Nebraska Transportation Center

MID-AMERICA TRANSPORTATION CENTER

NEBRASKA
Good Life. Great Journey.
DEPARTMENT OF TRANSPORTATION

Report M063

Final Report
26-1121-4038-001

Piezocone Penetration Testing Device

Chung R. Song, Ph.D., A.E.
Associate Professor
Department of Civil Engineering
University of Nebraska-Lincoln

Binyam M. Bekele
Graduate Research Assistant

Brian Sawyer
Undergraduate Research Assistant

2018

Nebraska Transportation Center
262 Prem S. Paul Research Center at Whittier School
2200 Vine Street
Lincoln, NE 68583-0851
(402) 472-0141

"This report was funded in part through grant[s] from the Federal Highway Administration [and Federal Transit Administration], U.S. Department of Transportation. The views and opinions of the authors [or agency] expressed herein do not necessarily state or reflect those of the U.S. Department of Transportation."

PIEZOCONE PENETRATION TESTING DEVICE

Submitted By

Chung R. Song, Ph.D., A.E.
Principal Investigator

Binyam M. Bekele
Graduate Research Assistant

Brian Sawyer
Undergraduate Research Assistant

and

University of Nebraska-Lincoln

Submitted to

Nebraska Department of Transportation

1500 Nebraska Highway 2

Lincoln, Nebraska 68502

Project Duration (7/1/2016 to 12/30/2017)

February 2, 2018

TECHNICAL REPORT DOCUMENTATION PAGE

1. Report No. M063	2. Government Accession No.	3. Recipient's Catalog No.
4. Title and Subtitle Piezocone Penetration Testing Device		5. Report Date January 3, 2017
		6. Performing Organization Code:
7. Author(s) Chung R. Song, Binyam M. Bekele and Brian Sawyer		8. Performing Organization Report No. 26-1121-4038-001
9. Performing Organization Name and Address University of Nebraska-Lincoln, Department of Civil Engineering 262 Prem Paul Research Center at Whittier School 2200 Vine St, Lincoln, NE 68503		10. Work Unit No. 11. Contract or Grant No.
12. Sponsoring Agency Name and Address Nebraska Department of Transportation (NDOT) 1500 Nebraska Highway 2 Lincoln, NE 68502		13. Type of Report and Period 14. Sponsoring Agency Code
15. Supplementary Notes		

16. Abstract

Hydraulic characteristics of soils can be estimated from piezocone penetration test (called PCPT hereinafter) by performing dissipation test or on-the-fly using advanced analytical techniques. This research report presents a method for fast estimation of hydraulic conductivity of overconsolidated soils based on the piezocone penetration test. The method relies on an existing relationship developed for the determination of hydraulic conductivity of normally consolidated soils on-the-fly. The present research revises this relationship so that it can be applied for overconsolidated soils by incorporating a proper correction equation. The revised relationship provides a pore pressure representing the hydraulic conductivity of a hypothetical "equivalent normally consolidated soil". The revised relationship was developed with piezocone indices (Q_t, F_r, and B_q) based on well documented laboratory test and PCPT data. In this regard, PCPT data from Nebraska Department of Transportation (NDOT) was used as a primary data base to determine the correction equation. Then, the proposed revised relationship was verified for other sites in the USA, Canada, and South Korea. This study showed that the proposed method provides a reasonably good prediction of hydraulic conductivity of overconsolidated soils. In addition, the method also accurately predicted the hydraulic conductivity of normally consolidated soils.

17. Key Words Hydraulic conductivity; Overconsolidated soil; PCPT; Piezocone indices		18. Distribution Statement	
19. Security Classification (of this report) Unclassified	20. Security Classification (of this page) Unclassified	21. No. of Pages 88	22. Price

TABLE OF CONTENTS

LIST OF TABLES

LIST OF FIGURES

ACKNOWLEDGMENTS

The authors would like to thank Nebraska Department of Transportation (NDOT) for the financial support needed to complete this research. Also, NDOT Technical Advisory Committee (TAC) for their technical support, discussion and comments.

DISCLAIMER

The contents of this report reflect the views of the authors, who are responsible for the facts and the accuracy of the information presented herein. This document is disseminated under the sponsorship of the U.S. Department of Transportation's University Transportations Centers Program, in the interest of information exchange. The U.S. Government assumes no liability for the contents or use thereof.

ABSTRACT

Hydraulic characteristics of soils can be estimated from piezocone penetration test (called PCPT hereinafter) by performing dissipation test or on-the-fly using advanced analytical techniques. This research report presents a method for fast estimation of hydraulic conductivity of overconsolidated soils based on the piezocone penetration test. The method relies on an existing relationship developed for the determination of hydraulic conductivity of normally consolidated soils on-the-fly. The present research modifies this relationship so that it can be applied for overconsolidated soils by incorporating a proper correction equation. The correction equation provides a pore pressure representing the hydraulic conductivity of a hypothetical "equivalent normally consolidated soil". The correction equation was developed with piezocone indices (Q_t, F_r, and B_q) based on well documented laboratory test and PCPT data. In this regard, PCPT data from Nebraska Department of Transportation (NDOT) was used as a primary data base to determine the correction equation. Then, the proposed correction equation was verified for other sites in the USA, Canada, and South Korea. This study showed that the proposed method provides a reasonably good prediction of hydraulic conductivity of overconsolidated soils. In addition, the method also predicted the hydraulic conductivity of normally consolidated soils.

1 INTRODUCTION

1.1 Background

The piezocone penetration testing device is known as one of the two more reliable geotechnical testing devices (Lunne et al. 1997), and NDOT has one portable unit which is actively deployed on their existing drill rigs. The built-in piezometer in the piezocone measures the pore pressure response during penetration and used to profile soil layering systems.

For saturated soils, this piezometer is also used to conduct dissipation tests to obtain hydraulic conductivity or coefficient of consolidation. Dissipation tests usually takes four to eight hours, which considerably lowers the testing efficiency (speed) of this device. (Usually it takes one to two hours for one piezocone test without dissipation test while it takes one whole day with a dissipation test.)

Recently a technique was developed by Song and Pulijala (2010) to estimate the hydraulic conductivity or coefficient of consolidation without resorting to the dissipation tests. Song and Pulijala's 2010 method is essentially an advanced analytical technique that doesn't need any mechanical modification of the existing piezocone system. Infusing Song and Pulijala (2010) to the current piezocone system of NDOT will provide real time estimation of hydraulic conductivity information. Once this technique is incorporated into the current NDOT's piezocone system, the efficiency of the piezocone penetration testing device will be significantly improved with no or little additional cost.

1.2 General Insight of the New Technique

Several methods to evaluate hydraulic properties using the piezocone penetrometer have recently been developed. Rust et al. (1995) estimated the coefficient of consolidation from pore pressure dissipation data obtained during the arresting time for the drive rod connection (at every one meter interval). Manassero (1994) proposed an empirical approach to estimate the hydraulic conductivity of slurry walls. Song et al. (1999) estimated the hydraulic conductivity of soils from the pore pressure difference between u_2 and u_3 measured PCPT. It is noted that u_2 is measured pore pressure at the cone tip shoulder. u_3 is measured pore pressure at the cone shaft that is approximately 14 cm apart from u_2 location. When one compares pore pressure at the cone shaft that is approximately 14 cm time difference between the two measurements, one can see that the pore pressure at u_3 is usually different from that at u_2. The difference shall be due to the dissipation of excess pore pressure in seven seconds with reference penetration speed 2 cm/s of piezocone penetrometer. By analyzing this pore pressure dissipation, Song et al. (1999) were able to estimate the hydraulic conductivity of soils. Song and Pulijala (2010) further developed a technique so that the computation time is decreased and "on-the-fly" computation of the hydraulic conductivity of soils from piezocone penetration tests can be done.

Song and Pulijala's technique is based on the notion of simultaneous generation and dissipation of excess pore pressure at a given point. Pore pressure will be generated due to the imposed stress by the penetration and redistribution of in-situ stress condition. However, the notion of simultaneous generation and dissipation states that this generated pore pressure at a given point also contains dissipation information for previously generated pore pressure before the penetrometer reaches to that point.

Analytical solutions to solve the simultaneous generation and dissipation of excess pore pressure are available (Elsworth and Lee 200, Voyiadjis and Song 2003), but the computation costs are quite high due to sophisticated numerical techniques. The parametric studies and semi-empirical equations proposed by Song and Pulijala (2010) provide a simpler and faster way of determining the hydraulic conductivity from PCPT.

1.3 Objectives of the Project

The main objective of the project is to estimate hydraulic conductivity of soils on real time basis using NDOT's piezocone penetration test device. The following detailed objectives were planned:

(a) Real time determination of hydraulic conductivity of soils based on Song and Pulijala's 2010 equation.
(b) Find correlation between measured excess pore pressure and hydraulic conductivity of Nebraska's Soils (overconsolidated soils).
(c) Conduct experiments in a well-controlled environment to confirm the correlations obtained in (b).
(d) Implement Correlations in NDOT's piezocone penetration test (PCPT) device (Data Logger/Computer) so that the hydraulic conductivity profile is obtained 'on-the-fly' with other outputs such as tip resistance, side friction, pore pressure and soil classification.

2 LITERATURE REVIEW

2.1 Background

The piezocone sounding device is the most reliable, rapid, and cost-effective testing device utilized to determine the type, stratification, mechanical and transport behavior of soils (Lunne et al., 1997). Today, due to their cost effectiveness and mobility, they are widely used in geotechnical site investigation, quality control of construction, ground improvement and in deep foundations. In particular, the hydraulic characteristics of soils can be estimated from piezocone penetration test (called PCPT hereinafter) by performing dissipation test or on-the-fly using advanced analytical techniques. The hydraulic characteristics of soils predominantly controlled by the coefficient of consolidation and the hydraulic conductivity of soil solid matrix. In this chapter, a review of available methods and underlying concepts is carried out regarding the evaluation of hydraulic conductivity and coefficient of consolidation using dissipation and on-the-fly testing.

2.2 Pore Pressure Response in PCPT

Advancing the penetrometer into the soil continually exerts an axial force onto the soil elements at different depths. For saturated soils, this vertical penetration from the tip of the penetrometer induces excess pore water pressure. However, when the penetration is halted, dissipation of the excess pore pressure generated will be initiated and it will continue to dissipate until it comes to the initial hydrostatic condition. Based on the rate of dissipation of the excess pore pressure, the magnitudes of hydraulic conductivity and coefficient of consolidation can be obtained.

A typical pore pressure dissipation response shows a continuous reduction of excess pore pressure with time after arresting the penetrometer, which is like the response in oedometer tests as shown

in Fig. 2.1. This phenomenon is typically observable in normally consolidated or lightly overconsolidated soils for pore pressure filter locations u_1 and u_2 (Burns and Mayne, 1998). For heavily overconsolidated soils, there is a dilatory pore pressure dissipation at the u_2 location behind the cone (Burns and Mayne, 1998) as shown in Fig. 2.1.

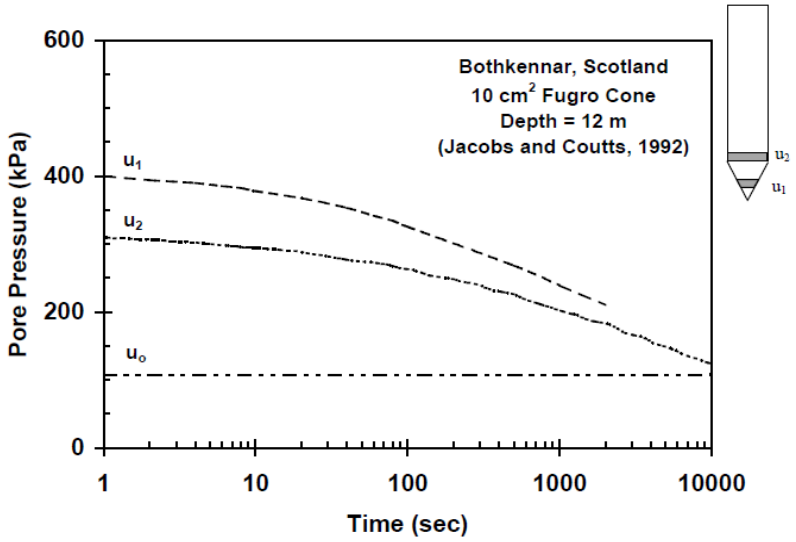

Fig. 2.1. Pore pressure dissipation response in normally consolidated and lightly overconsolidated soils (Burns and Mayne 1998)

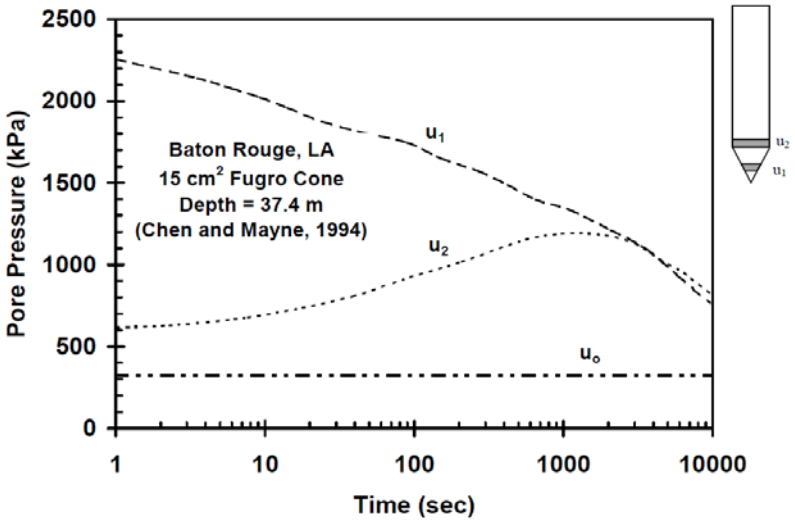

Fig. 2.2. Pore pressure dissipation response in overconsolidated soils (Burns and Mayne 1998)

In the dilatory pore pressure response, pore pressure tends to increase until a peak value is reached and then reduces with time to reach at a state of equilibrium pore pressure.

The pore pressure response for normally and lightly overconsolidated soils follows the solid line in Fig. 2.3 for a soil element located along the centerline of the travel path of the piezocone penetrometer as suggested by Voyiadjis and Song (2003). As the penetrometer approaches to the soil element, the additional stress from the penetrometer will induce excess pore pressure, and this pore pressure tends to increase until the moment the cone tip passes through the soil element. When the penetrating cone stops at this point, there is an immediate drop in pore pressure. After this, one may see a small increase in pore pressure due to the interaction between near field and far field. (near field: radially close to the cone, far field: radially far from the cone).

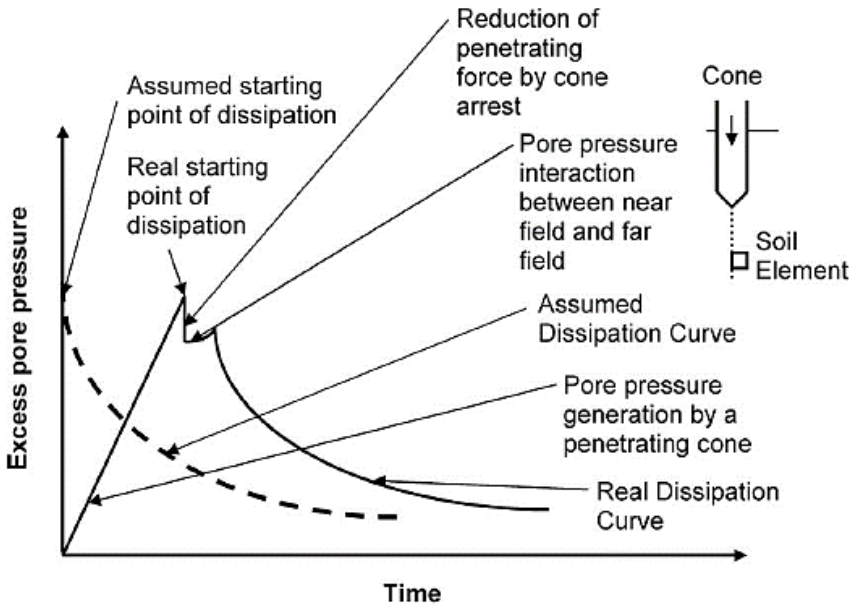

Fig. 2.3. Conceptual pore pressure response for soil element during piezocone penetration (Voyiadjis and Song 2003)

2.3 Evaluation of Hydraulic Conductivity from PCPT

This section briefly summarizes the major advancements in theoretical interpretations of piezocone penetration test based on dissipation curves and from on-the-fly methods.

The theoretical evaluation or interpretation of dissipation curves requires the parameter you are looking for, the magnitude of that parameter, the range of applicability it has, the length of time the dissipation is allowed, and the location that the pore pressure is measured; at the face, behind the cone or on the shaft (Baligh and Levandoux 1986). Baligh and Levandoux (1986) also discussed the difficulties in the theoretical evaluation of dissipation tests. These difficulties arise from the uncertainty associated with initial excess pore pressure determination and due to the complexity of a soil's mechanical behavior (non-linearity, anisotropy, rate dependency and non-homogeneity) caused by remolding due to penetration. Because of these complexities in theoretical interpretation of dissipation tests, few theoretical approaches have been developed, with nearly no developments before the 1980s.

In recent years, studies have concentrated on the evaluation of hydraulic parameters from PCPT on-the-fly. These techniques provide a real-time estimation of both the coefficients of consolidation and hydraulic conductivity continuously without resorting to dissipation tests. In addition to this, on-the-fly evaluation of these parameters can considerably increase the efficiency of PCPT through reduction of time consumed in performing dissipation tests. A brief discussion about both techniques from various points of view is made in the subsequent sections.

2.3.1 Prediction of Hydraulic Properties from Dissipation Curves

Torstensson (1977) (cited in Burns and Mayne 1998) did the first theoretical interpretation of dissipation test using cavity expansion theory for one-dimensional (radial) dissipation. In this work, the soil was assumed to behave as an elastic-perfectly plastic material. The Terzaghi-Rendulic uncoupled one-dimensional consolidation theory was used for the interpretation of the coefficient of consolidation. The coefficient of consolidation is estimated by computing the time

factor for 50% degree of consolidation using the following expression and matching it with the field dissipation data.

$$c = \frac{T_{50}}{t_{50}} r_o^{\,2} \tag{2.1}$$

where T_{50} is the time factor at 50% degree of consolidation. The T_{50} is predicted from this theory as a function of E_u/τ_f and depends on the type of cavity (cylindrical or spherical). E_u is equivalent undrained elastic modulus and τ_f is the maximum undrained shear strength. The t_{50} is the measured time at 50% of consolidation and r_o is an equivalent cavity radius. Torstensson stated that his method overestimated field values by a factor of approximately 2 from dissipation records, which were used to verify the model in normally consolidated clay. A sample dissipation curve from Torstensson (1977) is shown in Fig. 2.4.

Baligh and Levandoux (1986) did a comprehensive work for the prediction of dissipation tests that Torstensson did in 1977. The study used a strain path method to estimate the initial pore pressure for re-sedimented normally consolidated Boston blue clay (BBC) with rigidity index I_r = 100

.

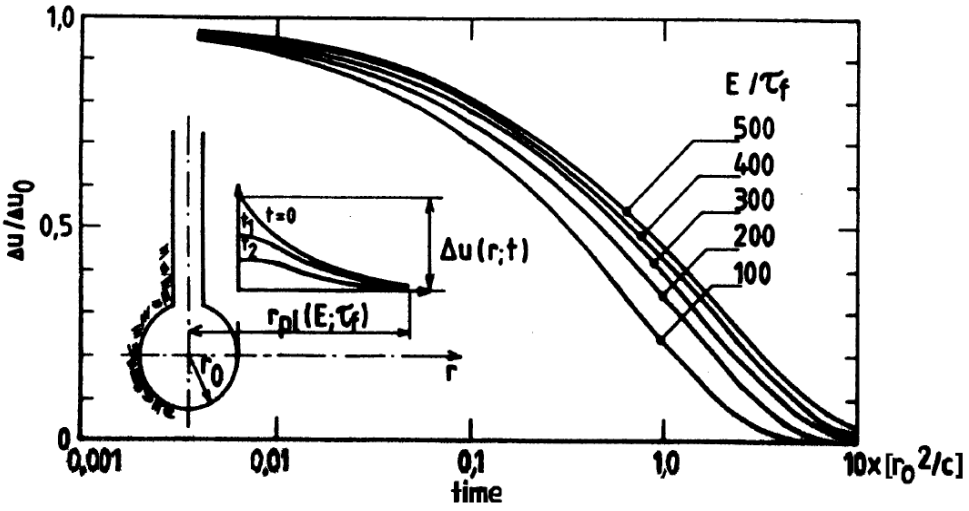

Fig. 2.4. Dissipation curve prediction from spherical cavity (Torstensson, 1977)

The rigidity index is defined as $I_r = {}^{G}/_{S_u}$, where G is the shear modulus and S_u is the undrained shear strength of the soil. This method was different from the cavity expansion method used by Torstensson (1977) and accounted for both vertical and horizontal (radial) dissipations. The basis for this interpretation method was the fact that penetration test is a strain controlled test.

The study utilizes linear material behavior. The authors argued that linear analysis provides valuable normalizations that can be applied to a wide range of soils. The work encompassed both uncoupled (Terzaghi theory) and coupled analysis (Biot's theory) of consolidation and the effect of cone angle, and anisotropy on dissipation response using finite difference analysis technique. Unlike Torstensson (1977), pore pressures were predicted at four different locations: At the cone tip, on the cone face, behind the cone, and on the shaft. Fig. 2.5 shows a sample dissipation curve predicted from this theory for an 18^o cone and using uncoupled consolidation analysis. Fig. 2.6 shows the comparison between uncoupled and coupled consolidation analysis for the 18^o cone.

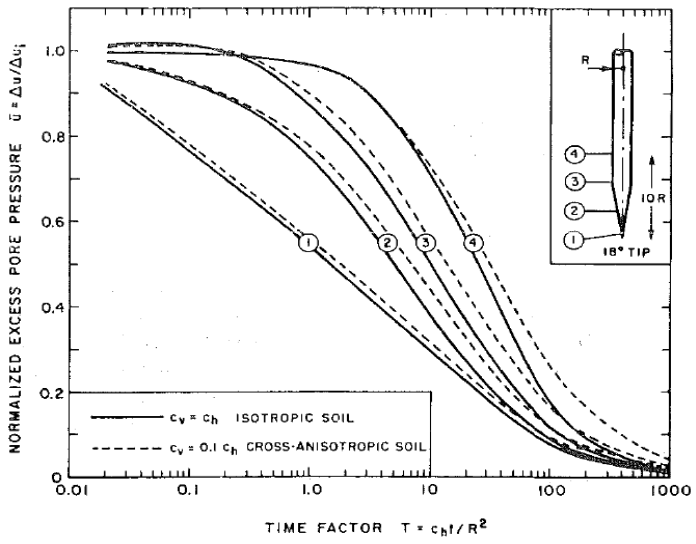

Fig. 2.5. Dissipation curve for 18^o (uncoupled analysis)

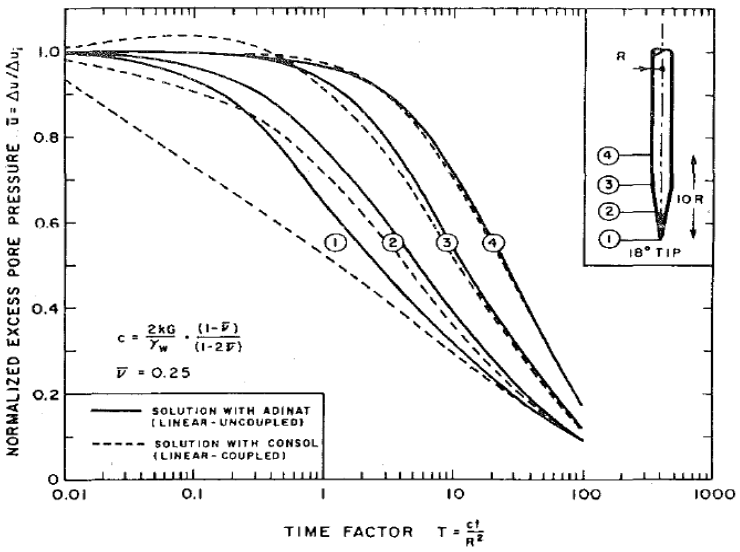

Fig. 2.6. Effect of coupling on the dissipation curves for 18^o cone (Isotropic Analysis)

In addition, based on field measurements of BBC at different locations on the cone and on the shaft behind it, predicted values showed excellent agreement for both the 18° and 60° cones despite the approximate nature of the strain path method. From this study, the following important points were concluded:

a) A tenfold decrease in vertical coefficient of consolidation has a minor effect on the dissipation rates. Therefore, dissipation is essentially controlled by the horizontal coefficient of consolidation, as shown in Fig. 2.6.

b) Dissipation around the blunt cones (60^o) are less sensitive to the filter location on the face of the cone and less susceptible to computational errors.

c) For the 18° cone, the effect of coupling the total stresses with the pore pressures has a minor effect on the dissipation rates after 20% consolidation, except at the cone tip, as shown in Fig. 2.6.

Houlsby and Teh (1988) extended the work of Baligh and Levandoux (1986) by incorporating large strain finite element technique besides the strain path method. This technique fulfills force equilibrium, which the strain path method failed to do. The soil penetrated by the cone was assumed to be an elastic-perfectly plastic material (obeys Von-Mises failure criterion), which was different from the material model used in Baligh and Levadoux (1986). Unlike the work of Baligh and Levandoux (1986), this study considered only uncoupled consolidation analysis. The pore pressure dissipations were estimated at different filter locations, as was done by Baligh and Levandoux (1986). A sample dissipation curve is shown in Fig. 2.7 for I_r=100.

The study conducted by Houlsby and Teh (1988) noted that due to the variation of I_r from soil to soil, the dissipation curves are not unique at a given filter location. The authors ultimately came up with a new method to merge a family of dissipation curves into a unified curve by modifying the time factor from T to T*. The modified time factor is obtained from the following expression:

$$T^* = \frac{c_h t}{R^2 \sqrt{I_r}} \tag{2.2}$$

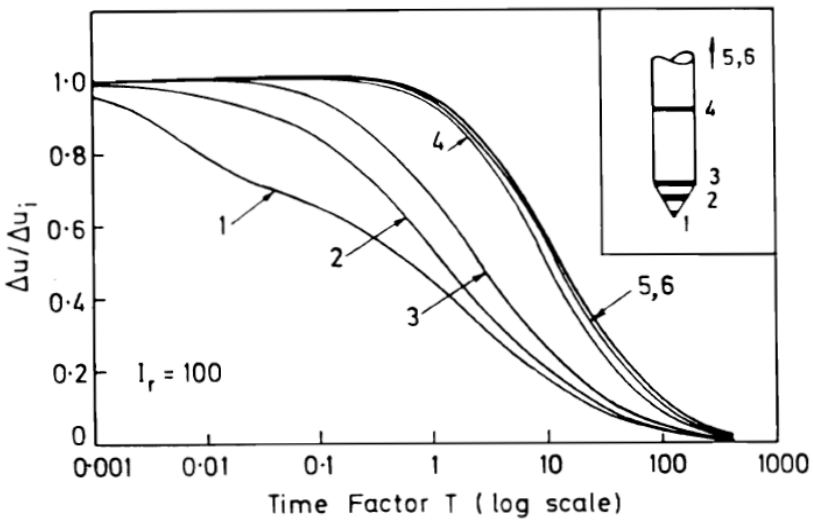

Fig. 2.7. Excess pore pressure dissipation curves at different locations for a soil with $\boldsymbol{I_r}$=100

where c_h is the horizontal coefficient of consolidation, R is the radius of the cone and I_r is the rigidity index. Fig. 2.8 shows the unified dissipation curves at the filter located behind the cone for different I_r values ranging from 50 to 500.

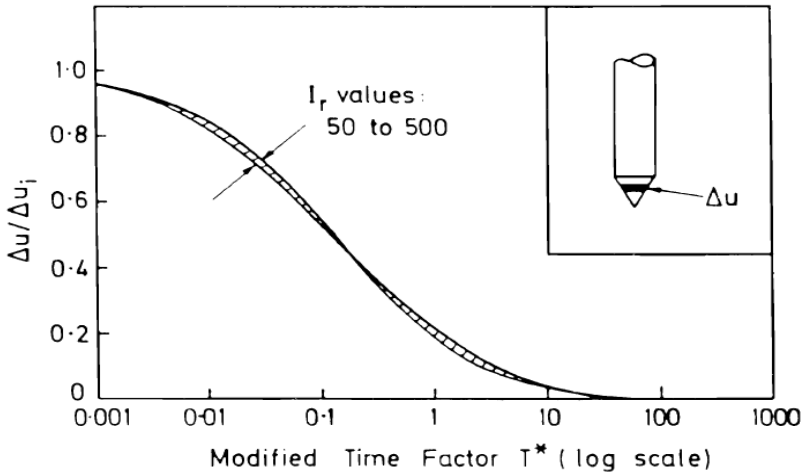

Fig. 2.8. Excess pore pressure dissipation for the modified time factor, T*

As a conclusion, the study stressed the importance of rigidity index to rationally interpret dissipation curves. The authors also believed that a unique interpretation of dissipation curves is achieved only if the time factor accounts for the effect of soil stiffness. Moreover, as Baligh and Levandoux (1986) concluded, this study also concluded that the dissipation rate is strongly controlled by the horizontal coefficient of consolidation.

Elsworth (1993) proposed a theoretical method of dissipation test interpretation which was quite different than the methods used in Torstensson (1977), Baligh and Levandoux (1986) and Houlsby and Teh (1988). The study utilized the volumetric dislocation model to analyze the cone penetration process and determine hydraulic conductivity and coefficient of consolidation. This method stated that both driving of the cone and dissipation of pore pressure occur concurrently. Thus, this method could model partial drainage conditions, which previous works were not able to do. In the proposed method of analysis, a point dislocation was assumed, which deviates from the

real physical system of the cone penetration test. Moreover, the soil was assumed to exhibit linear behavior and small deformation. The study concluded that the volumetric dislocation model showed close agreement with well-documented field results, especially for the coefficient of consolidation. The following general observations were made from this study:

a) Predicted results showed close agreement with well-documented field results, especially for the coefficient of consolidation.
b) Dissipation is controlled by pre-arrest rate of penetration and distance from the tip.
c) For the undrained case results at high penetration rate before cone arrest, this method showed a reasonable agreement with the methods based on static cavity expansion and strain path.

2.3.2 Prediction of Hydraulic Properties from On-The-Fly PCPT

Song et al. (1999) carried out a numerical simulation and experimental validation to estimate the permeability of soils on-the-fly using a two-point pore water measurement in PCPT. In the study, one point was measured above the cone (u_2) and the other measured above the friction sleeve (u_3). The authors mentioned that determination of hydraulic properties based on the dissipation test is relatively efficient, but still poses challenges to field engineers because of its time consumption and the impossibility of obtaining a continuous permeability profile. The analytical formulation used in this study was based on the coupled theory of mixtures using an updated Lagrangian reference frame. The pore pressure build-up was assumed to be a function of both the permeability and the stress-strain parameters. The penetration of the piezocone was identified as a time dependent, large strain problem. To account for this, the study used a non-linear, elastoplastic constitutive model (modified cam clay). Simultaneous generation and dissipation of excess pore water is considered (partial drainage condition) and thus removed the drawbacks of the

conventional method of estimating permeability from a dissipation test only. To validate the work, well documented actual field test results from PCPT were compared with the theoretically predicted values. Eventually, it was found that there is a clear relationship between $(\Delta u_2 - \Delta u_3)/\Delta u_2$ and permeability in the permeability range from 10^{-10} to 10^{-6} m/s. The threshold hydraulic conductivities 10^{-10} m/s and 10^{-6} m/s correspond to fully undrained and free drained conditions respectively. Moreover, it was indicated that these threshold values can be moved outward by changing the cone diameter and distance between u_2 and u_3.

Voyiadjis et al. (2003) proposed a method to determine the hydraulic conductivity of soils using the coupled theory of mixtures without carrying out a traditional dissipation test. This provides a real-time continuous hydraulic conductivity profile from a piezocone penetration test. In this study, it is noted that the traditional dissipation test has a non-reasonable assumption that the initial condition is a fully undrained condition. It is analyzed with incorrect initial time and initial pore water pressure. To overcome this drawback of the conventional method, the proposed method came up with a formulation of the coupled field equations for soils using the theory of mixtures in an updated Lagrangian reference frame, which was the same formulation used in Song et al. (1999). However, the procedure for the estimation of hydraulic conductivity in this study was quite different from the method used in Song et al. (1999) A trial and error method was employed in which an initial estimate of a hydraulic conductivity matrix is used to compute the pore pressure matrix. The computed pore pressure matrix is then compared with the measured pore pressure and if the difference is within 10%, then the assumed hydraulic conductivity is taken as a good estimate of the hydraulic conductivity of the soil. This procedure can be time-consuming unless a good initial estimation of hydraulic conductivity is made. This study also considered the effect of confining stress and a change in penetration speed on excess pore pressure. Fig. 2.9 shows the

variation of pore pressure with respect to penetration speed and confining stress. The effect of confining stress and penetration speed are assumed to be linear in this study.

To validate the method proposed here, theoretically predicted results were compared with well-documented field test data and experimental data from the calibration chamber system at Louisiana State University. Ultimately, it was found that the test data agreed well with their theoretical approach as shown in Fig. 2.10. The study also stressed that the method has a potential to determine hydraulic conductivities from the continuous pore pressure measurements. It was recommended by the authors to use the coupled theory of mixtures to predict the behavior of soils within the range of 10^{-7} and 10^{-4} dimensionless hydraulic conductivity values, where the dimensionless hydraulic conductivity is given by the expression $\left(\frac{k}{v}\right)\left(\frac{r}{r_{ref}}\right)$. k is the hydraulic conductivity, v is the penetration speed, r is the radius of the penetrometer head and r_{ref} is the radius of the reference penetrometer (1.784 cm)

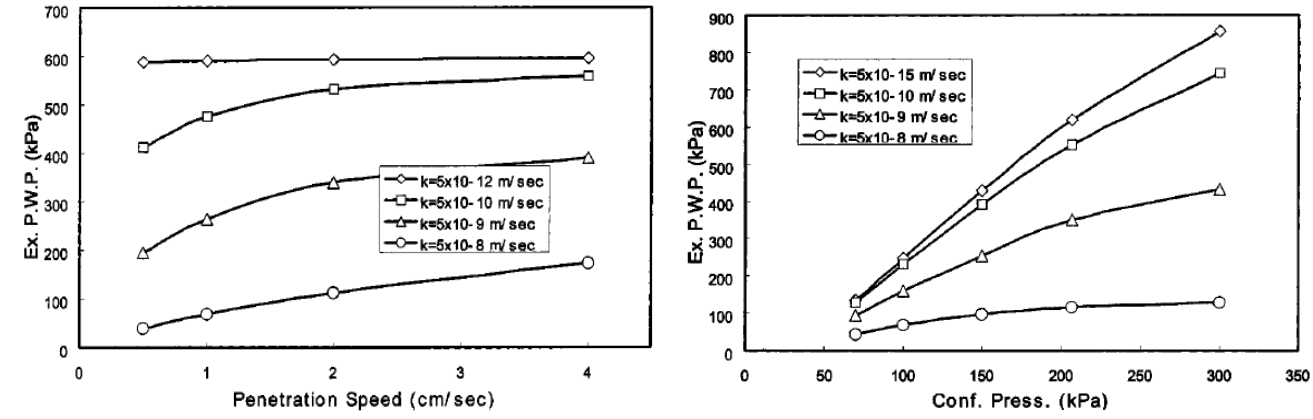

(a) (b)

Fig. 2.9. The effects of penetration speed (a) and confining stress (b) on excess pore pressure response of PCPT

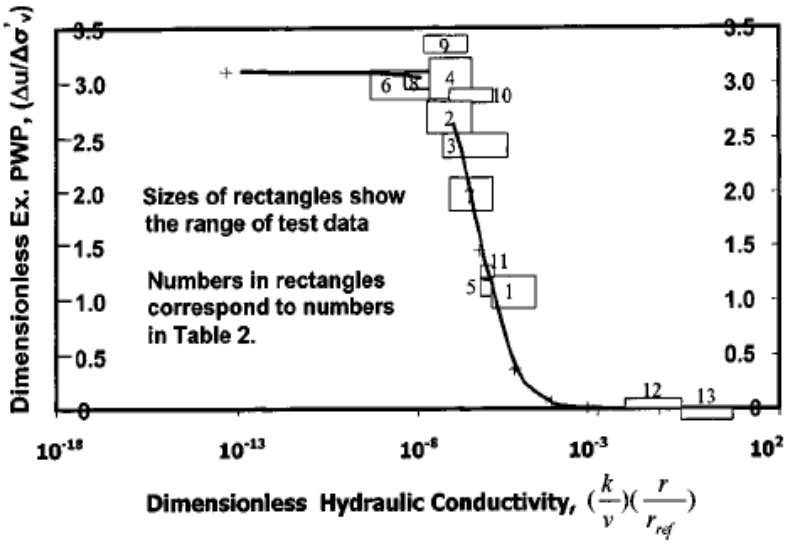

Fig. 2.10. Comparison of actual test data indicated by numbers from 1 to 13 with predicted results of dimensionless pore pressure and dimensionless hydraulic conductivity (M=1.2 and H=1.16)

Elsworth et al. (2005) proposed relationships (dislocation models) to represent the steady pore pressure developed around the penetrometer from a steady penetration rate. The approach used in this study is quite different from the method used in both Song et al. (1999) and Voyiadjis (2003). Like the aforementioned studies, this study has also targeted the determination of permeability on-the-fly from PCPT. A simple, generalized linear constitutive model was incorporated in this study. Dislocation models for both infinitesimal and finite radius penetrometers were formulated. In the infinitesimal radius penetrometer, a moving point dislocation was considered in which the penetrometer is assumed as a series of volumetric dislocations arranged along its trajectory. From this consideration, a relation is proposed to obtain the excess pore pressure developed at a given location. The main problem with the infinitesimal radius assumption is that the induced pore pressures are singular at the penetrometer tip. In the finite radius penetrometer, a finite migrating dislocation was assumed and approximate solutions were developed to determine the fluid pressure field around this migrating dislocation. The dislocation model obtained from this assumption was quite similar to the previous one, but has the advantage that it accommodates a finite sized

penetrometer. Further, the study incorporated piezocone indices (cone metrics) like Q_t, F_r and B_q which stand for normalized tip resistance, sleeve friction ratio and pore pressure ratio respectively into both the infinitesimal and finite radius dislocation models. Because the former suffered from shortcomings, the finite radius penetrometer dislocation model was used for further interpretations. Contour plots of permeability from each pair of indices B_q-Q_t, F_r-Q_t and B_q-F_r data are prepared from the relationships indicated below, which are derived by combining both finite radius penetrometer dislocation model and cone metrics.

$$K_D = \frac{1}{B_q Q_t} \tag{2.3}$$

$$K_D = \frac{1}{Q_t\left[1+\frac{1}{Q_t}-\frac{F_r}{\tan\phi}\right]} \tag{2.4}$$

$$K_D = B_q\left[\frac{F_r}{\tan\phi}-1+B_q\right] \tag{2.5}$$

Where B_q, Q_t and F_r are cone metrics, $tan\phi$ is the coefficient of friction at the sleeve-soil interface, K_D is the dimensionless permeability given by $(4k\sigma'_{vo})/(Ua\gamma_w)$, k is permeability, σ'_{vo} is the effective overburden pressure, U is the rate of penetration, a is the radius of the penetrometer, and γ_w is the unit weight of water. Data computed from the above three equations were correlated with known field data from two sites. It was concluded that the pair that contains Bq performed well in estimating permeability, and particularly Bq-Qt yielded the closest result. They also noticed that this method is applicable for a permeability range from 10^{-7} m/s to 10^{-4} m/s and standard penetration rate of 2 cm/s. These ranges showed a shift to the right in the order of magnitudes as compared to the ranges recommended in Song et al. (1999).

Lee at al. (2008) reported well-resolved measurements of hydraulic conductivity gathered from a newly developed in-situ permeameter. By using this measurement, the study examined the effect of tip-local disturbance and further examined the relative accuracy of hydraulic conductivity determinations from soil classification correlations (Robertson, 1990, as cited in Lee, 2008) from VisCPT measurements and from on-the-fly measurements of pore pressures using cone metrics (Elsworth et al., 2005 as cited in Lee, 2008). This work was performed at the Geohydrologic Experimental and Monitoring Site (GEMS) located in the floodplain of the Kansas River just north of Lawrence, Kansas. For testing, the in-situ permeameter was fabricated with tips of variable diameter (one with a sharp tip and the other with a large 4.5 cm length screen) to quantify the effect of disturbance in the testing zone. To validate the hydraulic conductivities measured with the in-situ penetrometers, calibration chamber tests were carried out with known hydraulic conductivities. For both tip diameters, the in-situ permeameter results closely agreed with the calibration chamber results, hence the in-situ permeameter results were used as a reference to examine the relative accuracy of the other methods. Presumed hydraulic conductivities were obtained from soil classification and grain size distribution (Robertson, 1990). VisCPT was used to directly capture a continuous real-time image of the soil. The soil grain size (sand) is obtained from image analysis of VisCPT and hydraulic conductivities are determined using Hazen formula. On-the-fly determination of hydraulic conductivity was done based on an approximate solution from the dislocation theory of finite radius penetrometer (Elsworth and Lee, 2005) without performing dissipation test. Using Bq-Qt plot, the dimensionless hydraulic conductivity K_D is used to estimate the hydraulic conductivity, *k*. The following conclusions were made in this study:

a) The results from the in-situ permeameter suggested a minor influence of tip-local disturbance. Thus, it indicated the feasibility of measuring hydraulic conductivity from CPT tip configuration.
b) On-the-fly determination of hydraulic conductivity required the tip-local pore pressure to be steady and partially drained.
c) If these conditions are satisfied, the on-the-fly PCPT sounding test has a practical means of accurately determining hydraulic conductivity.

Song et al. (2010) carried out extensive numerical simulations based on finite element analysis and proposed a more computationally and experimentally feasible method to determine hydraulic conductivity from Piezocone penetration testing. The basis for this method was the coupled relation of stress, deformation, pore water pressure and hydraulic conductivity. For this purpose, a coupled equation of mixtures derived by Abu-Farsakh (1998), as cited by Song et al. (2010), was used and modified cam-clay constitutive modeling is adopted to mimic the stress-strain behavior of the soil. Furthermore, it was shown that the response of soils during PCPT is a coupled response of M, λ, κ, pore pressure and hydraulic conductivity, where M is the slope of the critical state line, λ is the slope of the critical state line in $v - lnp'$ axis, and κ is the slope of the recompression line in $v - lnp'$ axis. The first two parameters indicate the stress-deformation characteristics. The effect of λ on the both pore water pressure and hydraulic conductivity of soils was considered to be negligible and thus it was discarded from further consideration. For this, it was reasoned that the constrained modulus corresponding to λ is much lower than that to κ, and thus a relatively smaller stress change is required for a given strain level in strain-controlled tests like PCPT. For such small induced stresses, the induced pore water pressure will be small and hence have negligible use in estimating hydraulic conductivity of the soil. A unique technique from the

previous works (Song et al., 1999; Voyiadjis et al., 2003) called variable separation was used in order to uncouple each variable and write one in terms of the other. Using this technique, explicit equations for pore water pressure in terms of κ, *k* and M were derived. From these equations and from mathematical manipulations, a logic that can estimate the hydraulic conductivity of soils as a function of u, κ and M is expressed as shown in [Eq. (2.6)].

$$k = \left\{ \frac{1 - 0.002436\left[u - 350(M - 1.0) + 160\log\frac{\kappa}{0.1} \right]}{1{,}893.7\left[u - 350(M - 1.0) + 160\log\frac{\kappa}{0.1} \right]} \right\} \tag{2.6}$$

where:

k is the hydraulic conductivity in m/sec,

u is the excess pore pressure in kPa,

κ is the recompression slope of void ratio vs. natural log pressure curve (dimensionless),

M is the slope of the critical state line (dimensionless).

The authors have indicated the following limitations of this equation:

a) Not applicable to sensitive clays

b) Applicable to λ/κ ratio from 0.1-0.2

c) Applicable for hydraulic conductivity range from $5x10^{-9}$ to $5x10^{-5}$ cm/s

d) Soils are assumed in a normally consolidated state

e) Assumed isotropic hydraulic conductivity

2.4 Conclusion

Estimation of hydraulic conductivity from PCPT can be done either by theoretically interpreting a dissipation curve or on-the-fly from the pore pressure response recorded during piezocone testing. The theoretical interpretation of dissipation curves is based on the prediction of the relationship

between the time factor and the excess pore pressure as penetration of the cone is halted. The key findings from the reviewed literatures are summarized as follows:

a) Dissipation is controlled mostly by the horizontal coefficient of consolidation
b) The prediction of the initial excess pore pressure is very important
c) The rigidity index is also important in theoretical modeling of dissipation curves
d) Most of the theories assume undrained condition

Analytical methods to interpret piezocone penetration data in order to determine hydraulic conductivity on-the-fly are also available. These methods rely on the assumption of a partial drainage condition in which excess pore pressure generation and dissipation occur at the same time (Song et al. 1999, Voyiadjis and Song 2003, Elsworth and Lee 2005). These methods use sophisticated numerical techniques and the associated costs are quite high. However, the semi-empirical equation proposed by Song and Pulijala (2010) is simple to use and provides an efficient way of determining hydraulic conductivity.

3 PRELIMINARY EVALUATION OF HYDRAULIC CONDUCTIVITY BASED ON LABORATORY TEST AND PCPT

3.1 Background

In this chapter, preliminary evaluation of hydraulic conductivity of soils using laboratory data and piezocone penetration test data is presented. Relevant data for all analyses carried out in this research were obtained from the Nebraska Department of Transportation (NDOT). Prior to the investigation of hydraulic conductivity, data collected from NDOT were organized so that data analysis could be executed quite easily.

The equation proposed by Song and Pulijala (2010) with some modifications and form changes, has been used to analyze the hydraulic conductivity based on PCPT data. In addition to this, hydraulic conductivity was also analyzed based on laboratory test data. From the collected PCPT and laboratory data, it has been determined that a majority of soil in Nebraska is overconsolidated soil as depicted by the OCR values of the soils and the negative or small magnitude of pore pressure measured from PCPT. However, it can be recalled from the previous literature discussion above, the equation proposed by Song and Pulijala (2010) is intended to be used for normally consolidated soils. To apply this preexisting equation to the specific soil examined in this project, measured excess pore pressure from PCPT should be adjusted for the overconsolidated soil condition before it is introduced into the equation. The details of the activities done in this research report are presented and discussed herein after.

3.2 Data Collection and Organization

Piezocone penetration test results of several projects along with their borehole log data were acquired from NDOT. The piezocone penetration data consisted of the cone resistance, the sleeve friction resistance and the pore pressure measured at u_2 position. The data collected from NDOT also consisted of laboratory test data of soil samples recovered from PCPT test holes. The primary target parameters from laboratory tests were the consolidation test results, which include the coefficient of consolidation, compression and recompression indices (C_v, C_c and C_r respectively).

Data collected from a total number of 28 projects were reviewed. Of the data obtained from the 28 projects, only 15 projects were utilized due to laboratory data or borehole log data that didn't contain the primary target parameters needed. The comparison of laboratory determined hydraulic conductivity and PCPT based hydraulic conductivity was done at discrete depths or points. This is because the laboratory tests are based on soil samples that are collected at discrete depths. Hence, the data available for comparison was dependent on the number of laboratory tests carried out for a given borehole. The depth of the groundwater table for each project was also collected and organized either directly from the borehole log or indirectly from the pore pressure distribution measured during PCPT. The summary of the data used is shown in ***Appendix A***.

3.3 Estimation of Hydraulic Conductivity from Laboratory Test Results

Before the estimation of the adjustment factors that should be applied to the measured excess pore pressure from PCPT, hydraulic conductivity estimation based on laboratory results was performed. In this regard, consolidation test results were used to determine the hydraulic conductivity of the soil samples collected at different specific depths in each borehole. The hydraulic conductivity of a soil can be determined from a consolidation test using [Eq. (3.1)] as shown below.

$$k = c_v m_v \gamma_w \tag{3.1}$$

where k is hydraulic conductivity (L/T), m_v is coefficient of volume compressibility (1/F) and γ_w is unit weight of water (F/L^3). The coefficient of volume compressibility is given by:

$$m_v = \frac{-\partial e}{(1+e_o)\partial(\Delta\sigma')} \tag{3.2}$$

where e and e_o are void ratio and initial void ratio respectively, and σ' is the effective vertical stress. The change in void ratio (Δe) for normally consolidated soil can be computed using [Eq. (3.3)].

$$\Delta e = C_c \log\left(\frac{\sigma_o'+\Delta\sigma'}{\sigma_o}\right) \tag{3.3}$$

where C_c is compression index. The final void ratio after an application of Δσ' vertical stress is given by $e = e_o - \Delta e$.

Coefficient of consolidation, compression index and initial void ratio were calculated directly from the given consolidation test data from NDOT. But, the value of volumetric modulus of compressibility (m_v) was computed indirectly using [Eq. (3.2) & (3.3)]. Rearranging [Eq. (3.2)]. as shown in [Eq. (3.4)] and plotting void ratio (e) with change in effective stress (Δσ'), values of m_v were calculated for a level of stress equivalent to the cone resistance (q_t). A sample plot prepared for project 2-6(119) RO-1 and a computation of m_v at a depth of 7.43 m (24.76 ft) below the ground surface are discussed below.

Table 3.1 Computation of mv from the given consolidation test results

σ_o'	Δσ'	$(\sigma_o'+\Delta\sigma')/\sigma_o'$	$\log((\sigma_o'+\Delta\sigma')/\sigma_o')$	$C_c\log((\sigma_o'+\Delta\sigma')/\sigma_o')$	e	$e/(1+e_o)$
134.88	0	1.00	0.000	0.000	0.45	0.310
134.88	600	5.45	0.736	0.081	0.369	0.254
134.88	1200	9.90	0.995	0.110	0.340	0.234
134.88	1800	14.35	1.157	0.127	0.323	0.222
134.88	2400	18.79	1.274	0.140	0.310	0.213

134.88	3000	23.24	1.366	0.150	0.300	0.206
134.88	3600	27.69	1.442	0.159	0.291	0.200
134.88	4200	32.14	1.507	0.166	0.284	0.196
134.88	4800	36.59	1.563	0.172	0.278	0.191

N.B. stresses are in kPa

$$m_v = \frac{-\partial\left(e/1+e_o\right)}{\partial(\Delta\sigma')} \tag{3.4}$$

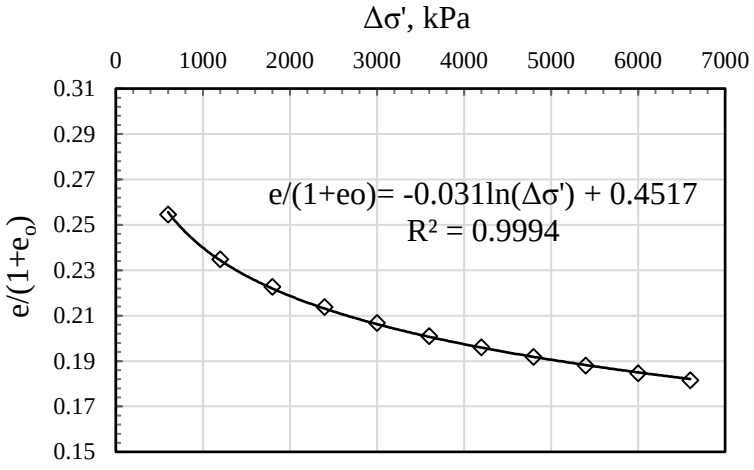

Fig. 3.1. Stain versus change in effective stress

From Fig. 3.1, the instantaneous slope (which in our case is the same as m_v) can be found by taking the first order derivative of void ratio with change in effective stress as indicated in [Eq. (3.4)]. Thus, $m_v = -\left(-0.0311/\Delta\sigma'\right) = \left(0.0311/\Delta\sigma'\right)$. Once we know the cone tip resistance, the value of m_v is obtained by substituting the cone tip resistance in Δσ'. For instance, at a depth of 7.43 m (24.76 ft), the cone tip resistance was found to be 2496 kPa. Then, m_v is calculated as $m_v = \left(0.0311/2496\,\text{kPa}\right) = 1.246x10^{-5}$ 1/kPa ($8.59x10^{-5}$ 1/psi). The coefficient of consolidation for the soil sample at this depth was found to be $7.25x10^{-6}$ m^2/s (6.74 ft^2/d). The hydraulic conductivity of the soil can be then computed by using [Eq. (2.1)] as:

$$k = c_v m_v \gamma_w = (7.25x10^{-6})(1.246x10^{-5})(9.81) = 8.86x10^{-10}\ \text{m/s} = 2.51x10^{-4}\ \text{ft/d}$$

In a similar fashion, the hydraulic conductivity at different depths where complete laboratory results exist was calculated. A table showing hydraulic conductivity computed from laboratory results is provided in ***Appendix B*** of this report. As a sample, Table 3.2 shows the hydraulic conductivity estimated from laboratory test results for project 2-6(119) RO-1.

Table 3.2. Hydraulic conductivity based on laboratory test results for project 2-6(119) RO-1

Depth	C_v	e_o	C_c	C_r	σ_o	σ_p	q_t	m_v	k	k
m	m^2/s				kPa	kPa	kPa	1/kPa	m/s	ft/d
2.34	7.08E-06	0.85	0.35	0.03	47.14	428.54	2161	3.52E-05	2.44E-09	6.92E-04
3.84	1.20E-05	0.76	0.38	0.04	68.26	449.28	1871	4.65E-05	5.49E-09	1.56E-03
5.96	7.61E-06	0.74	0.27	0.03	108.34	428.54	1631	3.86E-05	2.88E-09	8.18E-04
7.43	7.25E-06	0.45	0.11	0.02	134.88	331.68	2496	1.25E-05	8.86E-10	2.51E-04

3.4 Estimation of Hydraulic Conductivity Based on PCPT

As it has been discussed in chapter one, one of the applications of the cone penetration test is for the determination of hydraulic conductivity. Although hydraulic conductivity can be estimated based on the traditional dissipation test or on the fly, the on the fly techniques are more advantageous in providing a quick and continuous profile of hydraulic conductivity with depth. Song and Pulijala (2010) came up with a simple semi-analytical approach to determine hydraulic conductivity on the fly as a function of excess pore pressure at the u_2 position. The critical state line slope (M) and slope of elastic swelling line (κ) are also the variables in this equation. A slightly modified form of the equation proposed by Song and Pulijala (2010) was used for the estimation of hydraulic conductivity based on PCPT and is shown in [Eq. (3.5)].

$$k = \left[\frac{\frac{f(\mathrm{M},\kappa)}{u} - 1}{282{,}095.22} \right]^{1.0564} \tag{3.5}$$

where,

k is hydraulic conductivity in m/s

u is the excess pore pressure measured at u_2 position

$f(\mathrm{M},\kappa) = (345.25\mathrm{M} + 62.32)(-0.32\log(\kappa/0.1)+1)$

M is the slope of the critical state line in p'-q axis

κ is the slope of elastic swelling line $v - \ln p'$ in axis

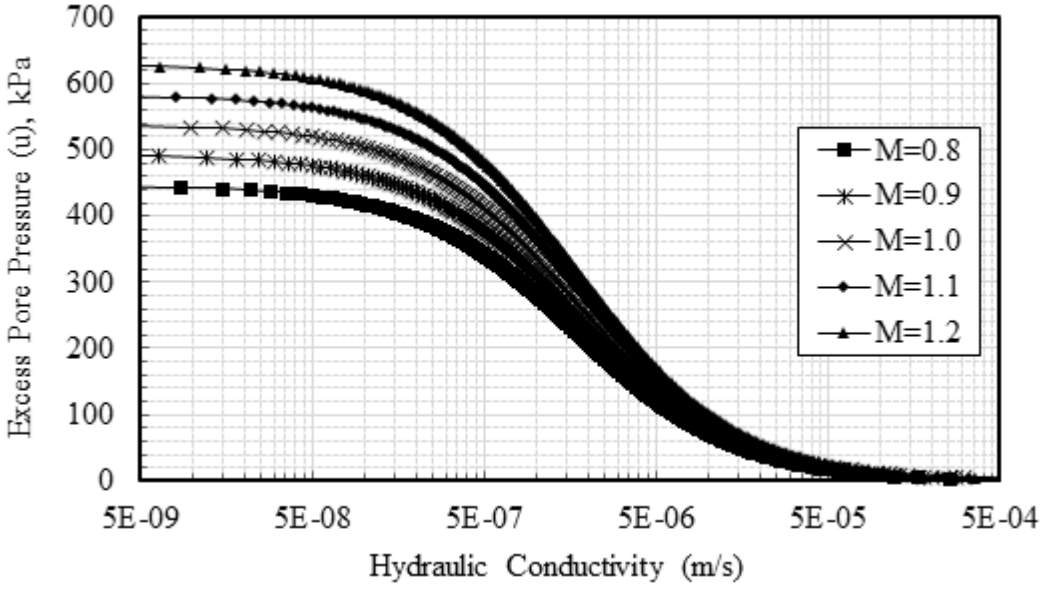

Fig. 3.2 Excess pore pressure Vs hydraulic conductivity for different values of M and $\kappa = 0.01$ based on Song and Pulijala (2010)

It should be noted however, [Eq. (3.5)] is only valid for hydraulic conductivity ranging from $5x10^{-4}$ m/s to $5x10^{-9}$ m/s. When the ratio of $f(\mathrm{M},\kappa)/u$ is less than unity, hydraulic conductivity of a given soil is less than $5x10^{-9}$ m/s.

For the sake of providing a continuous hydraulic conductivity profile, whenever [Eq. (3.5)] gave an undefined hydraulic conductivity, the upper bound hydraulic conductivity (i.e. $5x10^{-9}$ m/s) was assumed. Fig. 3.2 shows the relationship between hydraulic conductivity and excess pore pressure using [Eq. (2.5)]. 3.3 shows a sample calculation of hydraulic conductivity based on PCPT data for project 2-6(119) RO-1. A similar procedure is followed for the rest of the projects.

Table 3.3. Hydraulic conductivity based on PCPT for project 2-6(119) RO-1

GWT= 2.00 m

Depth	Pwp, u2	Static Pwp	Ex Pwp	Φ’	M	Cr	κ	k	k
m	kPa	kPa	kPa					m/s	ft/d
2.34	40.20	3.34	36.86	30	1.20	0.03	0.014	3.15E-05	8.93
3.84	103.50	18.05	85.45	30	1.20	0.04	0.018	1.14E-05	3.23
5.96	206.70	38.80	167.90	30	1.20	0.03	0.012	4.96E-06	1.40
7.43	68.10	53.22	14.88	30	1.20	0.02	0.010	8.94E-05	25.34

3.4.1 Strength and Compressibility Parameters (*M and κ*)

The slope of the critical state line is dependent on the angle of friction of a given soil. To get the proper value of the critical state line slope profile with depth, it is necessary to know the variation of the angle of friction of the soil with depth. There are several ways by which the value of angle of internal friction of a given soil can be identified. These methods mainly rely on laboratory tests or correlations from field tests.

Assessment of the laboratory results for the different projects indicated that the soils tested in almost all projects are mainly fine grained soils. The best means of finding the angle of friction of fine grained soils is to perform a triaxial test using high quality undisturbed soil samples (Robertson and Cabal 2010). Available correlations based on field tests mainly focus on sands and normally consolidated fine grained soils. In the absence of a reliable value, Robertson and Cabal (2010) recommended to assume a value of 28^o for clays and 32^o for silts. Based on the SBTn (normalized soil behavior type) chart provided by Robertson (1990, 2010), most of the soils were categorized in zone 3, 4, 5 and 9. Zones 3, 4, 5 and 9 stand for clay, clay-silt mixture, sand-silt mixture and very stiff fine grained soil respectively. As most of the soil fell in either the clay or silt category, an average angle of internal friction of 30^o was assumed. The critical state line slope

(M) was computed using [Eq. (3.6)]. For an angle of internal friction (ϕ') = 30^o, the critical state line slope (M) will be 1.20.

$$M = \frac{6\sin\phi'}{3-\sin\phi'} \tag{3.6}$$

The slope of the elastic swelling line (κ) was calculated from the recompression index (C_r), which was obtained from a consolidation test as shown in [Eq. (3.7)].

$$\kappa = \frac{C_r}{2.303} \tag{3.7}$$

3.4.2 Adjustment Factors to Compensate for Overconsolidation Effect

The equation proposed by Song and Pulijala (2010) is applicable to normally consolidated soils. Overconsolidated clays and very dense fine or silty sands give very low or even negative pore pressure readings at the pore pressure sensor behind the cone or at the u_2 position (Lunne et al. 1997). Therefore, if one uses the equation of Song and Pulijala without using proper adjustment factors for the pore pressure measured for soils stipulated above, then the hydraulic conductivity estimation will result in higher values. As evidence, comparison of the hydraulic conductivity estimated based on laboratory test results (Table 3.2) and based on PCPT (Table 3.3) clearly shows that the estimated hydraulic conductivity values by the equation are larger than those estimated based on laboratory results. To close the gap between the two estimations, there was a need to apply adjustment factors to compensate for the overconsolidation effect. To find out the proper adjustment factors, the following methodology was adopted:

1. Back analysis of the excess pore pressure that should be used in [Eq. (3.5)] was done by equating the hydraulic conductivity based on laboratory test results with the Song and Pulijala's equation.

2. Then, the adjustment factors were computed by dividing the excess pore pressure obtained in step (1) by the measured excess pore pressure based on PCPT.
3. A correlation was determined between the adjustment factors obtained in step (2) and SBTn chart parameters Q_t, F_r and B_q (Robertson 2010). These parameters are chosen because they reflect the type of soil penetrated during PCPT. From this correlation, a unique adjustment function was proposed which mainly relies on the type of the soil.

$$Q_t = \frac{q_t - \sigma_{vo}}{\sigma'_{vo}} \qquad F_r = \frac{f_s}{q_t - \sigma_{vo}} x100\% \qquad B_q = \frac{u_2 - u_o}{q_t - \sigma_{vo}} \tag{3.8}$$

where, Q_t is normalized cone resistance, F_r is normalized friction ratio, and B_q is pore pressure ratio. q_t is corrected cone resistance, f_s is sleeve friction and u_2 is pore pressure measured behind the cone. Table. 3.4 shows how the adjustment factors are computed on the basis of equating laboratory test result based hydraulic conductivity with [Eq. (3.5)].

Table 3.4. Computation of adjustment factors and SBTn parameters

Depth	**Pwp, u_2**	**Hydro static Pwp**	**Ex Pwp**	**Adj. Factor (C)**	**Adj. Ex Pwp**	**k (PCPT)**	**k (Lab)**	**Q_t**	**F_r**	**B_q**	**SBTn Zone**
m	kPa	kPa	kPa		kPa	m/s	m/s		%		
2.34	40.20	3.34	36.86	16.44	606.18	2.43E-09	2.44E-09	51.40	5.89	0.02	4
3.84	103.50	18.05	85.45	6.89	588.59	5.48E-09	5.49E-09	32.95	3.61	0.05	4
5.96	206.70	38.80	167.90	3.68	617.35	2.88E-09	2.88E-09	20.76	4.76	0.11	4
7.43	68.10	53.22	14.88	42.45	631.76	8.83E-10	8.86E-10	28.16	5.14	0.01	4

The adjustment factors (designated as C) were computed in the same fashion for the remaining 14 projects. After compiling the adjustment factors and the SBTn parameters at each depth for the 15 projects, a satisfactory correlation was obtained between the two. A single non-dimensional factor (designated as N) which was a function of Q_t, F_r and B_q was found to have the best correlation with the adjustment factors among any combinations of Q_t, F_r and B_q. The expression for N is given below in [Eq. (3.9)].

$$N = \left| \frac{Q_t B_q}{F_r} \right| \tag{3.9}$$

In [Eq. (3.9)], one should note that the absolute value of N should be taken while evaluating the

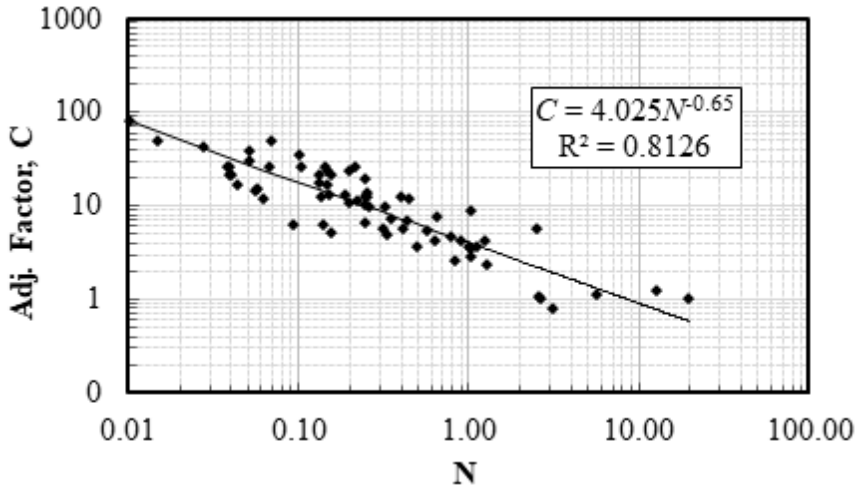

Fig. 3.3. Correlation between adjustment factors and non-dimensional factor N

adjustment factors, because in some instances (e.g. very stiff soil strata) the value B_q will be negative. The proposed correlation between N and C is shown in Fig. 3.3 and the complete data used for this analysis is shown in ***Appendix C***.

From the correlation, the adjustment factors can be estimated using the relationship shown in [Eq. (2.10)]. Then, hydraulic conductivity can be estimated from [Eq. (3.5)] by multiplying the measured pore pressure (u) with the adjustment factors estimated from [Eq. (3.9)].

$$C = \pm 4.025 N^{-0.65} \tag{3.10}$$

When the measured excess pore pressure is negative, the negative of the adjustment factor computed from [Eq. (3.9)] should be used and vice versa. The adjustment factors can be estimated on the fly once the level of the ground water table is fixed. Another advantage of [Eq. (2.10)] is that adjustment factors can be estimated in a continuous profile as far as the non-dimensional

normalized SBTn parameters are computed. ***Appendix D*** shows the estimation of hydraulic conductivity from PCPT after applying adjustment factors.

3.5 Sample Hydraulic Conductivity Profiles with Depth

In this section, sample hydraulic conductivity profiles plots are shown. These plots include the variation of hydraulic conductivity with depth estimated by PCPT before adjustments and after adjustment. In Fig. 3.4 the dotted rectangular shape indicates the hydraulic conductivity ranges estimated from consolidation test results. There is a significant deviation between the unadjusted hydraulic conductivity and laboratory test result. However, after applying the adjustment factors, the hydraulic conductivity deviates by an order of 1~2 from the measured hydraulic conductivity obtained from laboratory test.

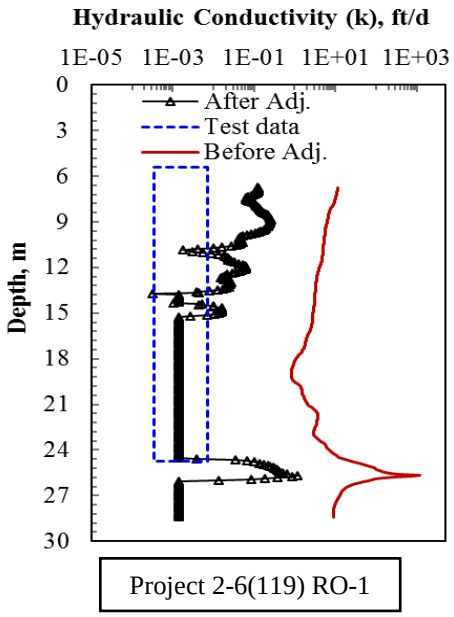

Project 2-6(119) RO-1

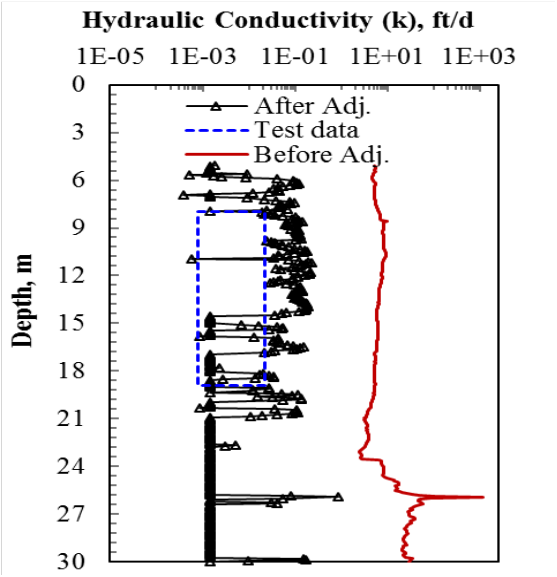

Project 2-6(119) RO-3

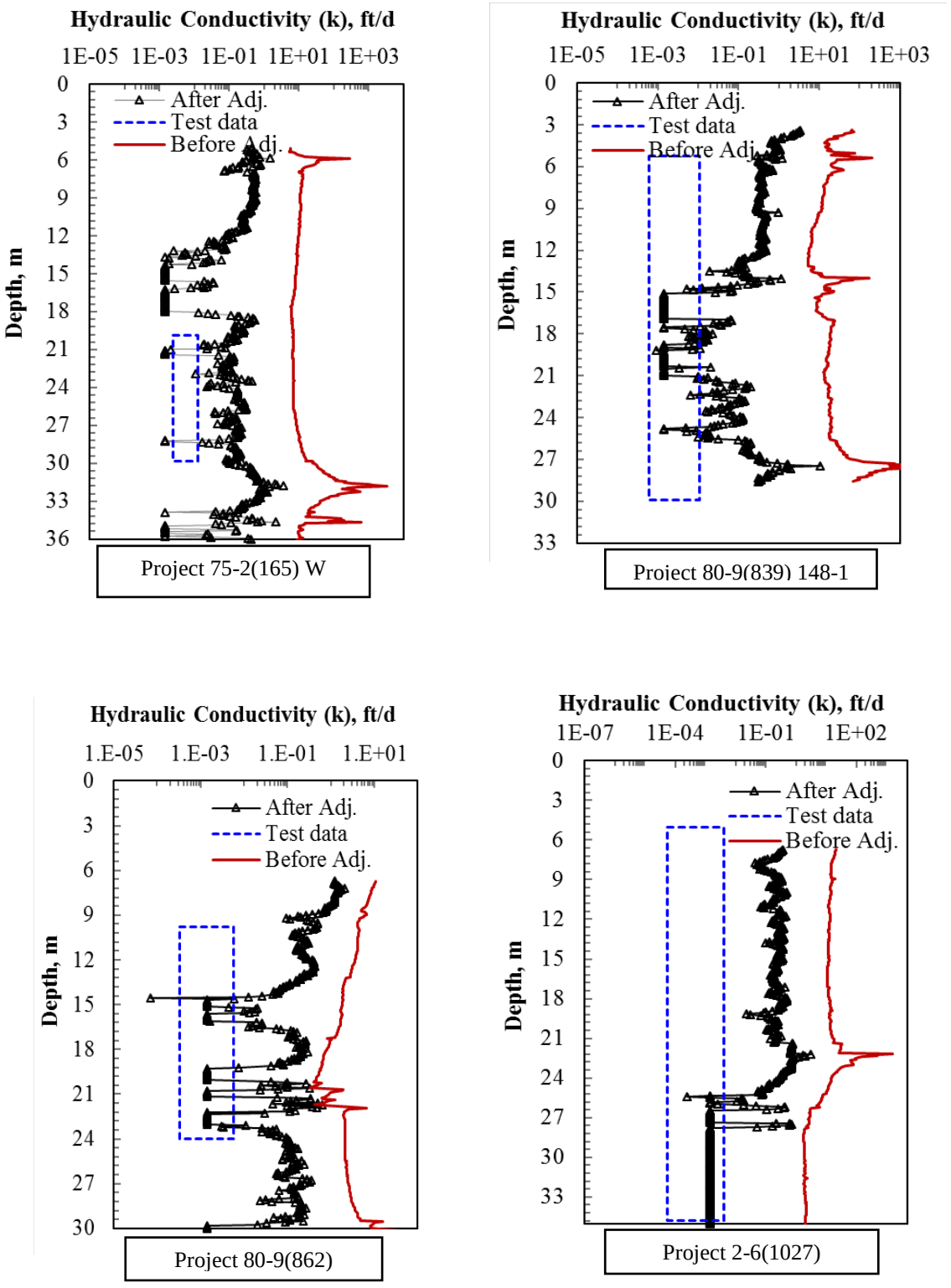

Fig. 3.4. Predicted hydraulic conductivity profiles with depth based on PCPT

4 ADDITIONAL EVALUATIONS ON THE CORRELATION AND CASE STUDIES

4.1 Introduction

Further evaluation and modification was done on the correlation obtained from the previous assessment in chapter 3. The evaluation has been done regarding the difference between positive and negative measured pore pressure on the hydraulic property of Nebraska soil. Moreover, the evaluation process included the investigation of the data points that are used for the estimation of the correlation between the non-dimensional factor *N* and adjustment factor C by plotting those data points on the SBTn (normalized soil behavior type) chart proposed by Robertson (2010). Based on this evaluation, a slight modification was made on the previously established relation between N and SBTn parameters (Q_t, F_r and B_q).

Case studies from well documented sites from the USA, Canada and South Korea are also included in this report. From these studies, quite satisfactory results are obtained for the estimation of hydraulic conductivity on the fly modified Song and Pulijala (2010). Hydraulic conductivity estimated based on the SBTn chart is compared with the results obtained from the proposed correlation.

Finally, an attempt was made to produce software to assist in the determination of hydraulic conductivity on the fly using visual basic for applications (VBA). Though the program has not progressed to completion, the foundational work completed so far regarding the VBA-based program is presented at the end of this report.

4.2 Evaluation of Data Points with negative and Positive Pore Pressure Ratio (B_q)

4.2.1 Qualitative Evaluation

In the previous evaluation, an absolute value of the non-dimensional parameter N was taken without proper justification. The previously proposed N and its correlation with C was taken as:

$$N = \left| \frac{Q_t B_q}{F_r} \right| \tag{4.1}$$

$$C = \pm 4.025 N^{-0.65} \tag{4.2}$$

where Q_t, B_q and F_r are normalized cone resistance, pore pressure ratio, and friction ratio respectively. It was assumed that if the measured excess pore pressure assumes a negative sign then the negative of the computed adjustment factor from [Eq. (4.2)] should be considered. Moreover, through this correlation, it was explicitly shown that the sign of B_q is minimally important for the prediction of adjustment factors. Qualitatively, the effect of the sign of B_q on hydraulic properties can be discussed with the help of the SBTn chart proposed by Robertson (2010), as shown in Fig. 4.1.

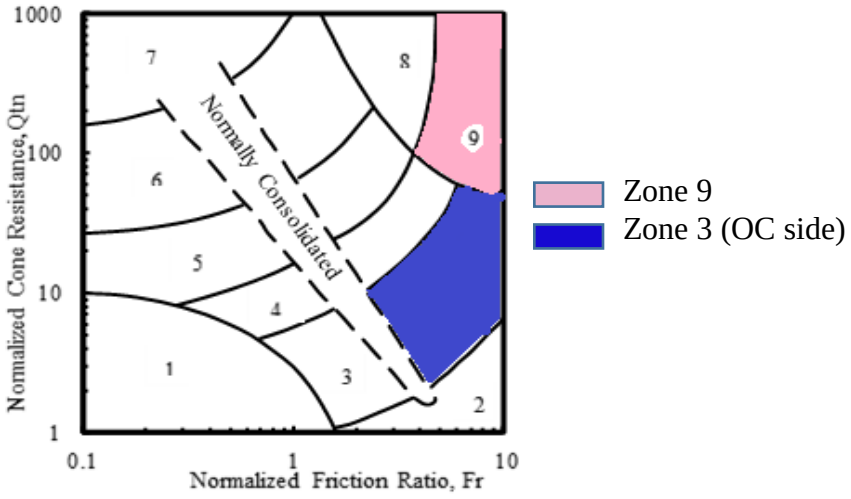

Fig. 4.1. Normalized soil behavior type (SBTn) chart (after Robertson 2010)

From Fig. 4.1, which shows two regions in the SBTn chart where one is zone 3 (overconsolidated side) and the other is zone 9 (very stiff fine grained soil region). Obviously, a large negative B_q is expected in zone 9 due to soils in this zone showing significant dilative characteristics. Whereas for zone 3, a small negative or small positive B_q is expected in the overconsolidated side. If one compares the upper and lower bound hydraulic conductivity of these two regions, zone 3 will have a value of 10×10^{-10} m/s to 10×10^{-9} m/s while zone 9 has a value of 1×10^{-9} to 1×10^{-7} m/s. From this, it is implied that though the sign of their B_q values can be substantially different, the hydraulic characteristics are still comparable.

Based on the above explanation, further evaluation can be made using the typical trends of excess pore pressure dissipation discussed in Burns and Mayne (1998). Now, consider Fig. 4.2 which shows the trends of dissipation of excess pore pressure measured at the u_2 filter location for normally and overconsolidated soils. Normally and lightly overconsolidated soils (contractive soils) show monotonic dissipation with time. On the other hand, moderately and heavily overconsolidated soils (dilative soils) display lower value of pore pressure before reaching a peak pore pressure and dissipate monotonically as witnessed in normally or lightly overconsolidated soils as shown in Fig. 4.2.

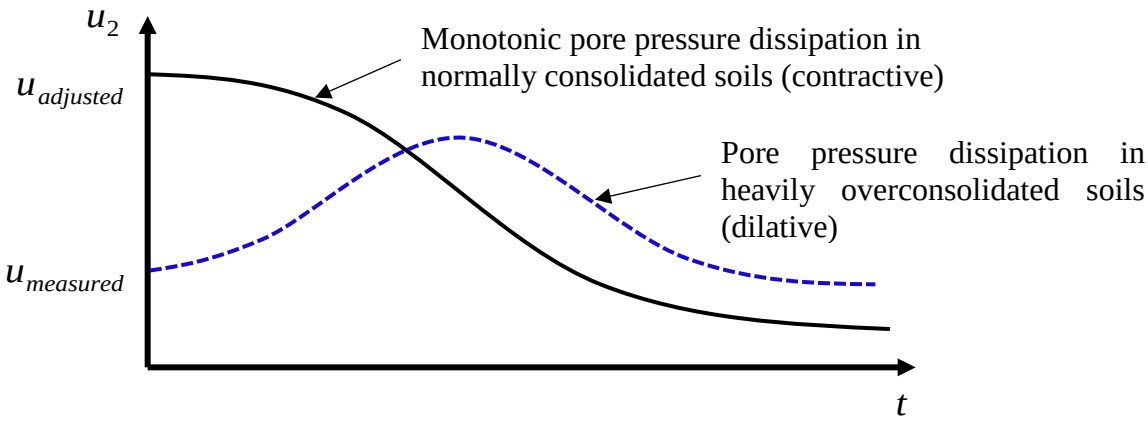

Fig. 4.2. Dissipation of pore pressure for contractive and dilative soils (adapted from Burns and Mayne 1998)

From Fig. 4.2, one can see that the hydraulic property of the two soils is similar, since the monotonic dissipation curves are parallel (dissipation after peak value for the OC soil). However, the initial pore pressure measured in the dilative soil is lower than the one measured in contractive soil due to their inherent characteristics. When adjustment factors are applied to the measured pore pressure ($u_{measured}$ in Fig. 4.2) of the dilative soil, it will be transformed to an initial pore pressure that would have been measured from an "equivalent" normally consolidated soil having an initial pore pressure designated as $u_{adjusted}$ in Fig. 4.2.

Going further, now consider a hypothetical initial small and large negative pore pressure measured from heavily overconsolidated soils with same hydraulic properties as shown in Fig. 4.3 though such dissipation trend has not been particularly noticed from literatures.

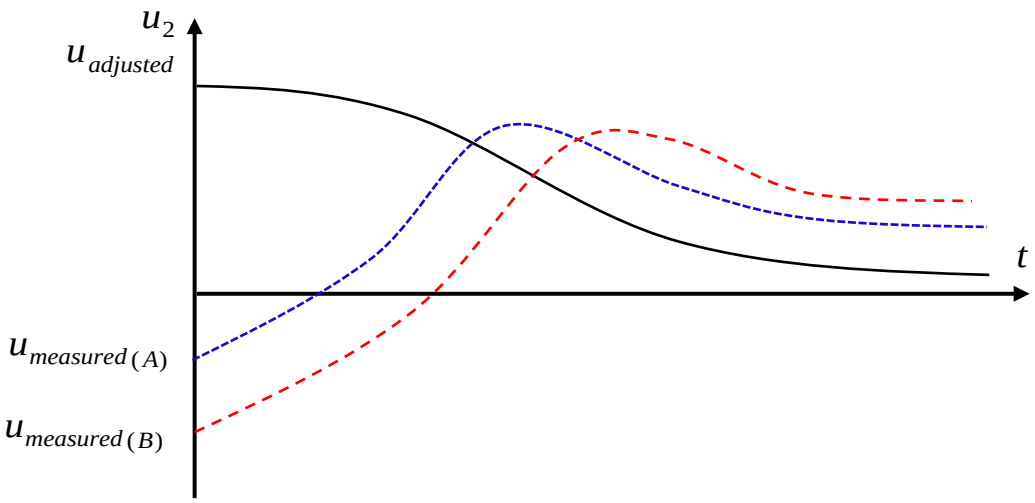

Fig. 4.3. Hypothetical dissipation of pore pressure in heavily overconsolidated soils

From Fig. 4.3, the adjustment factor required to transform a heavily overconsolidated soil with small negative excess pore pressure ($u_{measured\,(A)}$) will be larger than the adjustment factor required to change the one with large negative value ($u_{measured\,(B)}$). This is because the small negative pore pressure has lower magnitude compared to the larger negative pore pressure, so it requires a higher adjustment factor. From this, it can be claimed that for smaller positive and negative pore

pressures, the larger the adjustment factors expected and the larger the positive and negative pore pressures are, the smaller the adjustment factor needs to be. Therefore, if this explanation holds true, then the sign of B_q has less importance, and considering absolute value N, which is a function of B_q, is logical.

4.2.2 Quantitative Evaluation

The data set used for the derivation of the correlation between C and N is employed to verify the qualitative explanation given in 4.2.1 of this report. A total of 72 data points have been used to define the correlation in the previous evaluation in chapter 3. Among these 72 data points, 16 data points consisted of negative B_q, while the rest consisted of positive B_q. Each data set (one with positive B_q and the other with negative B_q) was organized independently along with their respective adjustment factors. Then, N is computed for each data set. For the negative B_q category, both computed N and C assumed negative values whereas the positive B_q category assumed positive N and C. Based on the discussion in the previous section, rather than taking the absolute value of B_q, this report intends to take the square of B_q. However, this consideration will be analyzed subsequently. N is modified to N^* as:

$$N^* = \frac{Q_t}{F_r} B_q{}^2 \tag{4.3}$$

Before data analysis is carried out, all 72 data points with Q_t and F_r values are plotted on the SBTn chart as shown in Fig. 4.4. The plot shows that all data points used in the correlation are relevant, since most of the points lie in the overconsolidated soils region. This may be desirable, as the correlation seeks to find an adjustment factor to the pore pressure measured for overconsolidated soils. Fig. 4.5(a) shows N^* versus C for the two data sets (i.e. one with positive B_q and the other with negative B_q). To check the validity of the assumption made in the qualitative evaluation, the

mirror image of the data sets for negative B_q is taken to the positive side as shown in Fig. 4.5(b), and a trend line is obtained for each case.

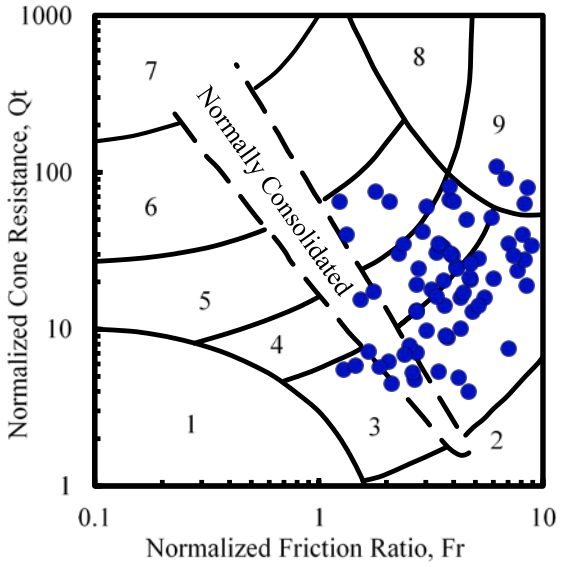

Fig. 4.4. Classification of soils in Nebraska using SBT_n chart

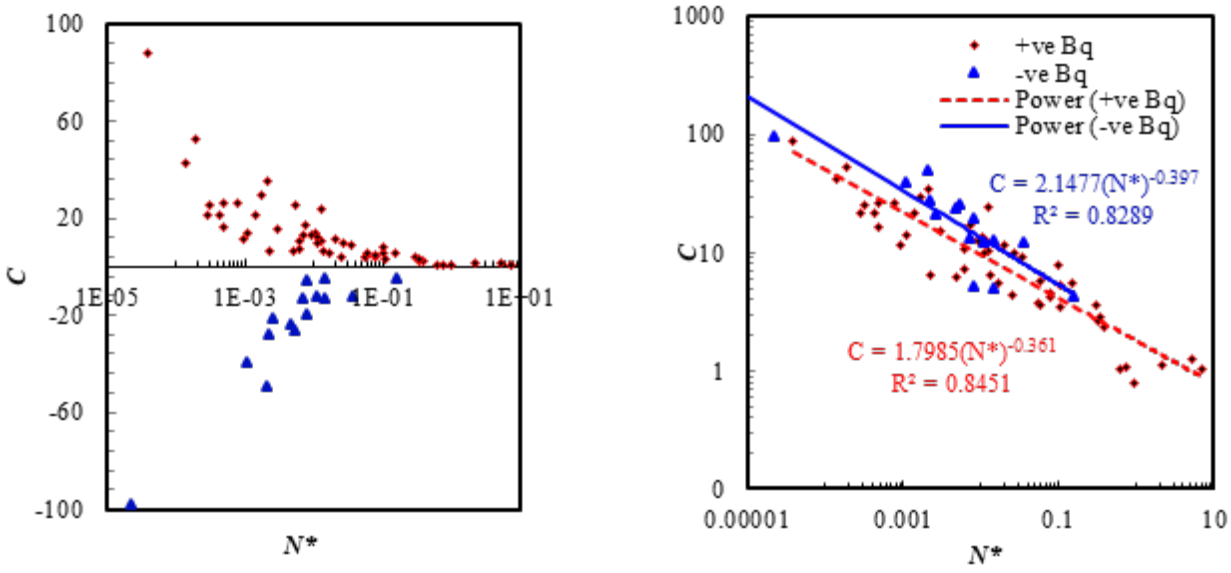

(a) (b)

Fig. 4.5. C vs modified N for negative and positive Bq data points (a) without reflection (semi log scale) (b) by reflection about N* axis (full log scale)

Referring Fig. 4.5(b), best fit power functions for positive and negative B_q are almost parallel. Moreover, the ratio of the estimated adjustment factors from the two functions is obtained to be approximately 1.50 and hence, it can be said that the deviation in the adjustment factors is not significantly large. More importantly, through the quantitative evaluation, it is shown that the sign of B_q has almost no effect on the prediction of adjustment factors. Considering this, a single modified trendline that encompass both data sets is proposed in Fig. 4.6.

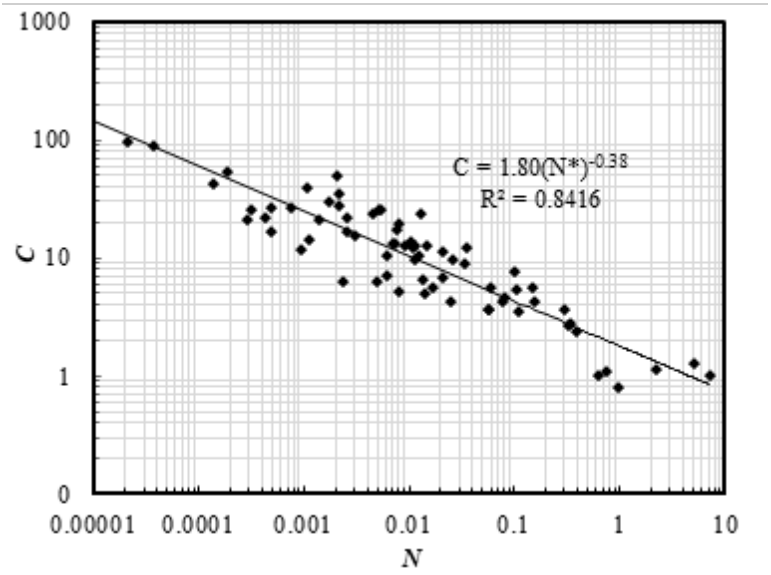

Fig. 4.6. C vs N* incorporating both negative and positive B_q

The modified correction equation with a coefficient of determination ($R^2 = 0.8416$) is given by:

$$C = 1.80\left(N^*\right)^{-0.38} \tag{4.4}$$

where C and N^* are adjustment factor and modified factor N, respectively.

4.3 Evaluation of the Correlation for other Sites

4.3.1 Yangsan Mulgeum, Korea (Dong A Geology 1997)

This site is the old delta area of the Nakdong River. The soils are primarily young alluvial deposits.

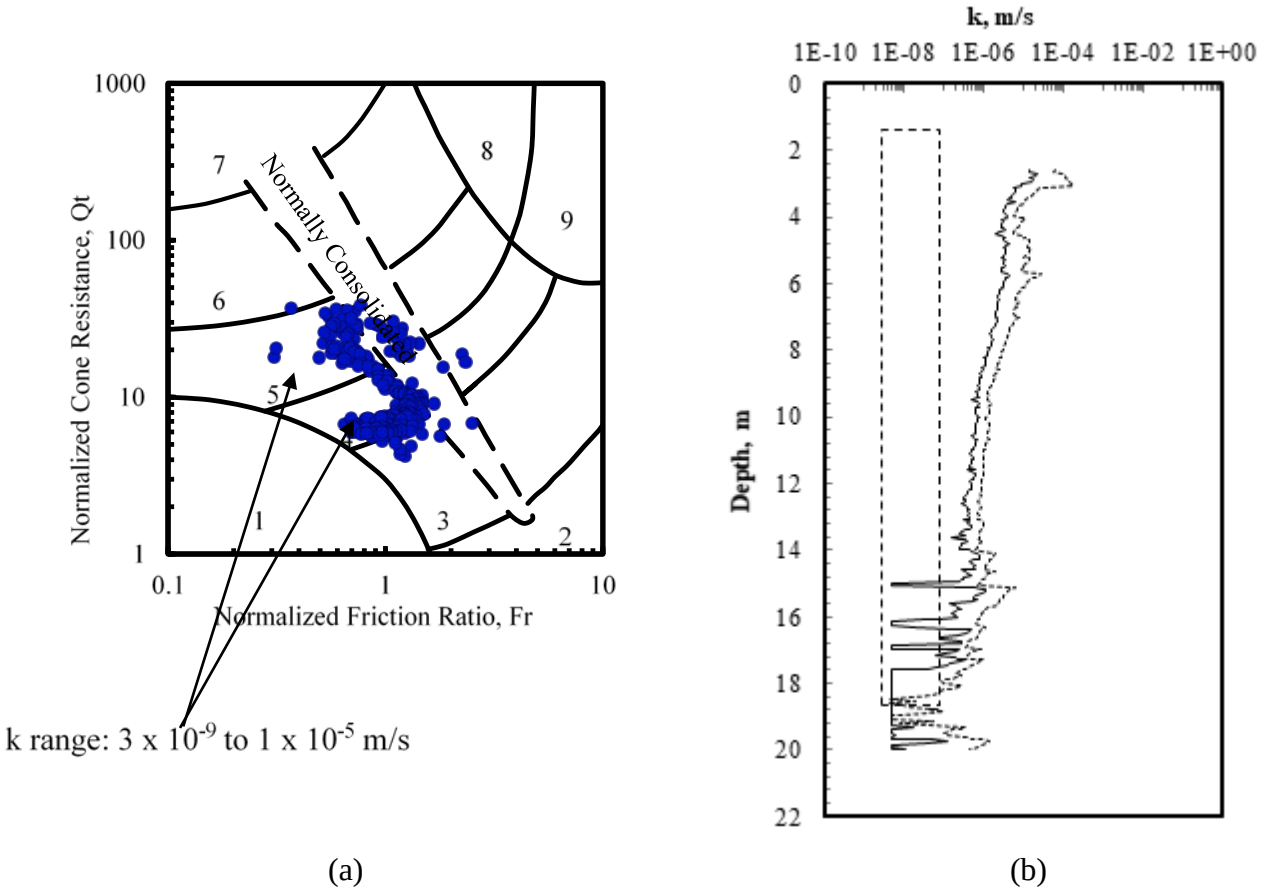

Fig. 4.7. (a) SBTn classification and range of hydraulic conductivity (b) Estimated hydraulic property profile with depth for Yangsan, Korea (data obtained from Dong A. Geology 1997)

According to Kim (2005), the area has approximately 10,000 years of sedimentary history, and the self-weight consolidation is still under progress. This area consists of clayey and silty fill materials, sedimentary layers consisting of clay, silty sand, silty clay, silt, sand, and gravel from the top. Pore pressure dissipation test using PCPT shows the coefficient of consolidation is (2-6) $\times 10^{-7}$ m^2/sec, and no other consolidation properties were provided.

Based on Robertson (2010), the soil is classified as silty clay to sandy silt with a hydraulic conductivity range from 3 x 10^{-9} m/s to 1 x 10^{-5} m/s as shown in Fig. 4.7(a). The ground water table is reported to be at a depth of 1 m.

From Fig. 4.7(a), the data points lean to the sensitive fine grained soils side. Some data points are also inside the normally consolidated soils zone. In Fig. 4.7(b), the estimated hydraulic conductivity shows good agreement with the laboratory measured hydraulic conductivity (indicated by the rectangular dotted plot), particularly towards deeper depths. Additionally, the estimated hydraulic conductivity is to the right of the measured hydraulic conductivity. This can be considered reliable, because it is common to have substantial deviation in laboratory and field hydraulic conductivity. Moreover, the unadjusted and adjusted hydraulic conductivity profiles are very close to each other. This may be because the soil is normally consolidated.

4.3.2 Frazer River, Canada (Crawford and Campanella 1991)

The area is located about 25 km South East from Vancouver on highway 99. The surface of this area is mostly floodplain, and the stratigraphy of the ground shows inter-bedded sand seams or peat layers. The subsurface soils are relatively uniform with a natural water content of about 45% and the liquid limit around 36%. According to consolidation test results, coefficients of compressibility, initial void ratios, vertical coefficients of consolidation, horizontal coefficients of consolidation, constrained modulus, and permeability are 0.3-0.5, 1.1-1.8, (0.6-2.8) × 10^{-7} m^2/s, (0.7-7) × 10^{-7} m^2/s, 1800-4 000 kPa, and (0.8-1.2) × 10^{-9} m/s respectively. The soil in the site is reported to be slightly overconsolidated to normally consolidated. In addition, from vane shear test results, it is reported that the soil shows high sensitivity in deeper depths. The ground water table is reported to be close to the ground surface. Based on Robertson (2010), the soil is classified as

silty clay to clayey silt with a hydraulic conductivity range from 3 x 10^{-9} m/s to 1 x 10^{-7} m/s as shown in Fig. 4.8(a).

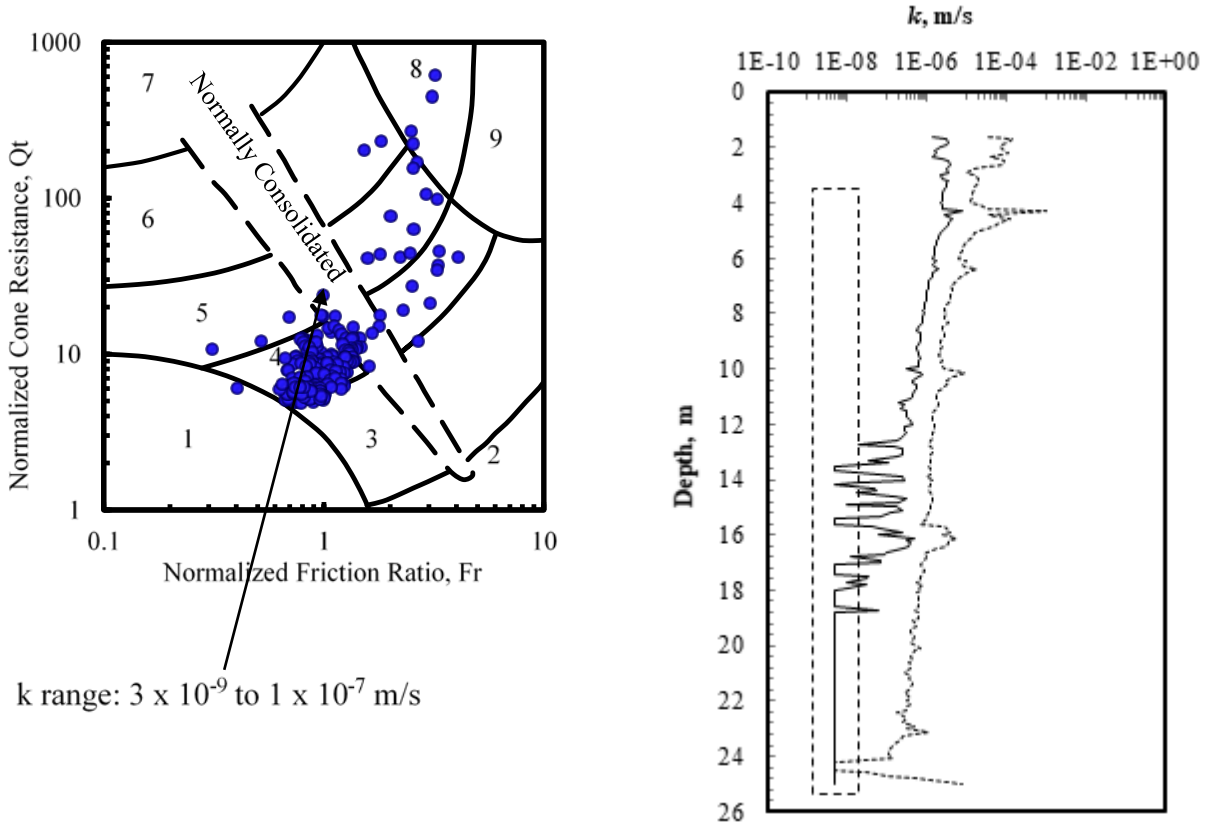

(a) (b)

Fig. 4.8. (a) SBTn classification and range of hydraulic conductivity (b) Estimated hydraulic property profile with depth for Frazer River (data obtained from Crawford and Campanella 1991)

The results in Fig. 4.8(a) shows that the soils are on the sensitive side, and some data points are also in the normally consolidated soils zone. Scatter data points exist in the slightly to very stiff sands and clayey soil zones, which are generally quite consistent with the reported nature of the soils (i.e. sensitive, normally consolidated to slightly overconsolidated). The hydraulic conductivity estimated from the modified Song and Pulijala's equation is quite closer to the measured hydraulic conductivity. The adjusted and unadjusted hydraulic conductivity are closer

in the shallower depths, which might imply the existence of normally consolidated soils, though there is significant deviation at deeper depths. This may be due to the increased sensitivity and effect of confining pressure in deeper depths. Moreover, the adjusted hydraulic conductivity ranges match those proposed by Robertson (2010) for zone 4 soils.

4.3.3 Cheongna (Section 1), Incheon, Korea (Kaya Engineering Co. 2007)

This area consists of overconsolidated soil in the upper layer and normally consolidated soil in the lower layer. Typical geotechnical properties show that the total unit weight is 1.57-1.95 t/m^3, liquid limit is 30-50%, natural water content is 20-40%, classification is CL, vertical coefficient of consolidation is (1-10) × 10^{-7} m^2/sec, horizontal coefficient of consolidation is (3-50) × 10^{-7} m^2/sec, coefficient of compressibility is 0.2-0.4, the depth of the soft layer is about 10 m, hydraulic conductivity is 4.82 x 10^{-8} m/s - 8.96 x 10^{-7} m/s, and OCR is 0.62~5.50. The soil in this area primarily falls under 3, 4 and 5. Most the data points are within the boundary between zones 3 and 4 which designates clay to silty clay soils. The hydraulic conductivity for these zones based on the SBTn chart ranges from 10^{-10} m/s to 10^{-7} m/s. Referring to Fig. 4.9(a), most the data points are in the overconsolidated soil zones. Some scattered data points show the soils are normally consolidated and somewhat sensitive. With the proper adjustment supplied to the unmodified Song and Pulijala (2010) equation based on the SBTn parameters, the estimated hydraulic conducted shows good agreement with the reported hydraulic conductivity of this area.

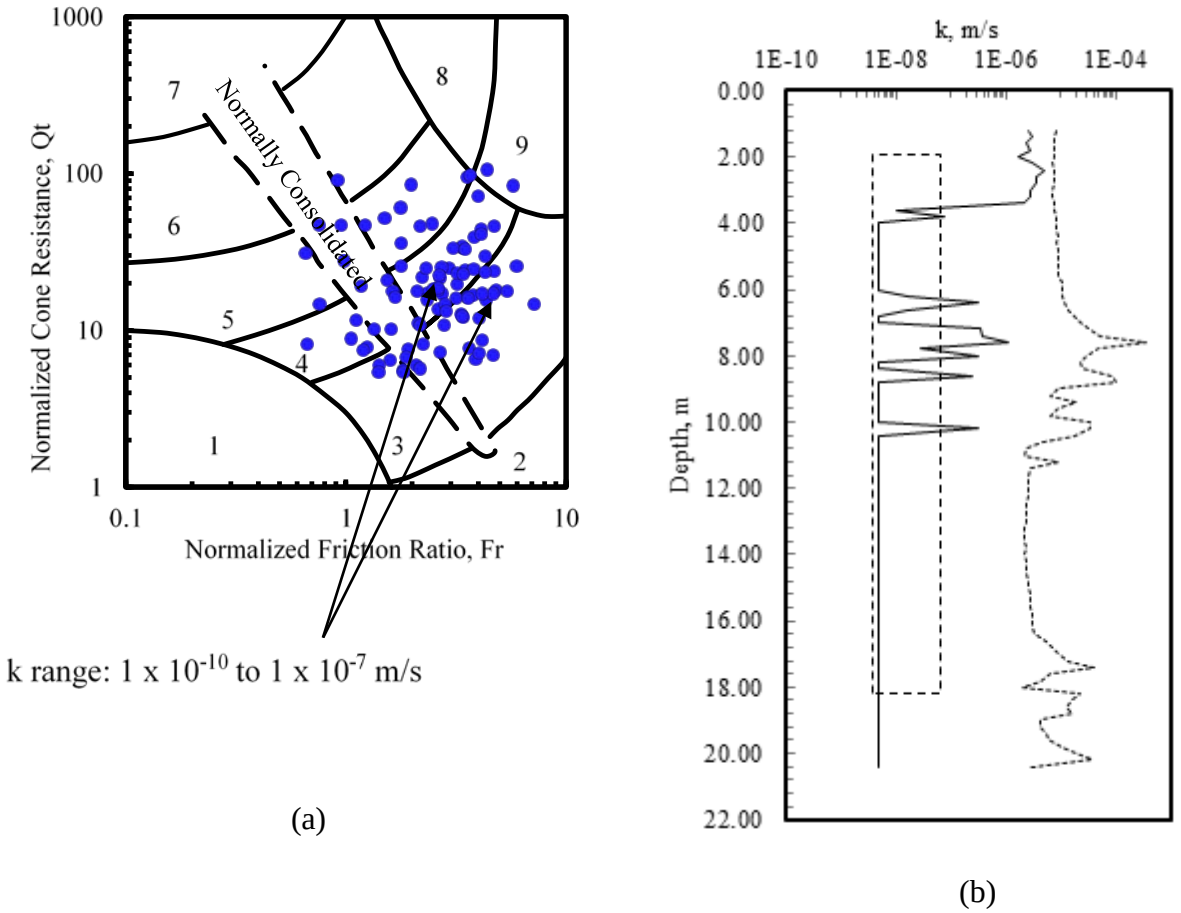

Fig. 4.9 (a) SBTn classification and range of hydraulic conductivity (b) Estimated hydraulic property profile with depth for Frazer River (data obtained from Kaya Engineering Co. 2007)

4.3.4 SR 49, Indiana, USA

The area is placed on the #49 road in Jasper County, Indiana. The normally consolidated clayey silty layers exist up to 25 m deep from the ground surface, and the ground water table is located at a level of 3 m below the surface. The average coefficient of consolidation evaluated from consolidation tests was about 3.6×10^{-7} m^2/sec. Fig. 4.10(b) shows the hydraulic conductivity estimated from the modified and unmodified Song and Pulijala (2010) equation. From the plot, the measured hydraulic conductivity is very close to the estimated hydraulic conductivity.

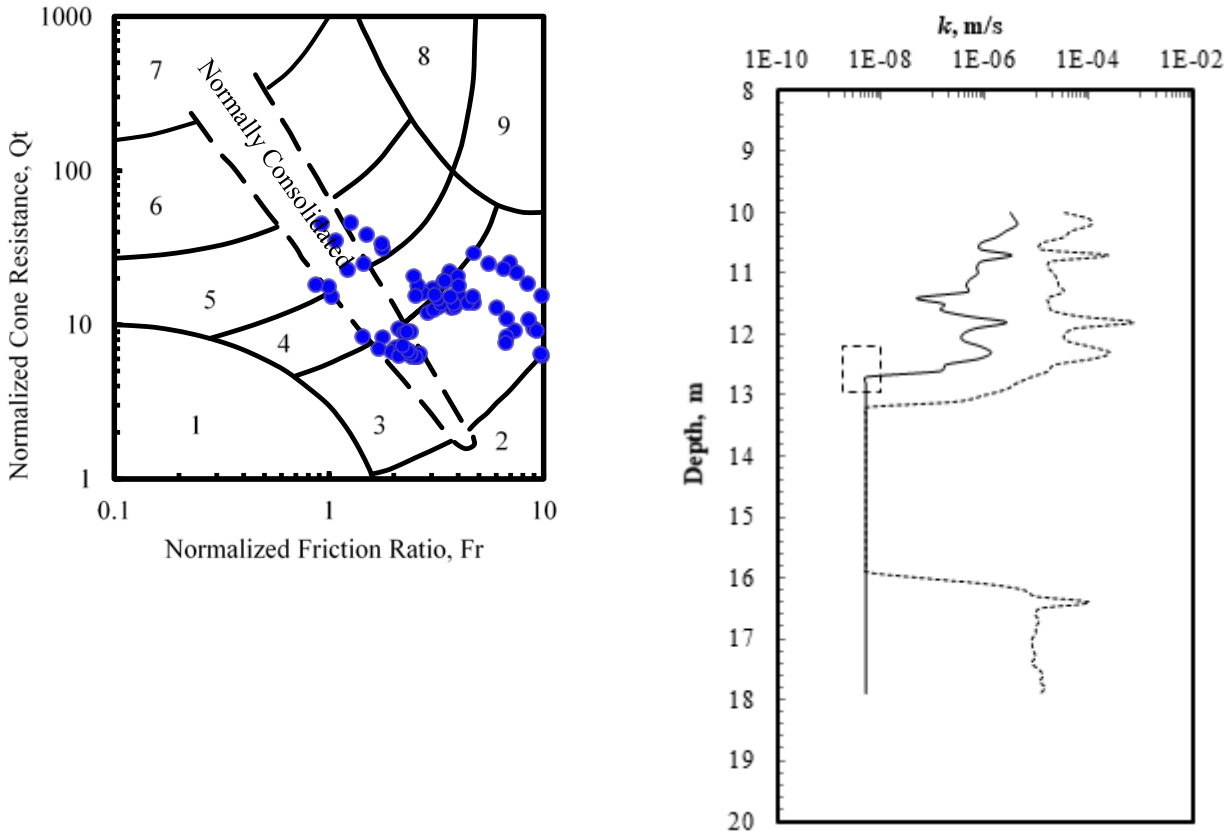

(a) (b)

Fig. 4.10 (a) SBTn classification and range of hydraulic conductivity (b) Estimated hydraulic property profile with depth for Frazer River (data obtained from Kaya Engineering Co. 2007)

4.4 Hydraulic Conductivity Determination Program

A goal in this project for the implementation of the correction factors is to code a spread sheet that allows NDOT engineers and field employees to easily apply the correction factors to the PCPT output to obtain a continuous hydraulic conductivity profile. This program should be simple to use for anybody with access to the PCPT output and the values for a few assumed parameters. This section details the progress made in "version 1" of the program, which will serve as a foundation for smoother and more capable future versions.

4.4.1 Program Development (Version 1)

This program was developed using Excel's built in language, Visual Basic for Applications (VBA). This is a language developed by Microsoft to interface well with Excel. This language enables a spreadsheet to be coded with a more powerful version of the macros that are commonly found within a cell. For example, the spreadsheet can be designed to automatically perform a series of tasks or display a user form that provides a graphic user interface that is easier to operate than directly interacting with an Excel datasheet.

VBA works in conjunction with a standard Excel spreadsheet, which serves as the backbone of the program. Traditional macros are still used on the spreadsheet for the intermediate calculations required to obtain the correction factors. For the initial input, the user selects the data file from the PCPT instrument output using the user form and inputs a few assumed parameters. This Visual Basic component of the Excel document then uses this information to provide a starting point for the standard Excel sheet containing macros. That sheet then runs the calculations to determine adjustment factors and determine a final hydraulic conductivity value. This can then be graphed and displayed on the user form. This functionality will be explained in more detail in the subsequent sections.

4.4.2 User Form

Visual Basic for Excel was used to allow for the input and interpretation of data obtained from PCPT testing. Because the method relies on a few assumed variables, the program's user form has text boxes to input the depth of the groundwater table, internal friction angle phi, and recompression index C_r. The goal of this program is to accept input of the output from the PCPT device, which will be in the format of an excel file—specifically .CSV. Additionally, it will accept

the user's input of our method's assumed parameters: Ground water table depth, ϕ, and C_r. These inputs will take place on the program's user form, which is shown in Fig. 4.11.

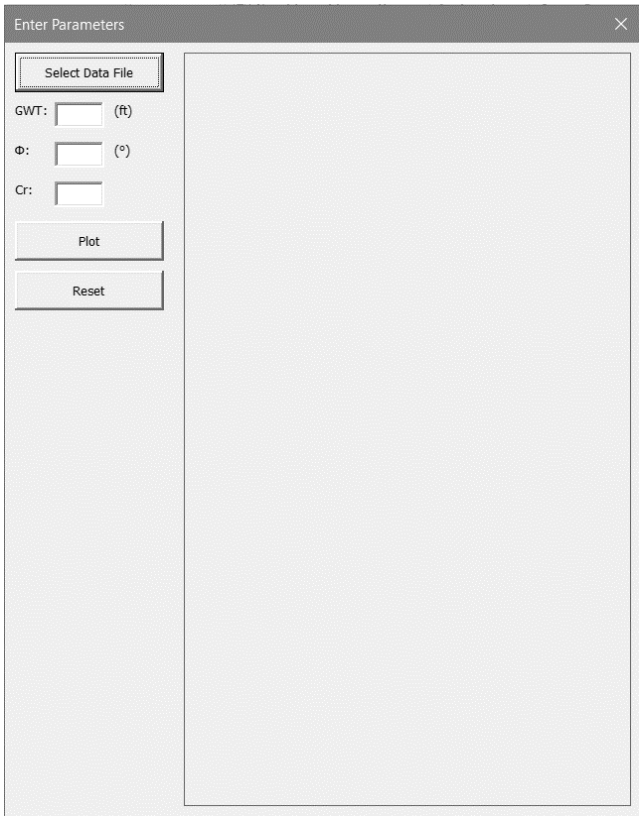

.

Fig. 4.11. VBA user form

When the "Select Data File" button is selected, a window pops up that allows the user to select the .CSV (or other Excel file type) from their computer that contains the PCPT output. This window should look familiar, and is shown in Fig. 4.12. Currently, the order of the columns in the source must be in the standard H, q_c, f_s, and u_2 order from left to right. These columns are copied from the source and pasted into the program's worksheet. When copying the data, the program moves downward along these first four columns until it finds an empty row. This allows the program to be used for any depth. These first four columns copied from the source are shown to the left of the

red line on Fig. 4.13, and the intermediate calculations are performed to the right of the red line using macros embedded in the cells.

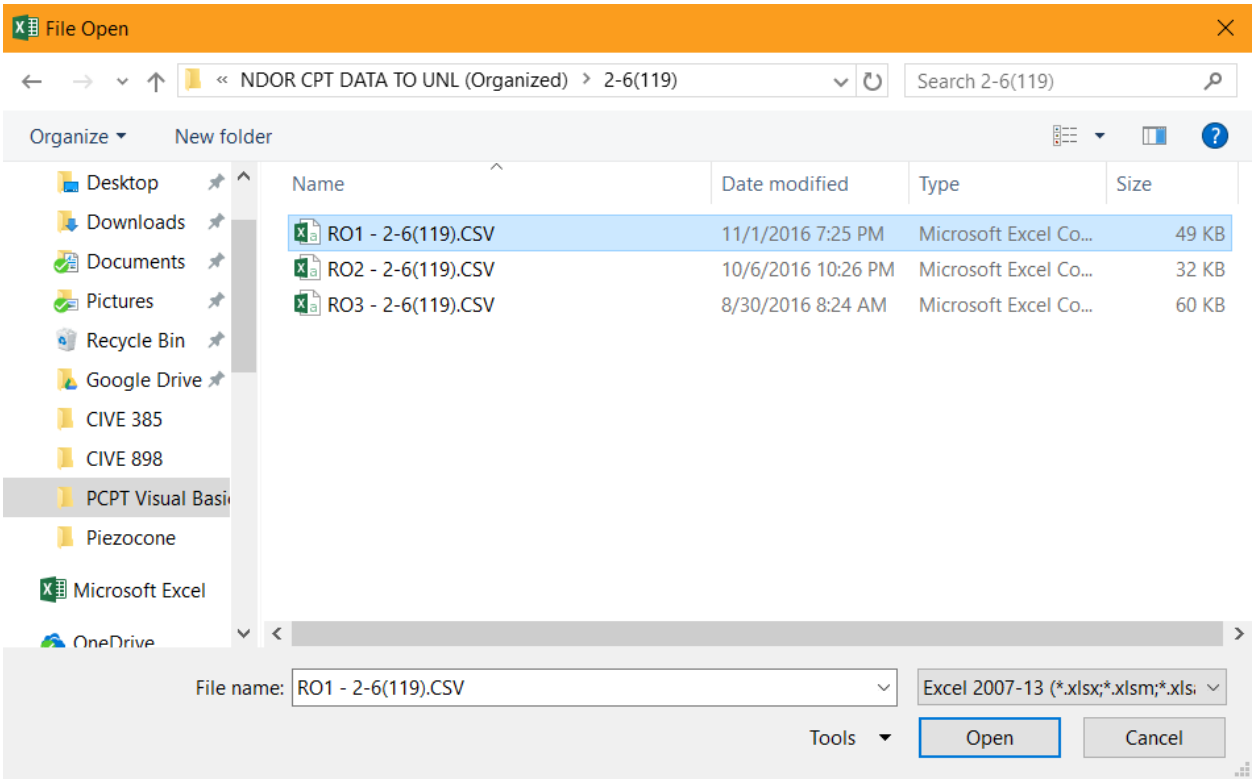

Fig. 4.12. User selection of PCPT

Referring again to **Error! Reference source not found.** 4.14, the GWT depth, ϕ', and C_r are typed into textboxes in the user interface. While the correction factors developed in this research use GWT depth in meters, M instead of ϕ', and κ instead of C_r, the input units on the user form were chosen because they are more commonly used in industry practice. The user's inputs are immediately converted to GWT depth in meters, M, and κ so that the equations developed in this research can be directly used. Once these inputs are included in the intermediate calculations, the final adjusted hydraulic conductivity profile has been determined. This profile is subsequently plotted for the user when they select the "Plot" button on the user form. Currently there are bugs

in the functionality of this element, but an edited image of the plotted output that will be available in version 2 of the program is depicted in Fig. 4.14.

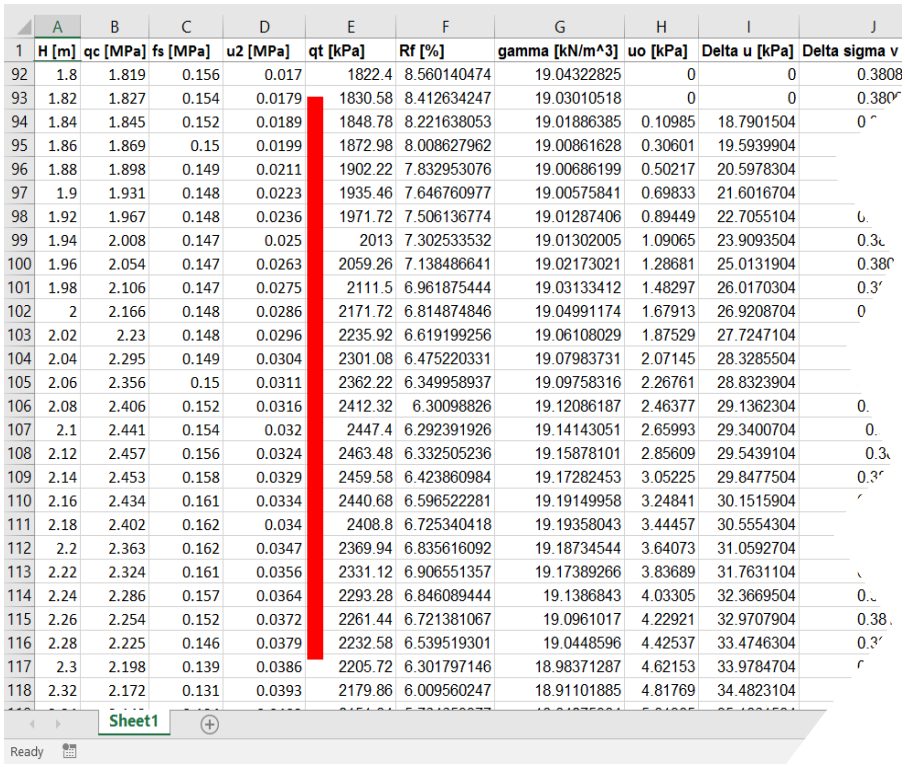

	A	B	C	D	E	F	G	H	I	J
1	H [m]	qc [MPa]	fs [MPa]	u2 [MPa]	qt [kPa]	Rf [%]	gamma [kN/m^3]	uo [kPa]	Delta u [kPa]	Delta sigma v
92	1.8	1.819	0.156	0.017	1822.4	8.560140474	19.04322825	0	0	0.3808
93	1.82	1.827	0.154	0.0179	1830.58	8.412634247	19.03010518	0	0	0.380
94	1.84	1.845	0.152	0.0189	1848.78	8.221638053	19.01886385	0.10985	18.7901504	0
95	1.86	1.869	0.15	0.0199	1872.98	8.008627962	19.00861628	0.30601	19.5939904	
96	1.88	1.898	0.149	0.0211	1902.22	7.832953076	19.00686199	0.50217	20.5978304	
97	1.9	1.931	0.148	0.0223	1935.46	7.646760977	19.00575841	0.69833	21.6016704	
98	1.92	1.967	0.148	0.0236	1971.72	7.506136774	19.01287406	0.89449	22.7055104	0.
99	1.94	2.008	0.147	0.025	2013	7.302533532	19.01302005	1.09065	23.9093504	0.3
100	1.96	2.054	0.147	0.0263	2059.26	7.138486641	19.02173021	1.28681	25.0131904	0.380
101	1.98	2.106	0.147	0.0275	2111.5	6.961875444	19.03133412	1.48297	26.0170304	0.3
102	2	2.166	0.148	0.0286	2171.72	6.814874846	19.04991174	1.67913	26.9208704	0
103	2.02	2.23	0.148	0.0296	2235.92	6.619199256	19.06108029	1.87529	27.7247104	
104	2.04	2.295	0.149	0.0304	2301.08	6.475220331	19.07983731	2.07145	28.3285504	
105	2.06	2.356	0.15	0.0311	2362.22	6.349958937	19.09758316	2.26761	28.8323904	
106	2.08	2.406	0.152	0.0316	2412.32	6.30098826	19.12086187	2.46377	29.1362304	0.
107	2.1	2.441	0.154	0.032	2447.4	6.292391926	19.14143051	2.65993	29.3400704	0.
108	2.12	2.457	0.156	0.0324	2463.48	6.332505236	19.15878101	2.85609	29.5439104	0.3
109	2.14	2.453	0.158	0.0329	2459.58	6.423860984	19.17282453	3.05225	29.8477504	0.3
110	2.16	2.434	0.161	0.0334	2440.68	6.596522281	19.19149958	3.24841	30.1515904	
111	2.18	2.402	0.162	0.034	2408.8	6.725340418	19.19358043	3.44457	30.5554304	
112	2.2	2.363	0.162	0.0347	2369.94	6.835616092	19.18734544	3.64073	31.0592704	
113	2.22	2.324	0.161	0.0356	2331.12	6.906551357	19.17389266	3.83689	31.7631104	
114	2.24	2.286	0.157	0.0364	2293.28	6.846089444	19.1386843	4.03305	32.3669504	0.
115	2.26	2.254	0.152	0.0372	2261.44	6.721381067	19.0961017	4.22921	32.9707904	0.38
116	2.28	2.225	0.146	0.0379	2232.58	6.539519301	19.0448596	4.42537	33.4746304	0.3
117	2.3	2.198	0.139	0.0386	2205.72	6.301797146	18.98371287	4.62153	33.9784704	
118	2.32	2.172	0.131	0.0393	2179.86	6.009560247	18.91101885	4.81769	34.4823104	

Sheet1

Ready

Fig. 4.13. Background

The reset button on the user form deletes the GWT, phi, and C_r values from the spreadsheet, along with the four columns imported from the PCPT readings.

4.4.3 Future Capabilities

Ideally, the code will become more generalized. As mentioned order, the columns from the PCPT source data must be in the order of H, q_c, f_s, and u_2. While this suits the current output style of NDOT's PCPT system, it will be better if the system can adapt to other configurations. For instance, if new equipment is purchased that does not have the same output order, the program should be able to detect a different order and copy the source data accordingly.

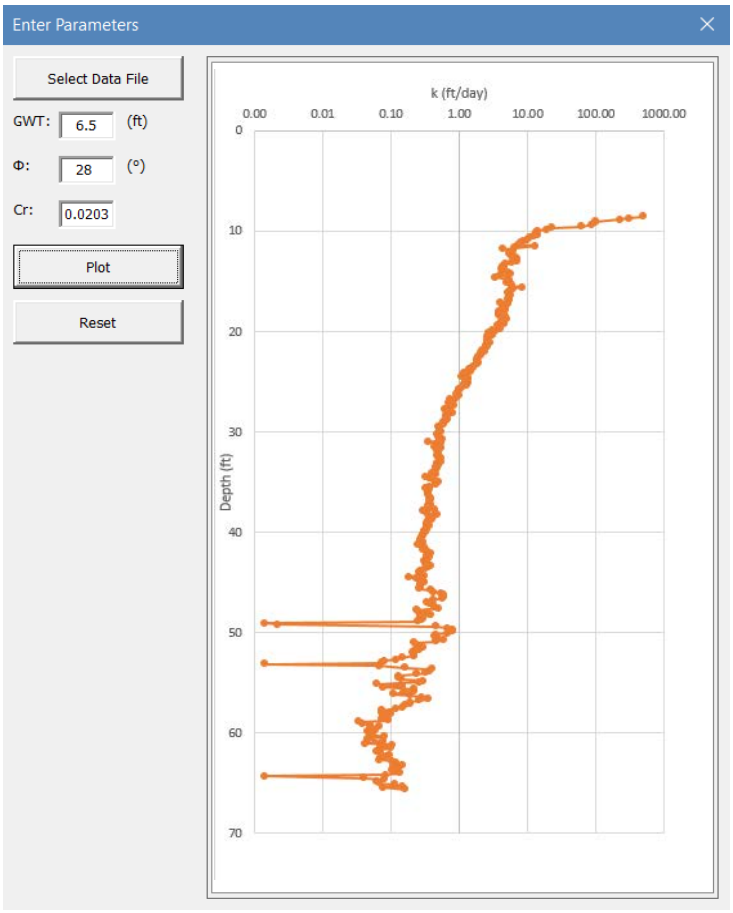

Fig. 4.14. Modified image of user form to display correct plot

The spreadsheet will be hidden from view of the users in future versions so that the program will be simpler. The calculations that occur on the spreadsheet will be able to occur in the background so that the user only needs to interact with the user form. This will also prevent the user from accidentally altering the spreadsheet which would cause errors in the system.

While the adjustment factors do require assumptions for GWT depth, M, and κ, these aren't simple parameters to estimate. Therefore, it may be wise to incorporate preset values for these into the program's user interface. For instance, there might be an eastern Nebraska option from a drop-down menu that will use a typical value for the region if those inputs cannot be easily estimated.

To allow this to be more customizable, the user might even be able to create their own presets within the user interface so that NDOT engineers can dynamically change the program's assumed parameters to suit regions with data collected after the completion of this project. To further simplify the process of choosing these assumed values, methods might be able to be borrowed from previous scholarly works that draw correlations between values determined from PCPT and estimated values for M and κ.

The reset button currently deletes the values from the spreadsheet, but it will not clear the plot unless the plot button is pressed again. Because the spreadsheet will be running in the background, it is important that the user form will accurately reflect the changes made on the spreadsheet. The input units are in customary units for industry use, but it might be helpful for the user to be able to toggle between units if necessary.

While the current progress provides a foundation for future development, more work is needed to refine the user experience. Additionally, the code should be more thoroughly commented for future edits if necessary. The final version of the code is planned to be an easy to use, standalone, and bug free software that NDOT can count on to reliably convert PCPT output to a continuous hydraulic conductivity profile.

5 IMPROVED CORRELATION BETWEEN ADJUSTMENT FACTORS AND SBTn PARAMETERS

5.1 General

In this chapter, further investigation and slight modification has been done on the previously established correlation. This modification was attained by expanding the already proposed correlation using the basic definition of SBTn parameters. This way, it was found out that the proposed non-dimensional factor N^* was dependent on skin friction and excess pore pressure alone without the effect of cone tip resistance. Despite this, an appreciable result has been obtained by considering the effect of skin friction and excess pore pressure through the existing correlation as demonstrated in the previous quarterly reports.

However, some literatures (e. g. Lunne et al. 1986a) already pointed out the non-reliability and non-repeatability of skin friction as compared to cone tip resistance when it is used as a parameter to estimate soil properties. Thus, a newly modified non-dimensional factor which is a function of cone tip resistance and excess pore pressure was proposed and its correlation with the required adjustment factors was investigated in this chapter. The newly proposed correlation along with the previously established one were used to evaluate hydraulic conductivities of Nebraskan soils as well as some other sites located in Korea, Canada and USA. The derivation and evaluation of adjustment equation based on skin friction (previous) and cone tip resistance (updated) is discussed in the following sections. Adjustment factors and correction factors are used interchangeably in this report and they refer to the same thing.

5.2 Previously Established Relationship

In the previous report, the relationship between SBTn parameters and the non-dimensional parameter *N* was given by:

$$C = \frac{Q_t}{F_r} B_q^{\ 2} \tag{5.1}$$

where *N** is modified non-dimensional factor; Q_t, F_r, B_q = normalized cone resistance, friction ratio, and pore pressure ratio respectively. A single trend line that encompasses data sets consisting of negative and positive B_q has been proposed after plotting variation of *N** with adjustment factor *C*. The proposed trendline is shown in Fig. 5.1 below.

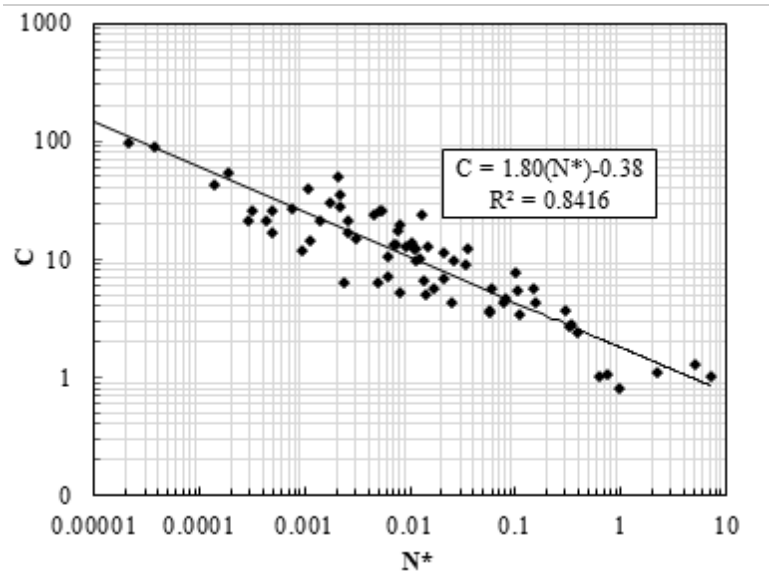

Fig. 5.1. C vs N* incorporating both negative and positive Bq

From Fig. 4.1, the modified adjustment equation based on N* was given as:

$$C = 1.80 N^{-0.38} \tag{5.2}$$

5.3 Improved Interpretation of Non-Dimensional Parameter

The adjustment factors which are intended to be a function of SBTn parameters can be rewritten using the mathematical expression given in [Eq. (5.3)]. The expression shown in the right-hand side of [Eq. (5.3)] is same as the expression shown in the right-hand side of [Eq. (5.1)] above, except the numerator and denominators are flipped. In this way, the relationship between the adjustment factor and non-dimensional parameter will be direct rather than an inverse relation like the one shown in Fig. 5.1.

$$N = \frac{F_r}{Q_t B_q{}^2} \tag{5.3}$$

The respective definition of the SBTn parameters in terms of PCPT parameters directly acquired from the test can be expressed by the following equations.

$$Q_t = \frac{q_t - \sigma_{vo}}{\sigma'_{vo}} \qquad F_r = \frac{f_s}{q_t - \sigma_{vo}} \text{x100\%} \qquad B_q = \frac{u_2 - u_o}{q_t - \sigma_{vo}} \tag{5.4}$$

Substitution of the corresponding definitions of Q_t, F_r, and B_q shown in [Eq. (4.4)] into [Eq. (4.3)] yields the following equation and designated as N_s:

$$N_s = \frac{f_s}{(\Delta u_2)^2} \sigma'_{vo} \text{ x 100\%} \tag{5.5}$$

where $N_s = N$; f_s = sleeve friction; Δu = excess pore pressure at u_2 position; and σ'_{vo} = in-situ effective overburden pressure. From [Eq. (5.5)], N_s is directly proportional to sleeve friction and effective overburden pressure, while it is inversely proportional to the square of measured excess pore pressure. When measured sleeve friction is high which is typical in cases of overconsolidated

and cemented soils, the value of required adjustment factor will be higher too. Similarly, when measured excess pore pressure is lower, a required adjustment factor value will be higher. However, in literature, it is stated that sleeve friction is the less repeatable and reliable among parameters obtained from PCPT (e.g. Lunne et al. 1986a). Thus, it was intended to substitute sleeve friction in [Eq. (5.5)] by net cone tip resistance ($q_t - \sigma_{vo}$) as shown in [Eq. (5.6)].

$$N_c = \frac{(q_t - \sigma_{vo})}{(\Delta u_2)^2}\sigma'_{vo} \tag{4.6}$$

where N_c = modified N based on net cone tip resistance. The substitution of net cone tip resistance yielded a parameter that resembles the factors that were used in (Campanella and Robertson 1981; Tumay et al. 1982) for profiling OCR from PCPT except the inclusion of effective overburden pressure and squaring of measured excess pore pressure to accommodate negative excess pore pressures. Backward assembly of [Eq. (5.6)] into an equivalent expression in terms of piezocone indices produced the equation shown below in [Eq. (5.7)]:

$$N_c = \frac{1}{Q_t B_q^{\ 2}} \tag{4.7}$$

[Eq. (5.7)] is similar in form to the non-dimensional parameter that was used in (Elsworth and Lee 2005) to estimate permeability of soils on-the-fly except B_q is squared in [Eq. (5.7)]. In subsequent discussions, both N_s and N_c were used to estimate required correction factor C and relative accuracy of these approaches in estimating hydraulic conductivity of overconsolidated soils was examined.

5.4 Results and Interpretation

Two sets of computed *C* and *N* based on PCPT data and oedometer data provided by NDOT were plotted to determine the correlation that exists between *C* and *N*. Fig. 5.2 [a & b] show C versus N plots on a full log scale for *N* computed based on [Eq. (5.5) and (5.6)] respectively.

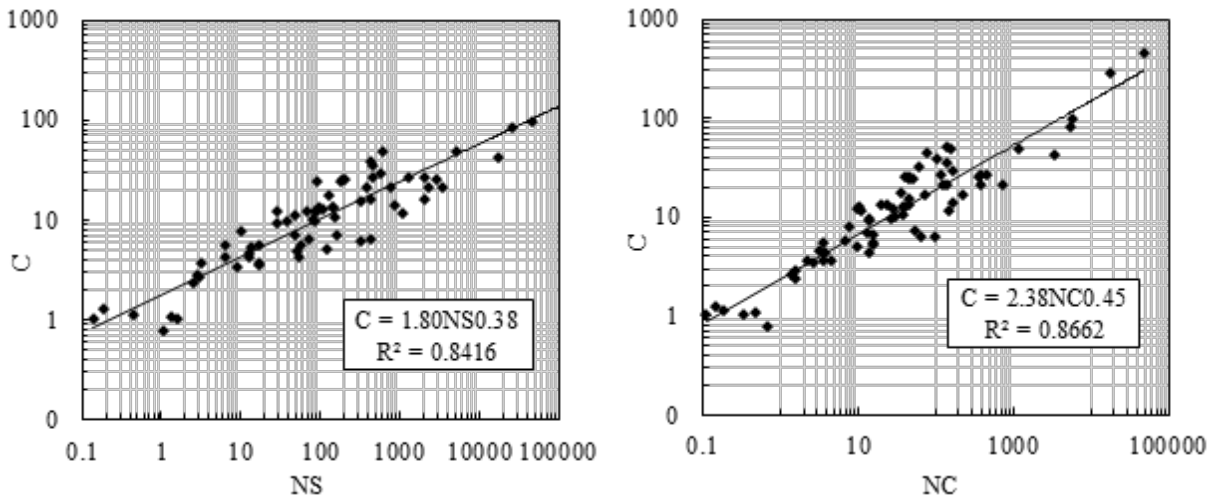

(a) (b)

Fig. 5.2. Correlation between *C* and *N* (a) based on sleeve friction (b) based on cone resistance

From Fig. 5.2 (a) & (b), it is shown that the lower bound for the correction factor, *C* is around unity, which indicates there is no need to apply correction to the measured excess pore pressure. The relationship of *C* with N_s and N_c can be expressed by the following two equations:

$$C = 1.80 N_S^{0.38} \tag{5.8}$$

$$C = 2.38 N_C^{0.45} \tag{5.9}$$

The correlations express the relationship between *C* and N_s and N_c for about 84 % and 87 % of the data set respectively, which can be considered as satisfactory. Once adjustment factors are obtained on the fly using either [Eq. (5.8) or (5.9)], adjusted excess pore pressure can be estimated using the following equation.

$$\Delta u_{adjusted} = \left| C.\Delta u_{measured} \right| \tag{5.10}$$

Then, adjusted excess pore pressure from [Eq. (5.10)] can be introduced into the equation of Song and Pulijala to give adjusted hydraulic conductivity. The modified Song and Pulijala equation after the incorporation of adjusted excess pore pressure will have the following form.

$$k_{adjusted} = \left[\frac{\frac{f(\mathrm{M},\kappa)}{\Delta u_{adjusted}} - 1}{282{,}095.22} \right]^{1.0564} \tag{5.11}$$

where $k_{adjusted}$ = adjusted hydraulic conductivity; $\Delta u_{adjusted}$ = adjusted excess pore pressure. It should be noted that $\Delta u_{measured}$ is obtained by subtracting the hydrostatic pore pressure from the measured u_2 pore pressure.

Fig. 5.3 shows computed hydraulic conductivity for six sites (project names are indicated in the top right corner of each plot) using the modified (adjusted) and unmodified Song and Pulijala equations. Laboratory determined κ and M = 1.20 are used to determine hydraulic conductivity on the fly from the unmodified and modified equations. Dotted rectangular plots in this figure show the range of hydraulic conductivity determined from oedometer test. Corrected hydraulic conductivity profiles from modified Song and Pulijala equation show some cut off boundaries at lower hydraulic conductivities. These boundaries are imposed in MS-Excel when $\frac{f(\mathrm{M},\kappa)}{\Delta u_{adjusted}}$,which is shown in [Eq. (4.11) above] is less than unity. This boundary hydraulic conductivity is 5 x 10^{-9} m/s which will designate the hydraulic conductivity of the soil is below it and cannot be specifically stated.

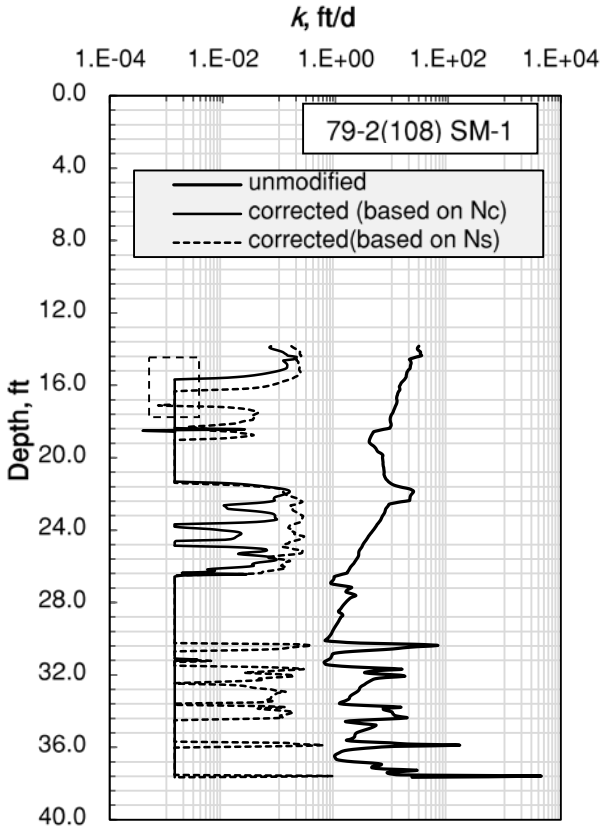
k, ft/d
1.E-04
1.E-02
1.E+00
1.E+02
1.E+04
79-2(108) SM-1
unmodified
corrected (based on Nc)
corrected(based on Ns)
Depth, ft
0.0
4.0
8.0
12.0
16.0
20.0
24.0
28.0
32.0
36.0
40.0

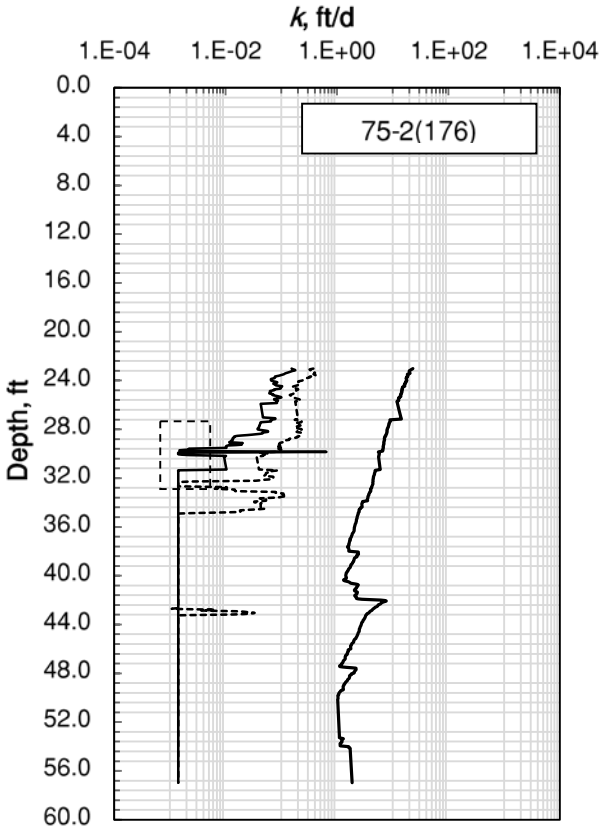
k, ft/d
1.E-04
1.E-02
1.E+00
1.E+02
1.E+04
75-2(176)
Depth, ft
0.0
4.0
8.0
12.0
16.0
20.0
24.0
28.0
32.0
36.0
40.0
44.0
48.0
52.0
56.0
60.0

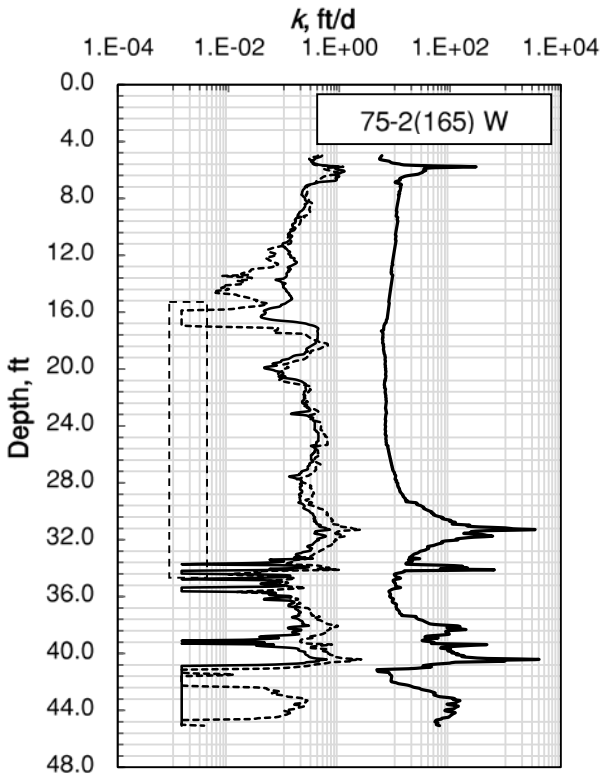
k, ft/d
1.E-04
1.E-02
1.E+00
1.E+02
1.E+04
75-2(165) W
Depth, ft
0.0
4.0
8.0
12.0
16.0
20.0
24.0
28.0
32.0
36.0
40.0
44.0
48.0

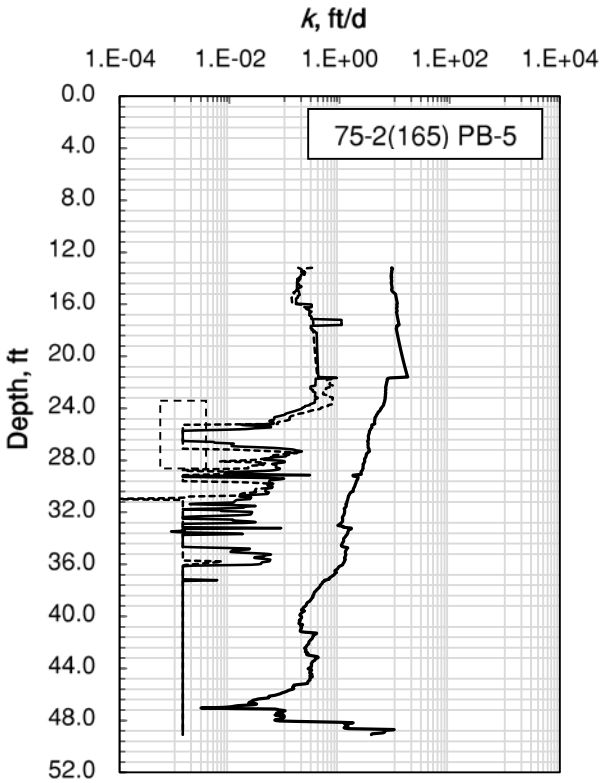
k, ft/d
1.E-04
1.E-02
1.E+00
1.E+02
1.E+04
75-2(165) PB-5
Depth, ft
0.0
4.0
8.0
12.0
16.0
20.0
24.0
28.0
32.0
36.0
40.0
44.0
48.0
52.0

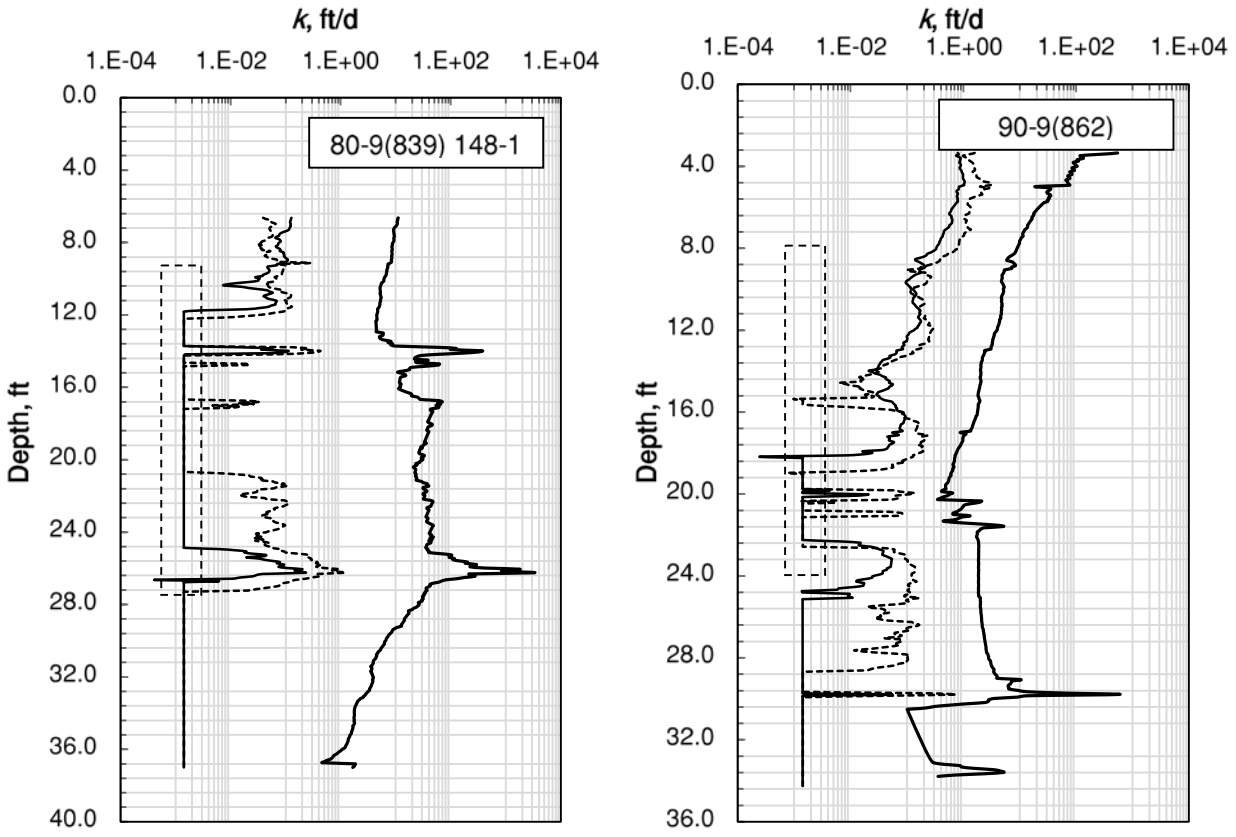

Fig. 5.3 Hydraulic conductivity estimated from modified Song and Pulijala (2010)

Hydraulic conductivity estimated by applying adjustment factors based on sleeve friction (N_s) and net cone tip resistance (N_c) have demonstrated similar patterns in Fig. 4.3. However, given the non-repeatability of sleeve friction and better coefficient of determination for the C-N_c correlation, correction factors determined from net cone tip resistance and excess pore pressure are more likely reliable. Furthermore, supremacy of cone tip resistance based prediction of hydraulic conductivity has been attested in some of the plots in Fig. 4.3. Therefore, following discussion will be restricted to C-N_c correlations.

5.5 Verification with other Test data

Some sites from Korea, Canada, and the US are selected and the same equation used for the prediction of hydraulic conductivity of overconsolidated soils in Nebraska is applied to PCPT data collected at these sites to verify the applicability of the equation to soil profiles found outside Nebraska.

5.5.1 Yangsan Mulgeum, Korea (Dong A Geology 1997)

This site is the old delta area of the Nakdong River. The soils are primarily young alluvial deposits. The layers of this area's profile starting from the surface consist of clayey and silty fill materials followed by sedimentary layers consisting of clay, silty sand, silty clay, silt, sand, and gravel. Pore pressure dissipation testing using PCPT shows the coefficient of consolidation is (2-6) $\times 10^{-7}$ m^2/sec. Based on Robertson (2010), the projection of PCPT result of this site shows that the soil is classified as silty clay to sandy silt with corresponding hydraulic conductivity ranging from 3 x 10^{-9} m/s to 1 x 10^{-5} m/s, as shown in Fig. 5.4(a). The ground water table is reported to be at a depth of 1 m. From Fig. 5.4(a), the data points lean to the sensitive fine-grained soils. Some data points are also inside the normally consolidated soils zone. In Fig. 5.4(b), the estimated hydraulic conductivity shows good agreement with the measured hydraulic conductivity (indicated by the rectangular dotted plot) at 15 m (50 ft.) below ground surface. Additionally, the estimated hydraulic conductivity is slightly to the right (i.e. more permeable) of the measured hydraulic conductivity. This can be considered reliable considering coefficient of consolidation from field performance is generally larger than laboratory test results (Robertson et al. 1992); the difference being a function of sensitivity and soil structure. Moreover, the uncorrected and adjusted

(corrected) hydraulic conductivity profiles are close to each other indicating the soil profile is normally consolidated.

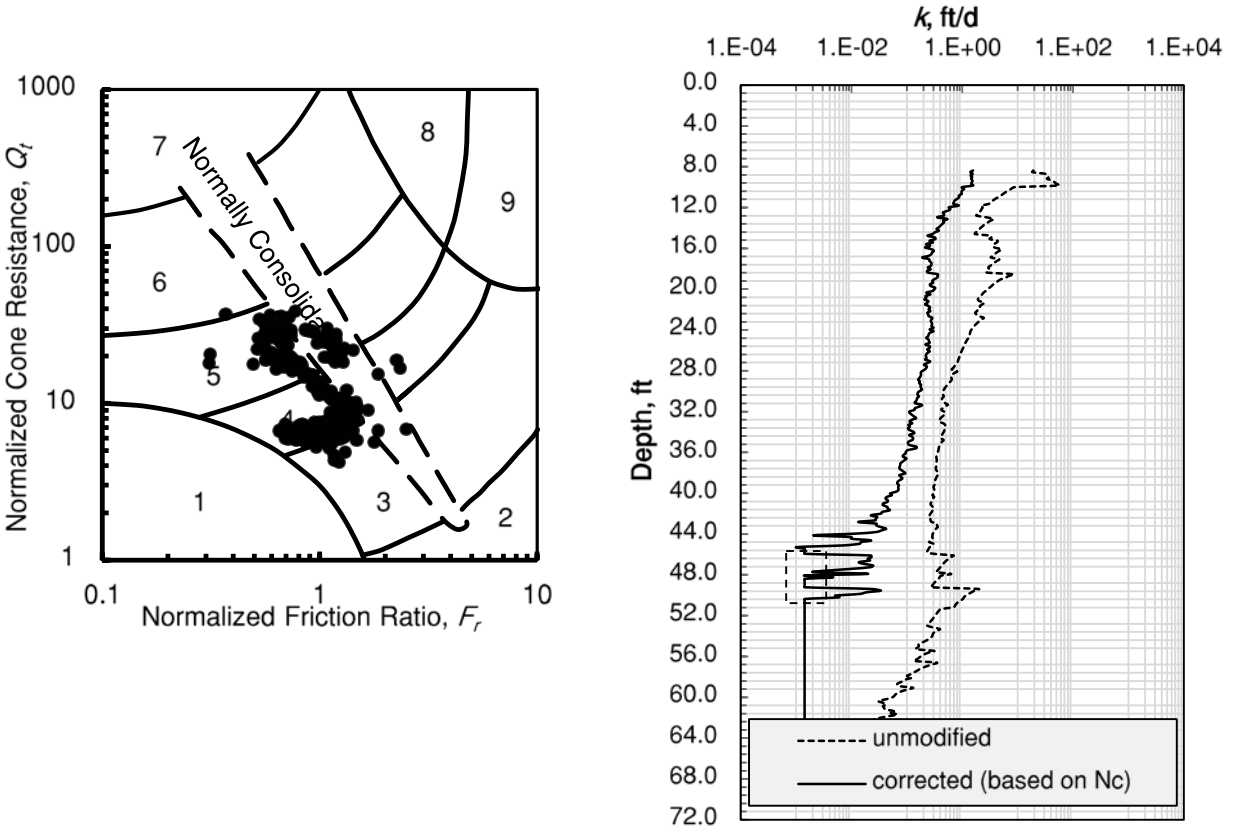

(a) (b)

Fig. 5.4. (a) SBTn classification (b) Estimated hydraulic property profile with depth for Yangsan Mulgeum, Korea (Data obtained from Dong A. Geology 1997)

5.5.2 Frazer River, Canada (Crawford and Campanella 1991)

The area is located about 25 km southeast of Vancouver on Highway 99. The surface of this area is mostly flood plain, and the stratigraphy of the ground shows inter-bedded sand seams and peat layers. The subsurface soils are relatively uniform with a natural water content of about 45% and a liquid limit about 36%. From consolidation test results, the range of coefficients of compressibility are 0.3-0.5, initial void ratios are 1.1-1.8, vertical coefficients of consolidation are (0.6-2.8) × 10^{-7} m^2/s, horizontal coefficients of consolidation are (0.7-7) × 10^{-7} m^2/s, constrained

moduli are 1,800-4,000 kPa, and permeability (0.8-1.2) × 10^{-9} m/s. The soil in the site is reported to be slightly overconsolidated to normally consolidated. In addition, from vane shear test results, it is reported that the soil shows high sensitivity in deeper depths. The ground water table is reported to be close to the ground surface. Based on Robertson (2010), the projection of PCPT result of this site shows that the soil is classified as silty clay to clayey silt with a hydraulic conductivity range from 3 x 10^{-9} m/s to 1 x 10^{-7} m/s Fig. 5.5(a).

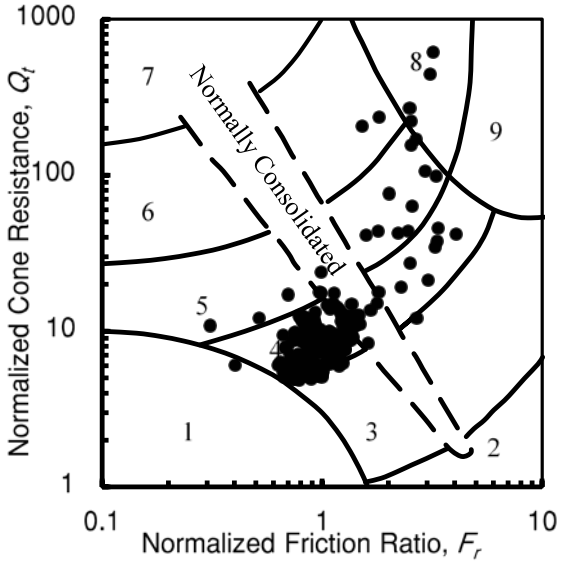

(a)

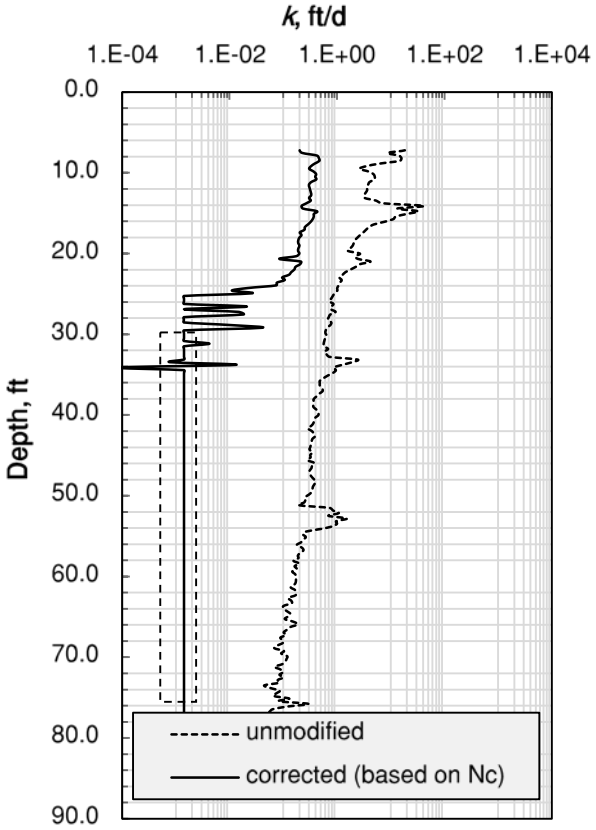

(b)

Fig. 5.5(a) SBTn classification (b) Estimated hydraulic property profile with depth for Frazer River (data obtained from Crawford and Campanella 1991)

The results in Fig. 5.5(a) shows that the soils are slightly sensitive, and some data points are scattered in the normally consolidated, slightly to very stiff sands and clayey soil zones, which are generally quite consistent with the reported nature of the soils (i.e. sensitive, normally consolidated to slightly overconsolidated). The hydraulic conductivity estimated from the modified Song and

Pulijala equation is quite close to the measured hydraulic conductivity (see Fig. 5.5(b)). Corrected and uncorrected hydraulic conductivities are closer in the shallower depths, which might imply the existence of normally consolidated soils, though there is significant deviation at deeper depths. This might be due to increased sensitivity implying lower hydraulic conductivity as observed in Robertson (2010). Moreover, corrected hydraulic conductivity ranges match those proposed by Robertson (2010) for zone 4 soils.

5.5.3 Cheongna (Section 1), Incheon, Korea (Kaya Engineering Co. 2007)

This area consists of overconsolidated soil in the upper layer and normally consolidated soil in the lower layer. Typical geotechnical properties show that the total unit weight is 1.57-1.95 t/m^3, liquid limit is 30-50%, natural water content is 20-40%, classification is CL, vertical coefficient of consolidation is (1-10) × 10^{-7} m^2/sec, horizontal coefficient of consolidation is (3-50) × 10^{-7} m^2/sec, coefficient of compressibility is 0.2-0.4, the depth of the soft layer is about 10 m, hydraulic conductivity is (4.82- 89.6) x 10^{-8} m/s, and OCR is 0.62-5.50. The soil in this area primarily falls under zones 3, 4, and 5. Data points in these zones are designated as clay to silty clay soils.

The hydraulic conductivity for these zones based on the SBTn chart ranges from 10^{-10} m/s to 10^{-7} m/s. Referring to Fig. 5.6(a), most of the data points are in the overconsolidated soils zones. The scattered data points also show some layers are normally consolidated and somewhat sensitive. Applying proper correction, the estimated hydraulic conductivity shows good agreement with the reported hydraulic conductivity of this area at the depth shown by the dotted rectangular plot in Fig. 5.6(b).

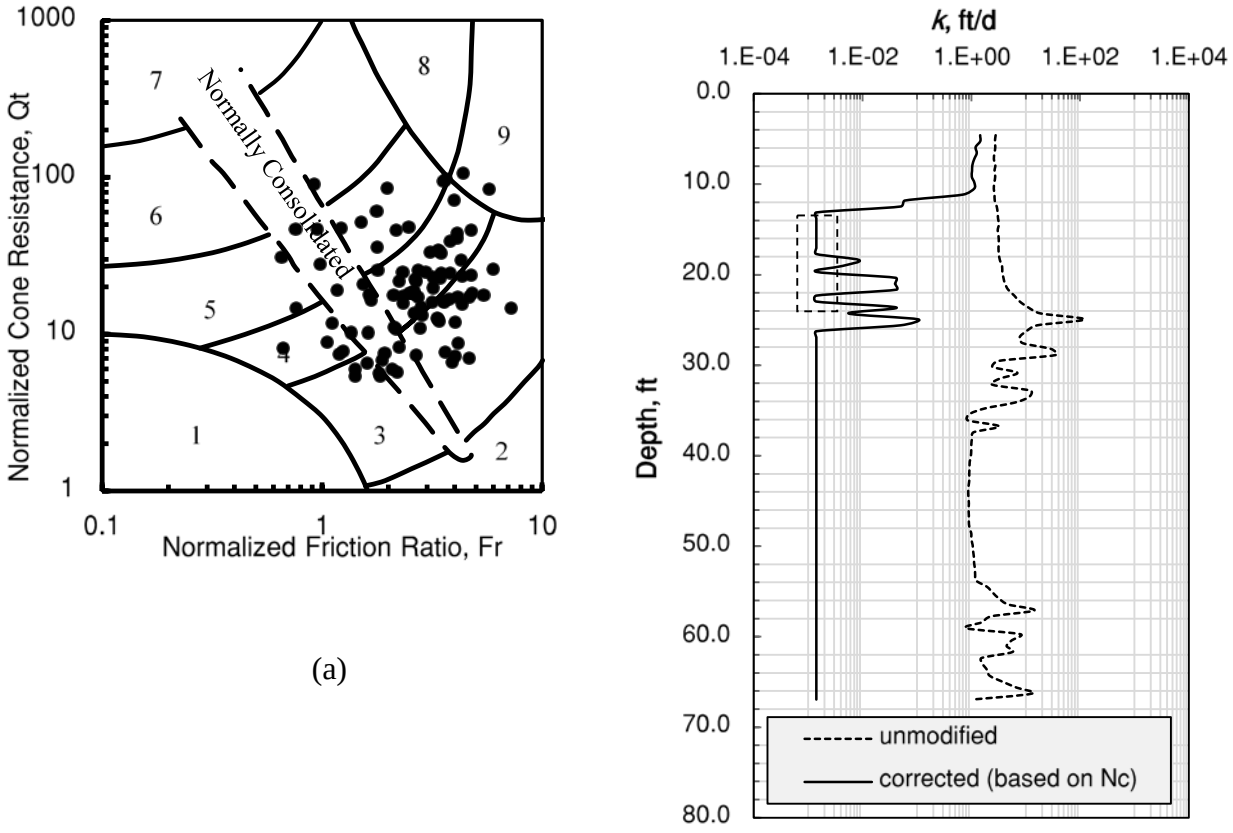

(a)

(b)

Fig. 5.6. (a) SBTn classification (b) Estimated hydraulic property profile with depth for Cheongna, Incheon, Korea (data obtained from Kaya Engineering Co. 2007)

5.5.4 SR 49, Indiana, USA (Kim 2005)

The area lies on the #49 road in Jasper County, Indiana. The normally consolidated clayey silty layers exist up to 25 m deep from the ground surface, and the ground water table is located at a level of 3 m below the surface. The average coefficient of consolidation evaluated from consolidation tests was about 3.6×10^{-7} m^2/sec. Fig. 5.7(b) shows adjusted and unadjusted hydraulic conductivity plots. From the plot, estimated adjusted hydraulic conductivity is close to measured hydraulic conductivity enclosed by the dotted rectangular plot. The projection of PCPT result of this site into Robertson (2010) chart showed data points are scattered in the silty clay and clayey silt zones which is consistent with reported classification of the soil. Range of hydraulic

conductivity estimated by (20) closely matches with measured hydraulic conductivity at 12.8 m depth.

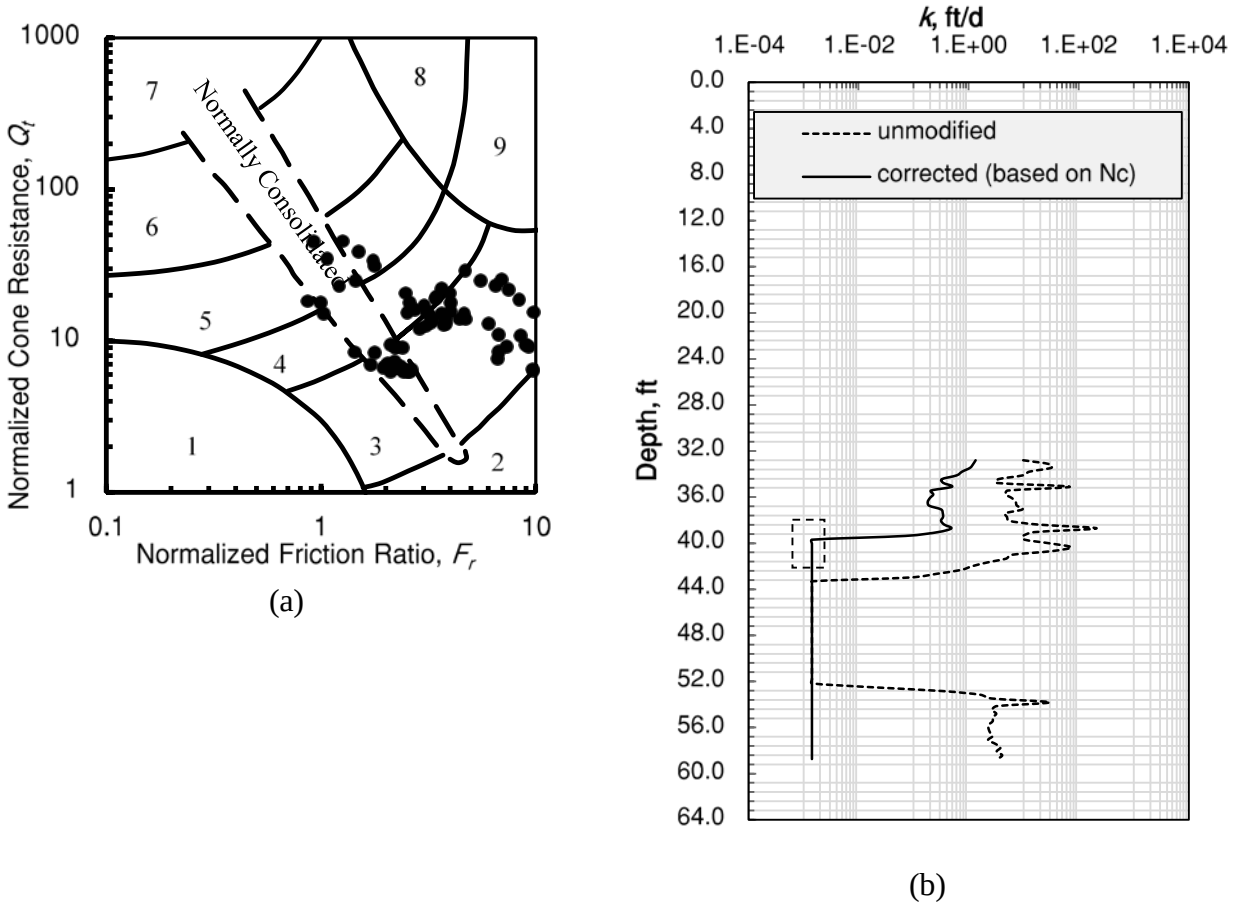

Fig. 5.7. (a) SBTn classification (b) Estimated hydraulic property profile with depth for SR 49, Indiana, USA (data obtained from Kim 2005)

6 PCPT DATA INTERPRETER USER GUIDE (VERSION 2)

The newest version of the program adds several improvements and conveniences to the original version. The previous version (in section 4.4) allows the user to extract information from PCPT output data files, input site specific conditions (GWT, average assumed friction angle, and recompression index), plot the hydraulic conductivity with depth according to this paper's correlation, and reset the form. The new version enables the user to change units between U.S. and Metric, toggle the correlation to be based on either tip resistance or sleeve friction (where the tip resistance correlation is typically more accurate), and export the chart to an excel sheet so that it can be manipulated or transferred to reports. The exported chart can express the entire depth of the data set on a single chart or break the data into up to four sections of 25 feet each (or meters if metric units are selected). The new version also includes a button to open a user manual which is built into the user form.

This program extracts the data output from piezocone penetration testing equipment and applies appropriate adjustments to plot a continuous hydraulic conductivity profile versus depth. The adjustments this program applies are consistent with those derived in this research concerning fast estimation of hydraulic conductivity for overconsolidated soils using piezocone test results.

If macros have not previously been enabled on the computer's installation of Excel, a security warning will be displayed which states "Macros have been disabled," with a button to the right allowing the user to "Enable Content" (Fig. 6.1). This button must be pressed for the program to begin. Alternatively, to avoid this step, the settings in Excel can be changed to allow macros to run automatically on startup. This is done using the following path: File > Options > Trust Center > Trust Center Settings > Macro Settings > Enable all macros. This is a global setting and will change

the settings of Excel as a whole, not just the PCPT program. This step is not necessary but recommended for convenience. It is important to note that if macros are not automatically enabled, the spreadsheet which normally runs in the background to execute necessary program functions can be edited, which if done and saved will result in the program no longer operating correctly.

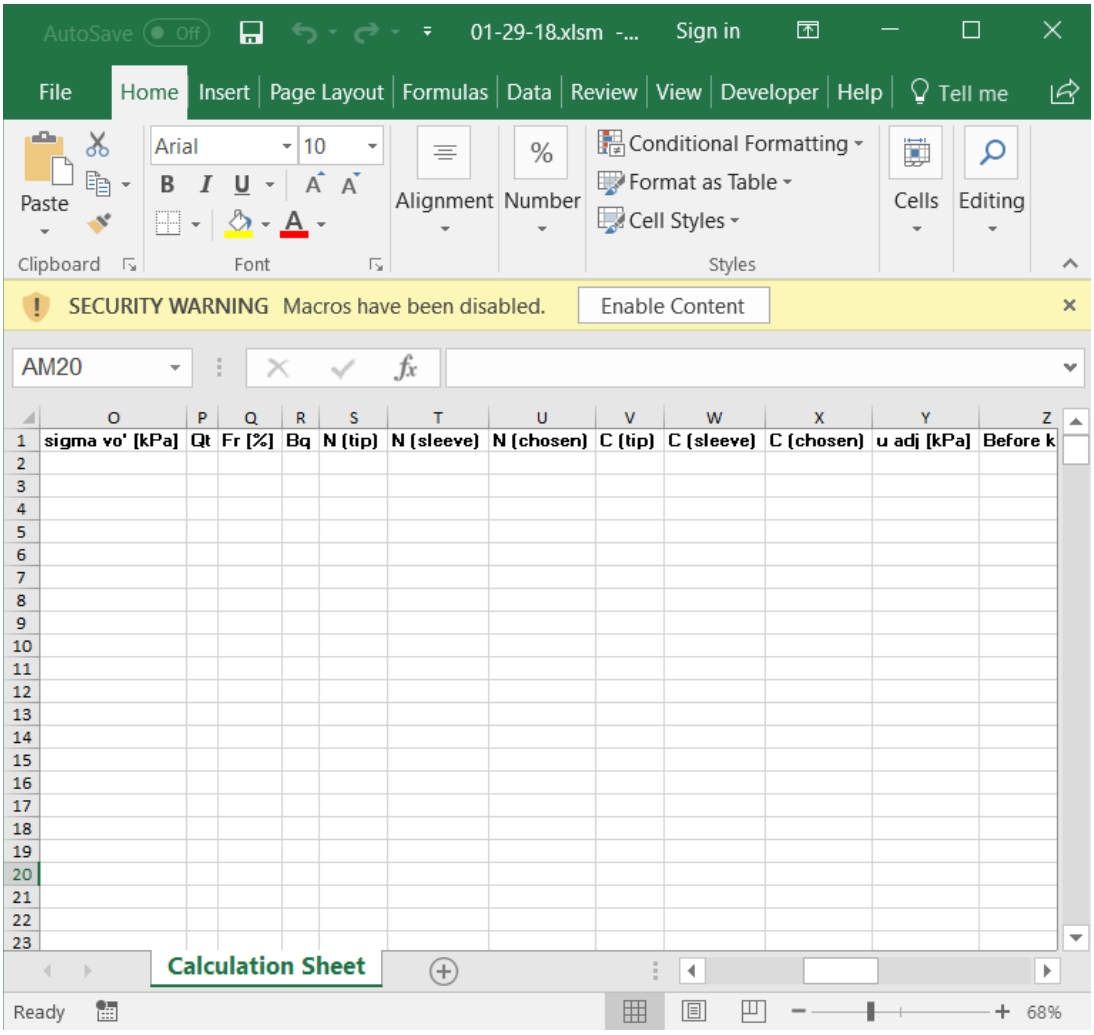

Fig. 6.1 Operating scree without macros enabled

The user form that is displayed on startup (Fig. 6.2) is the entire user interface for using the program—the user will never interact directly with the excel sheet which runs in the background. Once the user form appears on screen, “Select Data File” is clicked, which opens the PC’s file

explorer (Fig. 6.3) and allows for the selection of the piezocone's output ".CSV" data sheet (with columns A-D being H [m], qc [MPa], fs [MPa], and u2 [MPa], respectively, as shown in Fig. 6.4).

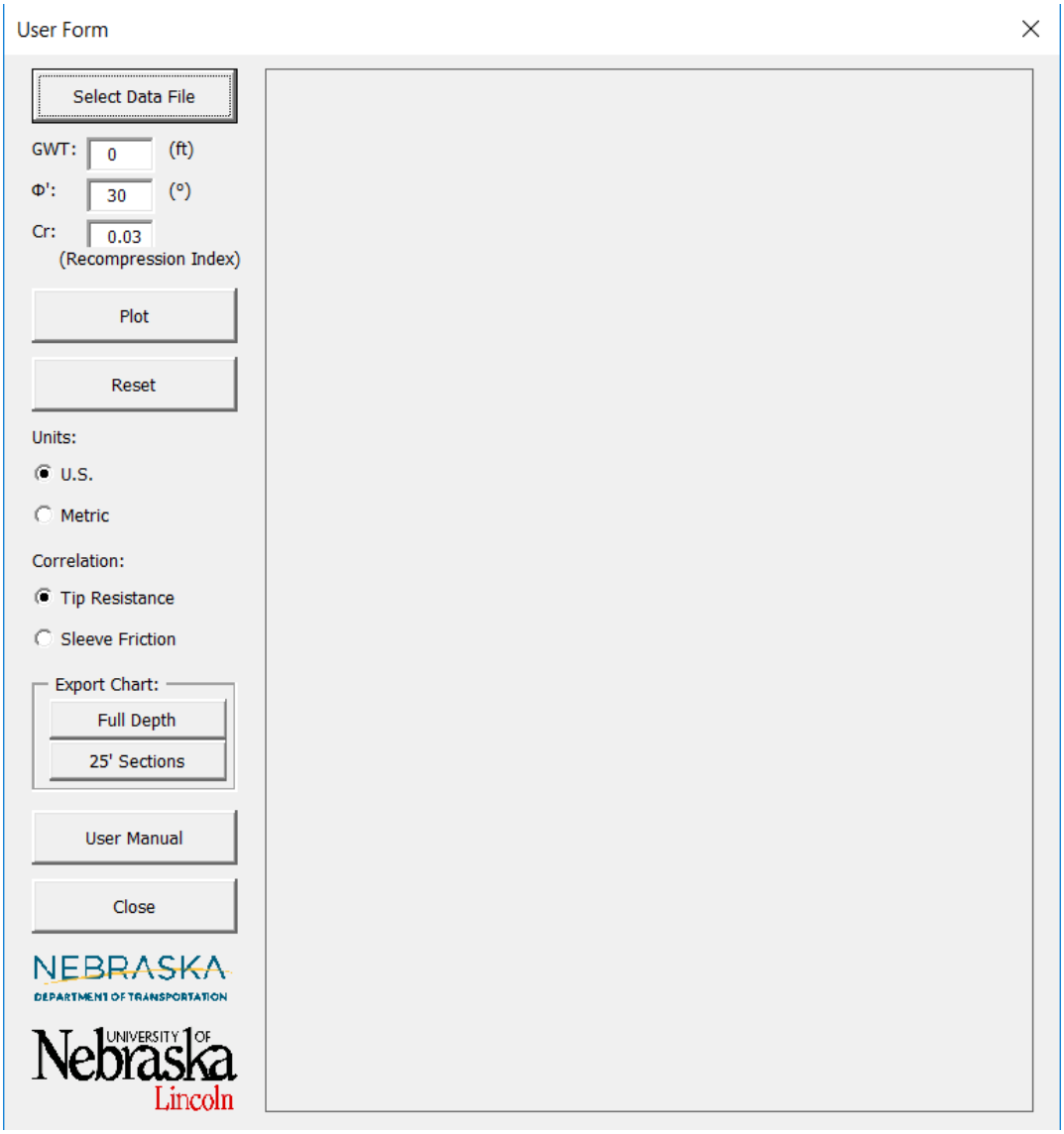

Fig. 6.2 User form on startup

Then, the user has the option to change the default values for GWT, friction angle, and recompression index. After this, press "Plot" to see the hydraulic conductivity profile in the space to the right. Fig. 6.5 shows the user form after plotting occurs. The reset function will tell the

program to no longer reference the previously selected data file and will erase the plot. Once this is pressed, a new data file can be selected for analysis.

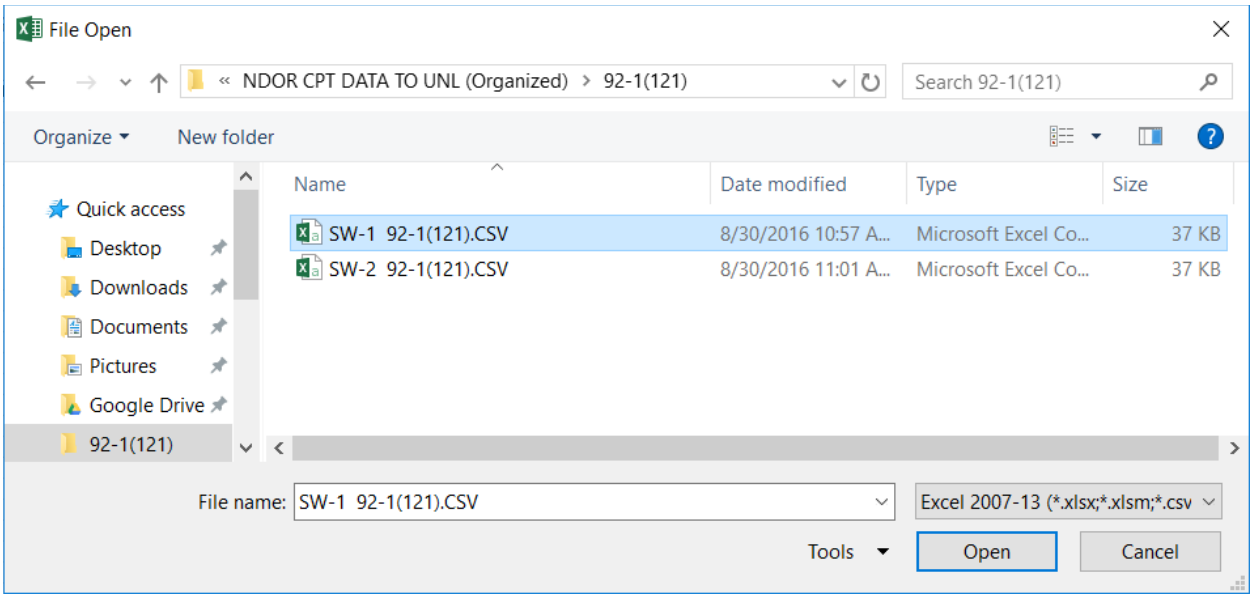

Fig. 6.3. File explorer to select PCPT data

The plot will by default show U.S. units of (ft/day) for k and (ft) for depth. This can be changed by selecting the bubble next to “Metric” under the “Units” heading. Additionally, the graph can be adjusted by changing the chosen correlation from tip resistance to sleeve friction The tip resistance correlation is regarded as the more accurate of the two, but both are included so the user can compare the two correlations found by this research.

The Export Chart button allows the user to save an excel sheet containing the plot shown on the user form along with the data table from which the plot is comprised. This tool allows the user to examine the computed hydraulic conductivity value for each depth that the piezocone took a reading. Additionally, this is the button that should be used if the user wishes to copy the graph into a report or print it. This graph can be edited the same way that graphs are typically edited in Microsoft Excel. Fig. 6.6 shows an example output resulting from this feature. In addition to

displaying the graph of the entire depth of the testing data, intervals of 25 feet or meters can be plotted to make report preparation easier.

	A	B	C	D
1	H [m]	qc [MPa]	fs [MPa]	u2 [MPa]
2	0	0	0	0
3	0.02	1.958	0.001	0.0033
4	0.04	4.408	0.001	0.006
5	0.06	6.767	0.001	0.0057
6	0.08	10.119	0.003	0.0047
7	0.1	13.043	0.012	0.004
8	0.12	15.83	0.025	0.0037
9	0.14	17.851	0.043	0.0057
10	0.16	19.017	0.066	0.0047
11	0.18	19.472	0.093	0.0047
12	0.2	18.789	0.115	0
13	0.22	17.733	0.126	-0.0023
14	0.24	16.549	0.129	-0.004
15	0.26	15.802	0.134	-0.004
16	0.28	15.456	0.141	-0.004
17	0.3	15.511	0.147	-0.003
18	0.32	15.775	0.151	-0.0013
19	0.34	16.23	0.151	-0.001
20	0.36	16.522	0.15	-0.0013
21	0.38	16.695	0.146	-0.0027
22	0.4	16.667	0.143	-0.0027
23	0.42	16.831	0.139	-0.0033
24	0.44	17.068	0.126	-0.004

Fig. 6.4 PCPT ".CSV" output columns A-D

If help is needed while using the program, the "User Manual" button can be pressed to provide an abridged set of directions to help with operating the program. This is shown in Fig. 6.7.

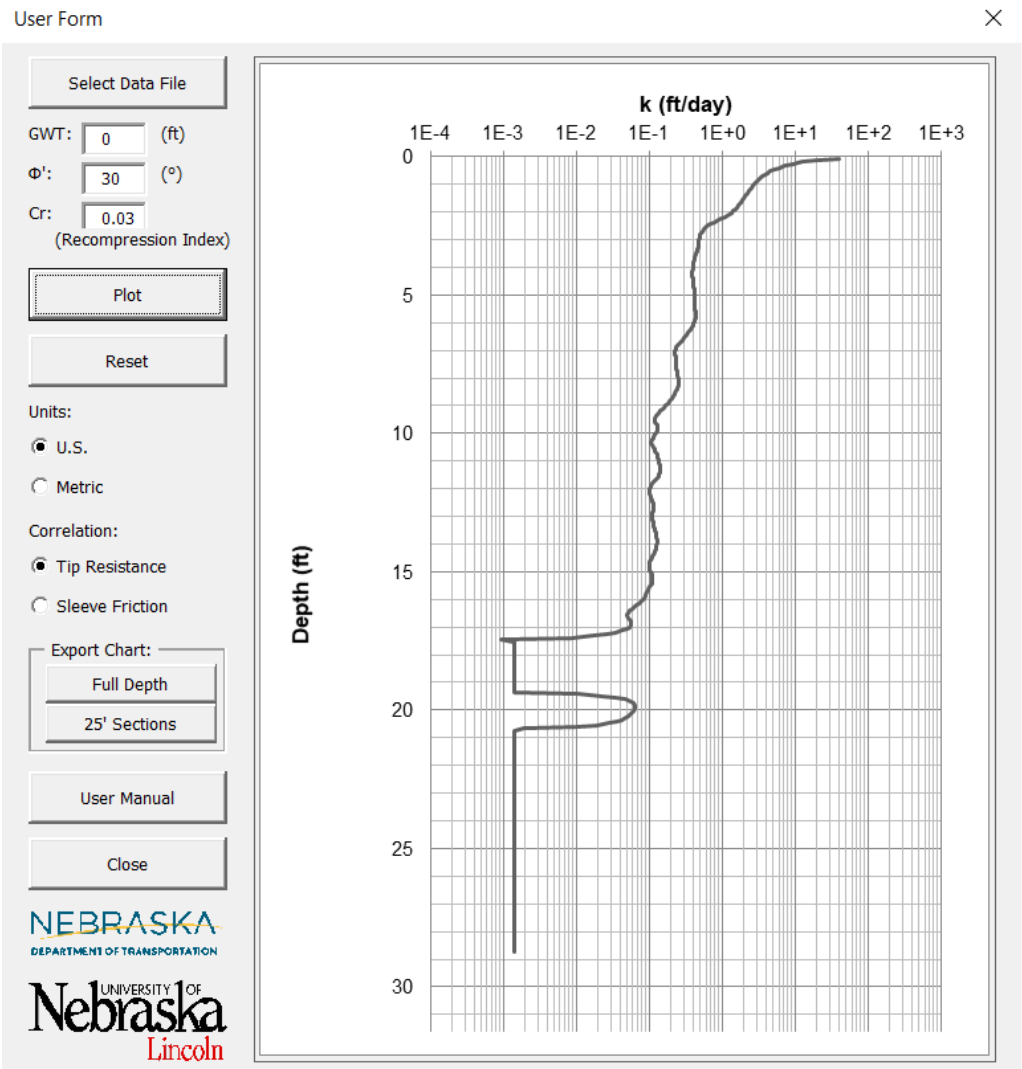

Fig. 6.5 Plotted hydraulic conductivity profile on user form

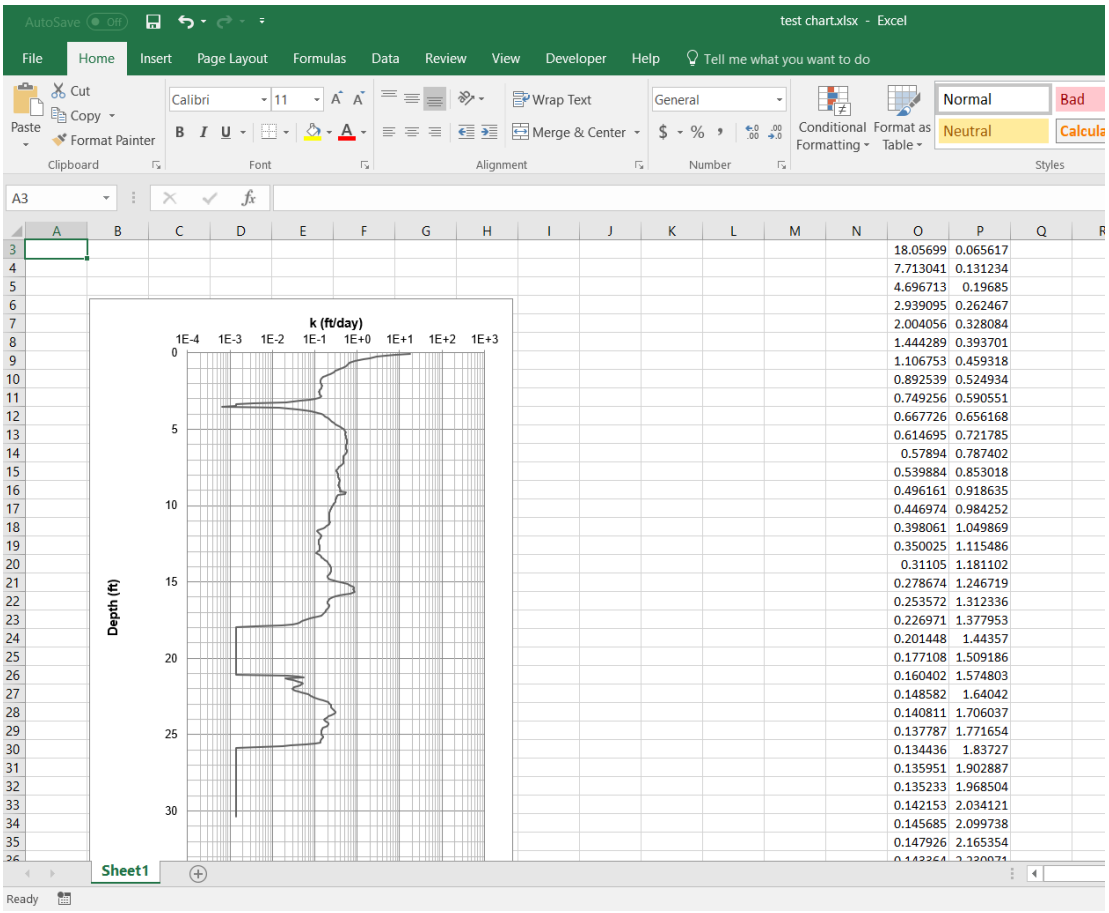

Fig. 6.6 Excel sheet resulting from “Export Chart” button

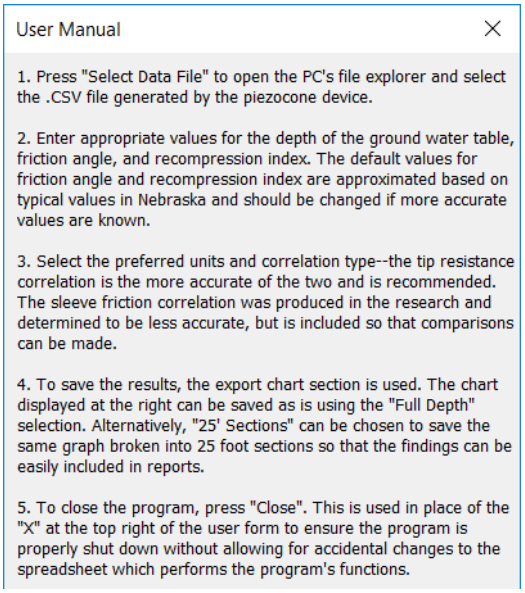

Fig. 6.7 Built in user manual

7 CONCLUSION

The piezocone penetration testing device is known as one of the two more reliable geotechnical testing devices. The built-in piezometer in the piezocone measures the pore pressure response during penetration and used to profile soil layering systems. For saturated soils, this piezometer is also used to conduct dissipation tests to obtain hydraulic conductivity or coefficient of consolidation. A recent technique by Song and Pulijala (2010) eliminates the disadvantage of dissipation tests and provided a more efficient way of determining hydraulic conductivity of soils. The fundamental principle of this techniques is simultaneous generation and dissipation of pore water pressure.

The main objective of this project was to estimate hydraulic conductivity of soils on a real time basis using NDOT's piezocone penetration test device. Further, focus was given to obtain correction factors for measured pore pressure during PCPT. These correction factors were necessitated as majority of Nebraskan soils are overconsolidated soils. Measured pore pressure in overconsolidated soils are either negative or very small so that these factors will compensate overconsolidation effects.

Correction factors were computed by matching up laboratory determined hydraulic conductivities with PCPT based hydraulic conductivities obtained using Song and Pulijala's equation. An attempt was made to correlate the correction factors to SBTn chart parameters so that correction factors can be obtained 'on-the-fly'. The effect of sign of Bq was also investigated. It was found that the sign of Bq has no significant influence on the correction factors. A correlation having a coefficient of determination 86% between correction factor and non-dimensional parameter which is a function of SBTn parameters Qt, Fr and Bq was obtained. The correlation was verified with

hydraulic conductivity and PCPT data from other test sites outside Nebraska and satisfactory results has been obtained.

A VBA program to aid the determination hydraulic conductivity profile 'on-the-fly' was developed. The program can be used as a standalone program to compute hydraulic conductivity once PCPT data has been acquired.

References

Burns, S. and Mayne, P. (1998). Penetrometers for Soil Permeability and Chemical Detection. Georgia Institute of Technology, Atlanta.

Campanella, R.G., Robertson, P.K. (1981). "Applied cone research". *Cone Penetration Testing and Experience*, ASCE, New York, 343-362.

Crawford, C. B., and R. G. Campanella. (1991). "Comparison of field consolidation with laboratory and in situ tests." *Canadian Geotechnical Journal* 103-112.

Dong A Geology. (1997). Piezocone testing report-settlement and stability control for constructing Yangsan Mulgum Housing Complex. *Dong A Geology Co.*

Elsworth, D. (1993). Analysis of piezocone dissipation data using dislocation methods." *J. Geotech. Engrg.*, 119 (10), 1601–1623.

Elsworth, D. and Lee, D.S. (2005). "Permeability determination from on-the-fly piezocone sounding." *J. Geotech. Geoenviron. Eng.*, 131 (5), 643–653.

Houlsby, G.T. et al. (1988). *Research at Oxford on the Analysis of the Piezocone Test,* Oxford: University of Oxford, Dept. of Eng. Science, U.K.

Kaya Engineering Co. (2005). "Technical review of ground improvement techniques for developing Chungra free trading area (District 1)". *Kaya Engineering.*

Kim, K. (2005). "Cone penetration test in clayey soil: Rate effect and application to Pile Shaft Resistance Calculations". Ph. D. Thesis, Purdue Univ. 218p.

Lee, Dae Sung, Derek Elsworth, and Roman Hryciw (2008). "Hydraulic Conductivity Measurement from On-The-Fly uCPT Sounding and from Viscpt". *Journal of Geotechnical and Geoenvironmental Engineering* 134 (12), 1720-1729.

Levadoux, J. N., and Baligh, M. M. (1986). “Consolidation after undrained piezocone penetration. I: Prediction.” *J. Geotech. Eng.*, 112 (7), 707–726.

Lunne, T., Eidsmoen, T., Gillespie, D., and Howland, J. (1986a). "Laboratory and field evaluation of cone penetrometers". *Use of In-Situ Tests in Geotechnical Engineering (GSP 6),* ASCE, New York, 714-729.

Lunne, T., Robertson, P. K., and Powell, J. J. M. (1997). *Cone penetration testing in geotechnical practice*, Blackie Academic & Professional, London, 48–71.

Manassero, M. (1994). "Hydraulic Conductivity Assessment of Slurry Wall using Piezocone Test"

Robertson, P., & Cabal, K. (2010). *Guide to Cone Penetration Testing* . Signal Hill: Gregg Drilling & Testing, Inc.

Robertson, P., Sully, J., Woeller, D., Lunne, T., Powell, J., and Gillespie, D. (1992). "Estimating coefficient of consolidation from piezocone tests". *Canadian Geotech. J.*, 29(4), 539-550.

Rust, E., Jacobsz, S. and van der Berg P. (1995). "Seepage analysis from Piezocone dissipation tests" *Proceedings CPT’95*, pp. 289-294.

Song, C. R. and S. Pulijala. (2010) “Hydraulic Property Estimation Using Piezocone Results”. *Journal of Geotechnical and Geoenvironmental Engineering* 136 (3): 456-463.

Song, C. R., Voyiadjis, G. Z., and Tumay, M. T. (1999). “Determination of permeability of soils using multiple piezo-element penetrometer.” *Int. J. Numer. Analyt. Meth. Geomech.*, 23 (13), 1609–1629.

Tumay, M.T., Acar, Y., deSeze, E., and Yimaz, R. (1982). "Soil exploration in soft clay with electric cone penetrometer". *Proc., 2nd European Symposium on Penetration Testing*, Amsterdam, 415-921.

Voyiadjis, G. Z., and Song, C. R. (2003). “Determination of hydraulic conductivity using piezocone penetration test.” *Int. J. Geomech.*, 3(3/4), 217–224.

Appendix A

Table A.1 Summary of project identifications and amount of data

							WT			
Project #	Total no. of bore holes	General Location	Station	No. of lab data points	No. used data points	PCPT data	WD	IAD	AD	Remark
2-6(119)	3	S. Beltway road- Rod's outdoor power	159+32, 48' RT	5	4	Y	N	N	N	Used
			160+47, 49' RT	5	3	Y	N	N	N	
			161+70, 45' RT	5	4	Y	N	Y	N	
2-6(1027)	1	148th Street / N-2	12+50, 50' RT	6	6	Y	N	Y	N	Used
12-5(112)	No BH log	-	-	-	-	-	-	-	-	-
14-4(1016)	4	-	-	-	-	-	-	-	-	-
34-7(124)	-	La Platte, NE	5599+55, 248' RT	-	-	**N**	Y	N	N	-
71-2(1005)	No BH log	I-80 to North of Kimball	765+70 CL	-	-	Y	N	N	N	-
75-2(165)	3	Plattsmouth to Bellevue-Fairview	1112+00 CL	4	3	Y	N	Y	N	Used
			7136+50, 20' RT	3	3	Y	N	Y	N	
75-2(176)	1	Chandler NB	224+90, 80' RT	3	2	Y	N	N	N	Used
75-2(1040)	9	Nebraska City South East	833+00, 150' RT	1	-	Y	N	N	N	Used
			825+00, 50' LT	3	2	Y	N	Y	N	
			821+20 CL	3	1	Y	N	Y	N	
75-2(1068)	5	Chandler Road NB	225+37, 166' RT	3	1	Y	N	N	N	Used
			205+20, 160' RT	2	1	Y	N	N	N	
79-2(108)	2	Agnew North and South	623+90, 80' RT	1	1	Y	N	N	Y	Used
				2	2	Y	N	N	Y	
80-9(829)	2	Church Road Over I-80	124+25, 25' LT	6	-	Y	N	Y	N	Friction was too small
			126+30, 25' RT	3	-	Y	N	Y	N	
80-9(837)	2	176th Street over I-80	4020+35, 20' RT	5	2	Y	N	N	Y	Used
			4018+10, 40' LT	4	3	Y	N	N	Y	
80-9(839)	2	148th over I-80	119+70, 60' LT	5	5	Y	N	N	Y	Used
			122+00, 30' LT	3	3	Y	N	N	Y	
80-9(849)	2	70th Street bridge-Lincoln	9010+59 RT	2	2	Y	N	Y	N	Used

							WT			
Project #	Total no. of bore holes	General Location	Station	No. of lab data points	No. used data points	PCPT data	WD	IAD	AD	Remark
			9013+50 LT	1	1	Y	N	Y	N	
80-9(850)	No BH log	-	-	-	-					
80-9-(856)	1	I-180 to Hwy 77	6312+05, 30' RT	3	2	Y	N	N	Y	Used
80-9(862)	1	I-80 NW 56th to US 77	411+50, 115' LT	5	5	Y	N	N	Y	Used
80-9(889)	-	-	-	-	-					
80-9(1185)	1	Expand I80 WB, I80/480 Intercha	1295+86, 110' LT	7	6	Y	N	Y	N	Used
85-2(111)	3	Ralston viaduct	23+12, 83' LT	11	3	Y	N	N	Y	Used
			21+75, 50' RT	6	3	Y	N	N	Y	
92-1(121)	2	Scottsbluff west viaduct	132+90, 58' RT	4	2	Y	N	N	N	Used
			127+30, 62' RT	3	2	Y	N	Y	N	
183-3(112)	2	Ansley viaduct	1009+50, 5' RT	8	-	Y	N	Y	N	Friction not recorded
			1013+75, 75' RT	6	-	Y	N	Y	N	
281-3(110)	6	Greeley South	160+00	3	-	Y	N	N	N	-
			231+00	3	-	Y	N	N	N	
			345+00, 20' RT	3	-	Y	N	N	Y	
			431+00	2	-	Y	N	N	N	
Camera Tower		-	-	-		-	-	-	-	-
83-3(106)	No BH log	Thedford South	-	-		-	-	-	-	-
M2075A		-	-	-		-	-	-	-	-
L93E(1009)	1	Charleston Link	317+70, 15' RT	2	-	Y	N	N	N	-

N.B. Y-available, N-Not available, BH-Borehole

Appendix B

Table B.1 Hydraulic conductivity estimated based on laboratory test results

Project	Depth	Lab							PCPT	m_v	k	k
		C_v	e_o	C_c	C_r	σ_o	σ_p	OCR	q_t			
	m	m^2/s				kPa	kPa		kPa	1/kPa	m/s	ft/d
2-6(119) RO-1	1.62	5.42E-06	0.65	0.19	0.03	27.94	504.58	18.06	2110.00	2.18E-05	1.18E-09	3.40E-04
	2.34	6.85E-06	0.85	0.35	0.03	47.14	428.54	9.09	2161.00	3.42E-05	2.30E-09	6.63E-04
	3.84	1.17E-05	0.76	0.38	0.04	68.26	449.28	6.58	1871.00	4.33E-05	4.95E-09	1.43E-03
	5.96	7.38E-06	0.74	0.27	0.03	108.34	428.54	3.96	1631.00	3.37E-05	2.44E-09	7.03E-04
	7.43	7.02E-06	0.45	0.11	0.02	134.88	331.68	2.46	2496.00	1.04E-05	7.17E-10	2.07E-04
2-6(119) RO-2	1.74	7.45E-06	0.61	0.14	0.02	31.39	297.22	9.47	3648.00	1.04E-05	7.72E-10	2.22E-04
	3.84	8.80E-06	0.84	0.48	0.04	46.46	656.64	14.13	1930.00	5.87E-05	5.07E-09	1.46E-03
	5.39	1.02E-05	0.79	0.40	0.04	74.40	656.64	8.83	1396.00	6.95E-05	6.93E-09	2.00E-03
	6.00	1.85E-06	0.77	0.26	0.03	83.04	207.36	2.50	2232.00	3.05E-05	5.54E-10	1.60E-04
	8.36	6.77E-07	0.37	0.09	0.02	132.34	525.31	3.97	3674.00	7.76E-06	5.15E-11	1.48E-05
2-6(119) RO-3	2.40	4.85E-06	0.74	0.31	0.03	46.18	387.07	8.38	1365.00	5.67E-05	2.70E-09	7.78E-04
	3.84	1.08E-05	0.83	0.38	0.04	80.40	442.32	5.50	1262.00	7.15E-05	7.57E-09	2.18E-03
	5.67	6.61E-07	0.99	0.41	0.03	102.00	248.88	2.44	754.00	1.19E-04	7.70E-10	2.22E-04
	7.46	2.97E-07	0.41	0.01	0.03	145.20	511.49	3.52	3234.00	9.59E-07	2.79E-12	8.04E-07
2-6(1027)	1.50	2.92E-07	0.87	0.33	0.02	29.28	414.72	14.16	1142.00	6.71E-05	1.92E-10	5.53E-05
	2.94	6.25E-07	0.80	0.25	0.03	42.72	168.00	3.93	703.00	8.58E-05	5.26E-10	1.51E-04
	4.44	3.33E-07	1.03	0.41	0.03	55.01	103.68	1.88	818.00	1.07E-04	3.51E-10	1.01E-04
	6.84	7.36E-06	0.66	0.25	0.02	79.30	511.44	6.45	1662.00	3.94E-05	2.84E-09	8.19E-04
	8.94	1.28E-06	0.57	0.16	0.03	102.48	373.20	3.64	2102.00	2.11E-05	2.65E-10	7.63E-05
	10.44	1.67E-06	0.54	0.14	0.03	118.70	622.08	5.24	2631.00	1.50E-05	2.45E-10	7.07E-05
75-2(165) PB-5	4.44	2.88E-06	0.88	0.38	0.03	80.64	311.04	3.86	756.00	1.16E-04	3.28E-09	9.43E-04
	5.96	6.88E-07	0.99	0.44	0.02	108.67	200.45	1.84	457.00	2.10E-04	1.42E-09	4.08E-04
	7.49	2.40E-07	0.95	0.24	0.02	136.90	136.92	1.00	837.00	6.39E-05	1.50E-10	4.33E-05

Project	Depth	Lab							PCPT	m_v	*k*	*k*
		C_v	e_o	C_c	C_r	σ_o	σ_p	OCR	q_t			
75-2(165) W	5.96	3.44E-06	0.94	0.28	0.02	67.73	145.15	2.14	1200.00	5.23E-05	1.76E-09	5.07E-04
	7.46	2.40E-06	1.09	0.28	0.02	78.53	165.89	2.11	470.00	1.24E-04	2.91E-09	8.38E-04
	8.94	1.15E-05	1.00	0.32	0.03	90.58	241.92	2.67	900.00	7.72E-05	8.73E-09	2.51E-03
75-2(176)	4.35	1.21E-06	0.75	0.25	0.03	84.43	328.32	3.89	1496.00	4.14E-05	4.93E-10	1.42E-04
	7.38	1.83E-06	0.71	0.24	0.01	134.78	490.75	3.64	769.00	7.93E-05	1.42E-09	4.09E-04
	8.82	1.32E-06	0.70	0.21	0.02	173.04	248.88	1.44	832.00	6.44E-05	8.36E-10	2.41E-04
75-2(1040) NE-5	0.40	2.51E-06	0.73	0.21	0.02	10.56	311.04	29.45	1040.00	5.07E-05	1.25E-09	3.59E-04
	2.36	7.24E-06	0.72	0.26	0.03	42.86	552.96	12.90	1800.00	3.64E-05	2.59E-09	7.45E-04
	4.53	3.33E-07	0.55	0.21	0.03	66.96	456.00	6.81	2889.00	2.04E-05	6.66E-11	1.92E-05
75-2(1040) NE-6	0.85	1.35E-06	0.89	0.28	0.01	18.48	283.20	15.32	1032.00	6.23E-05	8.28E-10	2.38E-04
	1.45	3.54E-06	0.81	0.42	0.02	29.86	656.64	21.99	910.00	1.11E-04	3.85E-09	1.11E-03
	4.50	1.06E-05	0.66	0.22	0.03	76.56	518.40	6.77	3427.00	1.68E-05	1.75E-09	5.04E-04
75-2(1068) H10	7.56	8.58E-06	0.83	0.36	0.02	132.00	359.52	2.72	4009.00	2.13E-05	1.79E-09	5.17E-04
	11.94	9.45E-06	0.61	0.19	0.03	217.68	552.96	2.54	3857.00	1.33E-05	1.23E-09	3.55E-04
79-2(108) SM-1	5.28	3.92E-07	1.01	0.22	0.02	90.00	90.00	1.00	1345.00	3.53E-05	1.36E-10	3.91E-05
79-2(108) SM-2	4.00	3.99E-08	1.16	0.31	0.06	68.64	165.84	2.42	406.00	1.53E-04	6.00E-11	1.73E-05
	6.00	7.74E-08	1.10	0.35	0.09	86.30	172.80	2.00	607.00	1.19E-04	9.06E-11	2.61E-05
80-9(837) SM-1	0.81	3.48E-06	0.91	0.32	0.03	13.10	186.72	14.25	3220.00	2.26E-05	7.73E-10	2.22E-04
	3.12	1.77E-06	0.77	0.31	0.02	53.04	359.04	6.77	3307.00	2.30E-05	4.00E-10	1.15E-04
	4.50	5.98E-06	0.74	0.21	0.02	78.24	152.16	1.94	3132.00	1.67E-05	9.81E-10	2.82E-04
	7.52	6.03E-06	0.74	0.23	0.03	135.60	518.40	3.82	2008.00	2.86E-05	1.69E-09	4.87E-04
	10.50	1.36E-06	0.48	0.14	0.02	190.32	355.20	1.87	1127.00	3.65E-05	4.86E-10	1.40E-04
80-9(837) SM-2	1.53	2.96E-06	0.87	0.38	0.03	29.04	345.60	11.90	1370.00	6.45E-05	1.87E-09	5.39E-04
	3.02	1.07E-05	0.82	0.30	0.02	54.72	283.20	5.18	1660.00	4.31E-05	4.53E-09	1.31E-03
	4.64	3.66E-06	0.59	0.17	0.01	79.44	172.80	2.18	5038.00	9.21E-06	3.31E-10	9.53E-05
	5.99	7.06E-06	0.71	0.28	0.03	111.84	345.60	3.09	1868.00	3.81E-05	2.63E-09	7.59E-04
80-9(839) 148-1	1.58	1.80E-06	0.74	0.24	0.03	31.92	324.48	10.17	2431.00	2.46E-05	4.35E-10	1.25E-04

Project	Depth	Lab							PCPT	m_v	k	k
		C_v	e_o	C_c	C_r	σ_o	σ_p	OCR	q_t			
	3.02	4.11E-06	0.76	0.27	0.02	59.76	193.44	3.24	1803.00	3.69E-05	1.49E-09	4.29E-04
	4.61	7.21E-06	0.56	0.22	0.02	83.52	131.28	1.57	2456.00	2.49E-05	1.76E-09	5.08E-04
	6.12	3.93E-06	0.56	0.16	0.02	112.08	414.72	3.70	2553.00	1.74E-05	6.73E-10	1.94E-04
	8.97	1.35E-05	0.49	0.15	0.02	172.32	532.32	3.09	2916.00	1.50E-05	1.98E-09	5.72E-04
80-9(839) 148-2	4.00	4.86E-06	0.69	0.31	0.02	67.97	345.60	5.08	1734.00	4.60E-05	2.19E-09	6.31E-04
	5.94	3.72E-06	0.70	0.21	0.02	114.48	228.00	1.99	3466.00	1.55E-05	5.64E-10	1.62E-04
	8.97	1.22E-05	0.66	0.28	0.02	177.41	518.40	2.92	2190.00	3.35E-05	3.99E-09	1.15E-03
80-9(849) A1	0.89	8.56E-07	0.53	0.12	0.02	20.06	290.40	14.47	1526.00	2.23E-05	1.88E-10	5.41E-05
	1.49	1.40E-07	0.53	0.11	0.02	32.74	483.84	14.78	2276.00	1.37E-05	1.88E-11	5.41E-06
80-9(849) A2	0.84	5.35E-07	0.62	0.08	0.02	28.42	324.72	11.43	970.00	2.21E-05	1.16E-10	3.33E-05
80-9(856)	1.52	2.10E-06	0.75	0.26	0.03	29.76	127.68	4.29	655.00	9.85E-05	2.03E-09	5.83E-04
	3.09	5.79E-06	0.79	0.30	0.02	45.84	725.76	15.83	464.00	1.57E-04	8.91E-09	2.57E-03
	7.43	9.81E-06	0.54	0.10	0.01	88.32	345.60	3.91	1910.00	1.48E-05	1.42E-09	4.09E-04
80-9(862) SM-1	1.56	1.15E-06	0.92	0.39	0.05	17.09	648.00	37.92	764.00	1.16E-04	1.32E-09	3.79E-04
	2.94	4.11E-06	0.67	0.21	0.03	29.52	276.48	9.37	1965.00	2.82E-05	1.14E-09	3.28E-04
	4.43	3.49E-06	0.60	0.34	0.05	43.49	449.28	10.33	1501.00	6.07E-05	2.08E-09	5.99E-04
	4.73	4.82E-06	0.79	0.27	0.02	70.42	580.61	8.25	1365.00	4.84E-05	2.29E-09	6.59E-04
	7.44	7.04E-06	0.97	0.24	0.02	83.71	622.08	7.43	1228.00	4.36E-05	3.01E-09	8.66E-04
80-9(1185)	1.47	2.07E-06	0.79	0.31	0.01	30.00	414.72	13.82	1027.00	7.23E-05	1.47E-09	4.23E-04
	2.51	4.16E-06	0.72	0.26	0.02	44.06	366.34	8.31	1651.00	4.02E-05	1.64E-09	4.72E-04
	2.99	3.15E-06	0.76	0.25	0.02	56.06	241.92	4.32	1172.00	5.20E-05	1.61E-09	4.62E-04
	4.49	4.96E-06	0.69	0.25	0.02	90.48	449.28	4.97	1412.00	4.47E-05	2.17E-09	6.26E-04
	5.99	7.08E-06	0.61	0.26	0.02	116.64	359.42	3.08	2763.00	2.53E-05	1.76E-09	5.06E-04
	9.12	2.18E-06	0.78	0.18	0.02	176.02	235.01	1.34	2027.00	2.20E-05	4.70E-10	1.35E-04
85-2(111) H1	3.00	4.27E-08	0.86	0.49	0.03	54.48	54.48	1.00	409.00	2.79E-04	1.17E-10	3.37E-05
	4.30	8.19E-07	0.68	0.24	0.02	74.59	100.80	1.35	850.00	7.20E-05	5.78E-10	1.67E-04
	5.80	4.92E-07	1.08	0.25	0.02	103.44	115.44	1.12	883.00	5.81E-05	2.80E-10	8.07E-05

Project	Depth	Lab							PCPT	m_v	k	k
		C_v	e_o	C_c	C_r	σ_o	σ_p	OCR	q_t			
	7.45	2.43E-06	0.72	0.21	0.02	131.42	262.56	2.00	870.00	6.08E-05	1.45E-09	4.18E-04
	8.77	9.80E-07	0.69	0.19	0.02	143.95	147.84	1.03	984.00	5.04E-05	4.85E-10	1.40E-04
	10.28	7.99E-07	0.77	0.27	0.02	187.78	207.36	1.10	735.00	8.87E-05	6.95E-10	2.00E-04
	16.28	1.02E-06	0.59	0.14	0.01	248.50	248.50	1.00	2884.00	1.29E-05	1.29E-10	3.70E-05
85-2(111) H3	2.42	2.07E-06	0.69	0.28	0.04	46.08	182.16	3.95	1014.00	7.10E-05	1.44E-09	4.14E-04
	3.75	3.86E-07	0.86	0.27	0.04	67.92	219.36	3.23	469.00	1.33E-04	5.03E-10	1.45E-04
	4.62	8.96E-07	0.84	0.25	0.03	87.60	147.84	1.69	499.00	1.18E-04	1.04E-09	2.98E-04
	5.91	2.96E-06	0.90	0.26	0.04	104.16	126.48	1.21	562.00	1.04E-04	3.02E-09	8.69E-04
	7.41	9.74E-07	1.03	0.45	0.04	117.36	230.16	1.96	663.00	1.44E-04	1.37E-09	3.96E-04
	8.96	2.38E-06	0.85	0.29	0.04	130.56	167.28	1.28	729.00	9.41E-05	2.20E-09	6.32E-04
9-1(121) SW-1	1.66	3.10E-06	1.19	0.45	0.04	25.92	76.03	2.93	1478.00	6.04E-05	1.83E-09	5.28E-04
	4.53	3.97E-07	1.17	0.51	0.02	71.38	89.86	1.26	1212.00	8.42E-05	3.28E-10	9.45E-05
	6.00	9.36E-06	0.87	0.33	0.03	98.06	622.08	6.34	3134.00	2.44E-05	2.24E-09	6.46E-04
	7.64	7.32E-06	1.89	0.19	0.01	125.18	359.42	2.87	913.00	3.13E-05	2.25E-09	6.48E-04
9-1(121) SW-2	4.62	5.97E-06	1.01	0.19	0.01	83.76	428.54	5.12	2954.00	1.39E-05	8.14E-10	2.35E-04
	6.00	8.33E-06	0.98	0.33	0.02	104.45	642.82	6.15	3160.00	2.29E-05	1.87E-09	5.39E-04
	7.60	1.04E-05	1.63	0.47	0.06	130.18	470.02	3.61	982.00	7.90E-05	8.09E-09	2.33E-03

Appendix C

Table C.1 Relationship between adjustment factors and N

Project		Qt	Fr	Bq	SBTn zone	Adj. Factor (C)	N
2-6(119)	2-6(119) RO-1	51.40	5.89	0.02	4.00	16.44	0.15
		32.95	3.61	0.05	4.00	6.89	0.44
		20.76	4.76	0.11	4.00	3.68	0.50
		28.16	5.14	0.01	4.00	42.46	0.03
	2-6(119) RO-2	108.24	6.21	0.01	N/A	21.46	0.16
		25.18	4.12	0.03	N/A	10.60	0.20
		13.21	2.74	0.05	4.00	10.25	0.25
		20.29	3.59	0.06	4.00	5.59	0.31
	2-6(119) RO-3	35.25	7.05	0.04	4.00	13.10	0.19
		24.47	4.09	0.04	4.00	13.56	0.25
		10.11	4.31	0.09	3.00	11.36	0.22
		40.20	8.15	0.01	4.00	25.71	0.04
2-6(1027)	2-6(1027)	19.05	8.44	-0.03	9.00	49.01	0.07
		14.01	3.65	-0.04	9.00	25.77	0.14
		12.94	2.73	-0.03	9.00	23.94	0.15
		29.54	3.96	-0.04	9.00	4.94	0.33
		23.77	7.74	-0.05	9.00	5.23	0.16
75-2(165)	75-2(165) PB-5	8.85	3.75	0.06	3.00	17.27	0.13
		4.02	4.68	0.08	3.00	25.56	0.07
		7.04	2.74	0.10	3.00	9.72	0.26
	75-2(165) W	18.00	3.19	-0.04	9.00	12.31	0.25
		4.78	2.66	-0.14	9.00	12.43	0.25
		9.17	3.69	-0.02	9.00	38.99	0.05
75-2(176)	75-2(176)	19.292	2.743	-0.019	N/A	21.52	0.13
		5.351	3.412	0.033	3.00	29.76	0.05
		5.276	2.631	0.067	3.00	12.74	0.14
75-2(1040)	75-2(1040) NE-5	75.45	1.79	0.06	5.00	5.58	2.54
		67.20	3.83	0.06	5.00	3.59	1.00
	75-2(1040) NE-6	64.62	4.01	0.04	5.00	4.33	0.63
75-2(1068)	75-2(1068) H10	26.38	4.76	0.01	N/A	21.48	0.04
		15.97	4.27	0.02	N/A	6.35	0.09
79-2(108)	79-2(108) SM-1	16.10	3.34	0.02	4.00	35.13	0.10
	79-2(108) SM-2	6.24	2.05	0.06	3.00	24.04	0.20
		7.82	2.54	0.18	3.00	5.35	0.57
80-9(837)	80-9(837) SM-1	12.97	4.83	0.00	N/A	88.39	0.010
		4.93	4.21	0.01	3.00	52.91	0.015
	80-9(837) SM-2	30.21	2.26	0.03	N/A	12.45	0.394
		60.57	3.04	0.02	N/A	7.15	0.347

Project		Qt	Fr	Bq	SBTn zone	Adj. Factor (C)	N
		15.93	5.47	0.01	N/A	26.19	0.038
80-9(839)	80-9(839) 148-1	79.97	8.54	0.00	N/A	285.05	0.01
		30.63	3.35	0.04	N/A	9.82	0.32
		27.63	8.26	0.00	N/A	97.45	0.01
		21.15	6.00	0.01	N/A	21.59	0.04
		17.19	4.41	0.04	4.00	6.23	0.14
	80-9(839) 148-2	21.28	4.71	0.06	N/A	6.52	0.25
		29.54	7.37	0.02	N/A	11.65	0.06
		14.02	5.15	0.02	3.00	14.23	0.06
80-9(849)	80-9(849) A1	91.09	6.84	-0.03	N/A	12.83	0.44
		80.63	3.82	-0.01	N/A	28.06	0.22
	80-9(849) A2	63.49	8.31	-0.03	N/A	19.53	0.25
80-9(856)	80-9(856)	33.84	3.50	0.11	4.00	3.44	1.02
80-9(862)	80-9(862) SM-1	64.86	2.07	0.03	5.00	9.08	1.04
		35.43	3.43	0.09	4.00	4.28	0.90
		30.33	3.87	0.10	4.00	4.57	0.79
		17.31	1.75	-0.12	9.00	4.30	1.23
80-9(1185)	80-9(1185)	65.35	1.24	0.37	6.00	1.02	19.57
		40.25	1.34	0.42	6.00	1.27	12.51
		34.84	2.39	0.39	6.00	1.12	5.68
		49.78	4.57	0.24	5.00	1.02	2.64
		24.34	2.78	0.29	4.00	1.07	2.55
85-2(111)	85-2(111) H1	6.86	2.41	0.14	3.00	5.70	0.41
		7.16	1.67	0.30	3.00	2.38	1.29
		4.50	2.12	0.40	3.00	2.64	0.84
		15.40	1.53	0.31	4.00	0.79	3.11
	85-2(111) H3	5.54	1.28	0.15	3.00	7.80	0.65
		5.89	1.46	0.28	3.00	3.64	1.11
		5.73	1.87	0.33	3.00	2.83	1.02
9-1(121)	9-1(121) SW-1	34.14	8.92	0.01	4.00	16.45	0.04
		7.53	7.02	0.05	3.00	15.20	0.06
	9-1(121) SW-2	41.73	2.91	0.01	5.00	26.32	0.10
		9.74	3.03	-0.05	9.00	13.11	0.15

Appendix D

Table D.1 Sample hydraulic conductivity computation based on PCPT

Project Name: -		2-6(119) RO-1			
GWT [ft]	6.66	M	1.2	κ	0.013

H [ft]	qc [psi]	fs [psi]	u [psi]	qt [psi]	R_f[%]	UW [kN/m3]	u2[kPa]	Uo [kpa]	Exc. Pore [kPa]	Δσv	σ_{vo} [kPa]	σ_{vo}' [kPa]	Qt []	Fr [%]	Bq []	Ic	Zone	Soil type	N	C	U_{adj}	k (ft/d)
0.07	40.18	1.31	0.32	40.24	3.24	15.04	2.20	0.00	0.00	0.301	0.30	0.301	920.58	3.25	0.008	-	-	-	2.25	2.38	0.00	
0.13	71.36	2.47	0.32	71.42	3.45	15.99	2.20	0.00	0.00	0.320	0.62	0.621	791.82	3.46	0.004	-	-	-	1.02	3.96	0.00	
0.20	101.24	3.48	0.30	101.30	3.44	16.52	2.10	0.00	0.00	0.330	0.95	0.951	732.78	3.44	0.003	-	-	-	0.64	5.37	0.00	
0.27	125.31	4.64	0.26	125.37	3.70	16.94	1.80	0.00	0.00	0.339	1.29	1.290	668.65	3.71	0.002	-	-	-	0.38	7.60	0.00	
0.33	145.47	5.51	0.17	145.51	3.79	17.19	1.20	0.00	0.00	0.344	1.63	1.634	612.67	3.79	0.001	-	-	-	0.19	11.71	0.00	
0.40	161.57	6.38	0.06	161.58	3.95	17.40	0.40	0.00	0.00	0.348	1.98	1.982	560.80	3.96	0.000	-	-	-	0.05	27.86	0.00	
0.47	174.63	7.11	-0.07	174.61	4.07	17.55	-0.50	0.00	0.00	0.351	2.33	2.333	514.74	4.08	0.000	-	-	-	0.05	27.32	0.00	
0.53	184.78	7.54	-0.20	184.74	4.08	17.64	-1.40	0.00	0.00	0.353	2.69	2.686	472.95	4.09	-0.001	-	-	-	0.13	15.37	0.00	
0.60	192.61	7.98	-0.32	192.55	4.14	17.72	-2.20	0.00	0.00	0.354	3.04	3.040	435.39	4.15	-0.002	-	-	-	0.17	12.54	0.00	
0.67	198.12	8.12	-0.42	198.04	4.10	17.75	-2.90	0.00	0.00	0.355	3.40	3.395	400.89	4.11	-0.002	-	-	-	0.21	11.18	0.00	
0.73	201.75	8.27	-0.49	201.65	4.10	17.78	-3.40	0.00	0.00	0.356	3.75	3.751	369.42	4.11	-0.002	-	-	-	0.22	10.76	0.00	
0.80	204.07	8.41	-0.54	203.96	4.12	17.81	-3.70	0.00	0.00	0.356	4.11	4.107	341.18	4.14	-0.003	-	-	-	0.22	10.84	0.00	
0.87	205.23	8.41	-0.57	205.12	4.10	17.81	-3.90	0.00	0.00	0.356	4.46	4.463	315.65	4.11	-0.003	-	-	-	0.21	11.02	0.00	
0.93	205.81	8.41	-0.58	205.69	4.09	17.81	-4.00	0.00	0.00	0.356	4.82	4.819	293.07	4.10	-0.003	-	-	-	0.20	11.38	0.00	
1.00	206.10	8.41	-0.58	205.98	4.08	17.81	-4.00	0.00	0.00	0.356	5.18	5.175	273.22	4.10	-0.003	-	-	-	0.19	11.91	0.00	
1.07	206.10	8.41	-0.58	205.98	4.08	17.81	-4.00	0.00	0.00	0.356	5.53	5.532	255.56	4.10	-0.003	-	-	-	0.18	12.44	0.00	
1.13	206.10	8.56	-0.57	205.99	4.15	17.83	-3.90	0.00	0.00	0.357	5.89	5.888	240.03	4.17	-0.003	-	-	-	0.16	13.32	0.00	
1.20	206.24	8.70	-0.52	206.14	4.22	17.85	-3.60	0.00	0.00	0.357	6.25	6.245	226.42	4.24	-0.003	-	-	-	0.14	14.73	0.00	
1.27	206.53	8.85	-0.45	206.44	4.29	17.87	-3.10	0.00	0.00	0.357	6.60	6.603	214.43	4.31	-0.002	-	-	-	0.11	17.00	0.00	
1.33	207.26	9.43	-0.33	207.19	4.55	17.94	-2.30	0.00	0.00	0.359	6.96	6.962	204.06	4.57	-0.002	-	-	-	0.07	22.22	0.00	
1.40	208.27	10.01	-0.16	208.24	4.81	18.01	-1.10	0.00	0.00	0.360	7.32	7.322	194.96	4.83	-0.001	-	-	-	0.03	38.43	0.00	
1.47	209.87	10.88	0.07	209.88	5.18	18.11	0.50	0.00	0.00	0.362	7.68	7.684	187.20	5.21	0.000	-	-	-	0.01	69.54	0.00	
1.53	211.90	12.04	0.36	211.97	5.68	18.23	2.50	0.00	0.00	0.365	8.05	8.049	180.46	5.71	0.002	-	-	-	0.05	26.72	0.00	
1.60	214.37	13.05	0.64	214.49	6.09	18.33	4.40	0.00	0.00	0.367	8.42	8.415	174.62	6.12	0.003	-	-	-	0.09	19.93	0.00	
1.67	216.83	14.21	0.90	217.01	6.55	18.43	6.20	0.00	0.00	0.369	8.78	8.784	169.22	6.59	0.004	-	-	-	0.11	17.20	0.00	
1.73	219.44	15.08	1.07	219.66	6.87	18.51	7.39	0.00	0.00	0.370	9.15	9.154	164.33	6.91	0.005	-	-	-	0.12	16.24	0.00	
1.80	222.34	15.81	1.12	222.57	7.10	18.57	7.69	0.00	0.00	0.371	9.53	9.525	159.99	7.15	0.005	-	-	-	0.11	16.60	0.00	
1.87	226.40	16.10	1.04	226.61	7.10	18.59	7.20	0.00	0.00	0.372	9.90	9.897	156.76	7.15	0.005	-	-	-	0.10	17.79	0.00	
1.93	232.93	16.24	0.84	233.10	6.97	18.61	5.80	0.00	0.00	0.372	10.27	10.270	155.39	7.01	0.004	-	-	-	0.08	20.71	0.00	
2.00	243.81	16.24	0.55	243.92	6.66	18.63	3.80	0.00	0.00	0.373	10.64	10.642	156.92	6.70	0.002	-	-	-	0.05	27.08	0.00	
2.07	261.07	16.10	0.22	261.11	6.17	18.65	1.50	0.00	0.00	0.373	11.02	11.015	162.33	6.20	0.001	-	-	-	0.02	48.20	0.00	
2.13	286.01	16.10	-0.09	286.00	5.63	18.68	-0.60	0.00	0.00	0.374	11.39	11.389	172.02	5.66	0.000	-	-	-	0.01	84.20	0.00	
2.20	319.08	15.95	-0.36	319.01	5.00	18.71	-2.50	0.00	0.00	0.374	11.76	11.763	185.85	5.03	-0.001	-	-	-	0.04	31.48	0.00	
2.27	359.40	16.10	-0.55	359.29	4.48	18.77	-3.80	0.00	0.00	0.375	12.14	12.139	202.94	4.50	-0.002	-	-	-	0.07	22.78	0.00	
2.33	404.51	16.24	-0.68	404.37	4.02	18.83	-4.70	0.00	0.00	0.377	12.52	12.515	221.62	4.04	-0.002	-	-	-	0.09	18.85	0.00	
2.40	451.07	16.53	-0.75	450.92	3.67	18.89	-5.20	0.00	0.00	0.378	12.89	12.893	239.97	3.68	-0.002	-	-	-	0.11	16.95	0.00	

Project Name: -		2-6(119) RO-1			
GWT [ft]	6.66	M	1.2	κ	0.013

H [ft]	qc [psi]	fs [psi]	u [psi]	qt [psi]	R_f[%]	UW [kN/m3]	u2[kPa]	Uo [kpa]	Exc. Pore [kPa]	Δσv	σ_{vo} [kPa]	σ_{vo}' [kPa]	Qt []	Fr [%]	Bq []	Ic	Zone	Soil type	N	C	U_{adj}	k (ft/d)
2.47	495.74	16.97	-0.80	495.58	3.42	18.95	-5.50	0.00	0.00	0.379	13.27	13.272	256.28	3.44	-0.002	-	-	-	0.12	15.93	0.00	
2.53	534.90	17.55	-0.83	534.73	3.28	19.02	-5.70	0.00	0.00	0.380	13.65	13.652	268.87	3.29	-0.002	-	-	-	0.13	15.42	0.00	
2.60	566.08	18.42	-0.87	565.91	3.25	19.10	-6.00	0.00	0.00	0.382	14.03	14.034	276.83	3.27	-0.002	-	-	-	0.13	15.10	0.00	
2.67	587.84	19.44	-0.91	587.66	3.31	19.18	-6.30	0.00	0.00	0.384	14.42	14.418	279.83	3.32	-0.002	-	-	-	0.13	15.04	0.00	
2.73	600.17	20.89	-0.97	599.97	3.48	19.27	-6.70	0.00	0.00	0.385	14.80	14.803	278.25	3.49	-0.002	-	-	-	0.13	15.20	0.00	
2.80	603.65	22.48	-1.00	603.45	3.73	19.35	-6.90	0.00	0.00	0.387	15.19	15.190	272.71	3.74	-0.002	-	-	-	0.12	15.85	0.00	
2.87	599.88	24.37	-1.02	599.67	4.06	19.44	-7.00	0.00	0.00	0.389	15.58	15.579	264.21	4.08	-0.002	-	-	-	0.11	16.89	0.00	
2.93	590.59	26.54	-0.99	590.40	4.50	19.54	-6.80	0.00	0.00	0.391	15.97	15.970	253.72	4.51	-0.002	-	-	-	0.09	18.68	0.00	
3.00	577.83	28.72	-0.93	577.65	4.97	19.62	-6.40	0.00	0.00	0.392	16.36	16.362	242.24	4.99	-0.002	-	-	-	0.08	21.08	0.00	
3.07	563.47	30.89	-0.87	563.30	5.48	19.69	-6.00	0.00	0.00	0.394	16.76	16.756	230.63	5.51	-0.002	-	-	-	0.06	23.80	0.00	
3.13	548.97	33.07	-0.83	548.80	6.03	19.76	-5.70	0.00	0.00	0.395	17.15	17.151	219.47	6.05	-0.002	-	-	-	0.05	26.56	0.00	
3.20	535.77	34.95	-0.86	535.60	6.53	19.81	-5.90	0.00	0.00	0.396	17.55	17.547	209.30	6.56	-0.002	-	-	-	0.05	27.77	0.00	
3.27	524.75	36.55	-0.99	524.55	6.97	19.86	-6.80	0.00	0.00	0.397	17.94	17.945	200.41	7.00	-0.002	-	-	-	0.05	26.81	0.00	
3.33	516.63	37.85	-1.23	516.38	7.33	19.89	-8.49	0.00	0.00	0.398	18.34	18.342	192.97	7.37	-0.002	-	-	-	0.06	24.32	0.00	
3.40	510.97	38.87	-1.61	510.65	7.61	19.92	-11.09	0.00	0.00	0.398	18.74	18.741	186.74	7.65	-0.003	-	-	-	0.08	21.25	0.00	
3.47	507.63	39.60	-2.09	507.22	7.81	19.94	-14.39	0.00	0.00	0.399	19.14	19.139	181.59	7.85	-0.004	-	-	-	0.10	18.49	0.00	
3.53	505.60	40.18	-2.61	505.08	7.95	19.95	-17.99	0.00	0.00	0.399	19.54	19.539	177.11	8.00	-0.005	-	-	-	0.12	16.41	0.00	
3.60	503.72	40.47	-3.12	503.09	8.04	19.96	-21.49	0.00	0.00	0.399	19.94	19.938	172.86	8.09	-0.006	-	-	-	0.13	14.92	0.00	
3.67	500.96	40.61	-3.55	500.25	8.12	19.96	-24.48	0.00	0.00	0.399	20.34	20.337	168.48	8.17	-0.007	-	-	-	0.15	13.97	0.00	
3.73	496.76	40.76	-3.86	495.98	8.22	19.96	-26.58	0.00	0.00	0.399	20.74	20.736	163.80	8.27	-0.008	-	-	-	0.16	13.52	0.00	
3.80	491.10	40.61	-4.03	490.29	8.28	19.95	-27.78	0.00	0.00	0.399	21.14	21.135	158.83	8.34	-0.008	-	-	-	0.16	13.37	0.00	
3.87	484.28	40.47	-4.05	483.47	8.37	19.94	-27.88	0.00	0.00	0.399	21.53	21.534	153.69	8.42	-0.008	-	-	-	0.15	13.60	0.00	
3.93	476.74	40.18	-3.95	475.95	8.44	19.93	-27.18	0.00	0.00	0.399	21.93	21.933	148.52	8.50	-0.008	-	-	-	0.15	14.07	0.00	
4.00	469.34	39.89	-3.73	468.60	8.51	19.92	-25.68	0.00	0.00	0.398	22.33	22.331	143.58	8.57	-0.008	-	-	-	0.13	14.85	0.00	
4.07	462.09	39.60	-3.45	461.40	8.58	19.90	-23.78	0.00	0.00	0.398	22.73	22.729	138.87	8.64	-0.008	-	-	-	0.12	15.88	0.00	
4.13	455.27	39.31	-3.12	454.65	8.65	19.89	-21.49	0.00	0.00	0.398	23.13	23.127	134.45	8.71	-0.007	-	-	-	0.11	17.24	0.00	
4.20	448.17	39.02	-2.77	447.61	8.72	19.87	-19.09	0.00	0.00	0.397	23.52	23.524	130.10	8.78	-0.006	-	-	-	0.09	18.93	0.00	
4.27	440.63	38.73	-2.42	440.14	8.80	19.86	-16.69	0.00	0.00	0.397	23.92	23.921	125.77	8.87	-0.006	-	-	-	0.08	21.01	0.00	
4.33	431.92	38.44	-2.09	431.51	8.91	19.84	-14.39	0.00	0.00	0.397	24.32	24.318	121.26	8.98	-0.005	-	-	-	0.07	23.58	0.00	
4.40	422.35	38.00	-1.75	422.00	9.00	19.82	-12.09	0.00	0.00	0.396	24.71	24.715	116.65	9.08	-0.004	-	-	-	0.05	26.88	0.00	
4.47	411.91	37.56	-1.45	411.62	9.13	19.80	-9.99	0.00	0.00	0.396	25.11	25.110	111.94	9.21	-0.004	-	-	-	0.04	31.01	0.00	
4.53	400.89	36.84	-1.19	400.65	9.20	19.76	-8.19	0.00	0.00	0.395	25.51	25.506	107.23	9.28	-0.003	-	-	-	0.03	35.83	0.00	
4.60	390.01	36.11	-0.94	389.82	9.26	19.73	-6.50	0.00	0.00	0.395	25.90	25.900	102.70	9.35	-0.002	-	-	-	0.03	42.30	0.00	
4.67	379.56	35.24	-0.71	379.42	9.29	19.69	-4.90	0.00	0.00	0.394	26.29	26.294	98.42	9.38	-0.002	-	-	-	0.02	51.44	0.00	
4.73	369.85	34.23	-0.51	369.75	9.26	19.65	-3.50	0.00	0.00	0.393	26.69	26.687	94.46	9.36	-0.001	-	-	-	0.01	64.51	0.00	
4.80	361.14	33.36	-0.32	361.08	9.24	19.61	-2.20	0.00	0.00	0.392	27.08	27.079	90.87	9.34	-0.001	-	-	-	0.01	87.97	0.00	
4.87	353.17	32.34	-0.13	353.14	9.16	19.57	-0.90	0.00	0.00	0.391	27.47	27.471	87.57	9.26	0.000	-	-	-	0.00	157.89	0.00	
4.93	346.06	31.47	0.03	346.07	9.09	19.53	0.20	0.00	0.00	0.391	27.86	27.861	84.58	9.20	0.000	-	-	-	0.00	421.76	0.00	
5.00	339.39	30.75	0.19	339.43	9.06	19.49	1.30	0.00	0.00	0.390	28.25	28.251	81.78	9.17	0.001	-	-	-	0.01	125.78	0.00	
5.07	333.30	30.02	0.33	333.36	9.01	19.46	2.30	0.00	0.00	0.389	28.64	28.640	79.20	9.12	0.001	-	-	-	0.01	87.27	0.00	
5.13	327.64	29.30	0.48	327.74	8.94	19.42	3.30	0.00	0.00	0.388	29.03	29.029	76.79	9.06	0.001	-	-	-	0.01	69.31	0.00	
5.20	322.27	28.72	0.62	322.40	8.91	19.39	4.30	0.00	0.00	0.388	29.42	29.417	74.51	9.03	0.002	-	-	-	0.02	58.73	0.00	

Project Name: -		2-6(119) RO-1			
GWT [ft]	6.66	M	1.2	κ	0.013

H [ft]	qc [psi]	fs [psi]	u [psi]	qt [psi]	R_f[%]	UW [kN/m3]	u2[kPa]	Uo [kpa]	Exc. Pore [kPa]	Δσv	σ_{vo} [kPa]	σ_{vo}' [kPa]	Qt []	Fr [%]	Bq []	Ic	Zone	Soil type	N	C	U_{adj}	k (ft/d)
5.27	316.91	28.14	0.78	317.06	8.87	19.36	5.40	0.00	0.00	0.387	29.80	29.804	72.30	9.00	0.003	-	-	-	0.02	50.97	0.00	
5.33	311.40	27.56	0.93	311.58	8.84	19.33	6.40	0.00	0.00	0.387	30.19	30.190	70.11	8.97	0.003	-	-	-	0.02	45.94	0.00	
5.40	305.60	27.12	1.10	305.82	8.87	19.31	7.59	0.00	0.00	0.386	30.58	30.577	67.91	9.00	0.004	-	-	-	0.03	41.51	0.00	
5.47	299.50	26.54	1.26	299.76	8.85	19.28	8.69	0.00	0.00	0.386	30.96	30.962	65.70	8.99	0.004	-	-	-	0.03	38.30	0.00	
5.53	292.98	26.11	1.44	293.26	8.90	19.25	9.89	0.00	0.00	0.385	31.35	31.347	63.46	9.04	0.005	-	-	-	0.03	35.64	0.00	
5.60	286.45	25.67	1.61	286.77	8.95	19.22	11.09	0.00	0.00	0.384	31.73	31.732	61.27	9.10	0.006	-	-	-	0.04	33.48	0.00	
5.67	280.21	25.09	1.77	280.57	8.94	19.19	12.19	0.00	0.00	0.384	32.12	32.115	59.19	9.09	0.006	-	-	-	0.04	31.72	0.00	
5.73	274.41	24.66	1.93	274.80	8.97	19.16	13.29	0.00	0.00	0.383	32.50	32.498	57.26	9.13	0.007	-	-	-	0.04	30.30	0.00	
5.80	269.63	24.08	2.07	270.04	8.92	19.12	14.29	0.00	0.00	0.382	32.88	32.881	55.59	9.08	0.008	-	-	-	0.05	29.02	0.00	
5.87	266.14	23.64	2.20	266.59	8.87	19.10	15.19	0.00	0.00	0.382	33.26	33.263	54.22	9.03	0.008	-	-	-	0.05	28.01	0.00	
5.93	264.11	23.06	2.34	264.58	8.72	19.07	16.09	0.00	0.00	0.381	33.64	33.644	53.18	8.88	0.009	-	-	-	0.05	26.88	0.00	
6.00	263.82	22.63	2.47	264.32	8.56	19.04	16.99	0.00	0.00	0.381	34.02	34.025	52.52	8.72	0.010	-	-	-	0.06	25.84	0.00	
6.07	264.98	22.34	2.60	265.50	8.41	19.03	17.89	0.00	0.00	0.381	34.41	34.406	52.17	8.57	0.010	-	-	-	0.06	24.89	0.00	
6.13	267.60	22.05	2.74	268.14	8.22	19.02	18.89	0.00	0.00	0.380	34.79	34.786	52.11	8.38	0.010	-	-	-	0.06	23.84	0.00	
6.20	271.08	21.76	2.89	271.65	8.01	19.01	19.89	0.00	0.00	0.380	35.17	35.166	52.22	8.16	0.011	-	-	-	0.07	22.82	0.00	
6.27	275.28	21.61	3.06	275.89	7.83	19.01	21.09	0.00	0.00	0.380	35.55	35.546	52.48	7.98	0.011	-	-	-	0.07	21.81	0.00	
6.33	280.07	21.47	3.23	280.72	7.65	19.01	22.28	0.00	0.00	0.380	35.93	35.926	52.84	7.79	0.012	-	-	-	0.08	20.85	0.00	
6.40	285.29	21.47	3.42	285.97	7.51	19.01	23.58	0.00	0.00	0.380	36.31	36.307	53.27	7.65	0.012	-	-	-	0.08	19.99	0.00	
6.47	291.24	21.32	3.63	291.96	7.30	19.01	24.98	0.00	0.00	0.380	36.69	36.687	53.83	7.44	0.013	-	-	-	0.09	19.04	0.00	
6.53	297.91	21.32	3.81	298.67	7.14	19.02	26.28	0.00	0.00	0.380	37.07	37.067	54.52	7.27	0.013	-	-	-	0.10	18.27	0.00	
6.60	305.45	21.32	3.99	306.25	6.96	19.03	27.48	0.00	0.00	0.381	37.45	37.448	55.35	7.09	0.013	-	-	-	0.10	17.58	0.00	
6.67	314.15	21.47	4.15	314.98	6.81	19.05	28.58	0.02	28.56	0.381	37.83	37.809	56.40	6.94	0.013	2.7	4.000	clayey silt to silty clay	0.11	17.01	485.78	1.21E-01
6.73	323.43	21.47	4.29	324.29	6.62	19.06	29.58	0.22	29.36	0.381	38.21	37.995	57.80	6.73	0.013	2.7	4.000	clayey silt to silty clay	0.11	16.44	482.74	1.25E-01
6.80	332.86	21.61	4.41	333.74	6.48	19.08	30.38	0.41	29.97	0.382	38.59	38.180	59.22	6.59	0.013	2.7	4.000	clayey silt to silty clay	0.12	16.04	480.70	1.27E-01
6.87	341.71	21.76	4.51	342.61	6.35	19.10	31.08	0.61	30.47	0.382	38.97	38.366	60.51	6.46	0.013	2.6	4.000	clayey silt to silty clay	0.12	15.71	478.84	1.30E-01
6.93	348.96	22.05	4.58	349.88	6.30	19.12	31.58	0.80	30.77	0.382	39.36	38.552	61.51	6.41	0.013	2.6	4.000	clayey silt to silty clay	0.12	15.58	479.54	1.29E-01
7.00	354.04	22.34	4.64	354.97	6.29	19.14	31.98	1.00	30.98	0.383	39.74	38.739	62.11	6.40	0.013	2.6	4.000	clayey silt to silty clay	0.13	15.55	481.71	1.26E-01
7.07	356.36	22.63	4.70	357.30	6.33	19.16	32.38	1.20	31.18	0.383	40.12	38.926	62.21	6.44	0.013	2.6	4.000	clayey silt to silty clay	0.12	15.60	486.35	1.20E-01
7.13	355.78	22.92	4.77	356.73	6.42	19.17	32.88	1.39	31.48	0.383	40.51	39.113	61.81	6.53	0.013	2.6	4.000	clayey silt to silty clay	0.12	15.70	494.16	1.10E-01
7.20	353.02	23.35	4.84	353.99	6.60	19.19	33.38	1.59	31.79	0.384	40.89	39.301	61.02	6.71	0.013	2.7	4.000	clayey silt to silty clay	0.12	15.92	506.11	9.61E-02
7.27	348.38	23.50	4.93	349.37	6.73	19.19	33.98	1.79	32.19	0.384	41.27	39.488	59.91	6.84	0.014	2.7	4.000	clayey silt to silty clay	0.12	16.04	516.51	8.43E-02
7.33	342.72	23.50	5.03	343.73	6.84	19.19	34.68	1.98	32.69	0.384	41.66	39.676	58.64	6.96	0.014	2.7	4.000	clayey silt to silty clay	0.12	16.11	526.61	7.34E-02
7.40	337.07	23.35	5.16	338.10	6.91	19.17	35.58	2.18	33.40	0.383	42.04	39.863	57.38	7.03	0.015	2.7	4.000	clayey silt to silty clay	0.12	16.05	535.92	6.37E-02
7.47	331.56	22.77	5.28	332.61	6.85	19.14	36.37	2.37	34.00	0.383	42.42	40.050	56.16	6.98	0.015	2.7	4.000	clayey silt to silty clay	0.12	15.82	538.01	6.16E-02
7.53	326.92	22.05	5.40	327.99	6.72	19.10	37.17	2.57	34.60	0.382	42.81	40.236	55.10	6.85	0.016	2.7	4.000	clayey silt to silty clay	0.13	15.51	536.67	6.30E-02
7.60	322.71	21.18	5.50	323.81	6.54	19.05	37.87	2.77	35.11	0.381	43.19	40.420	54.13	6.67	0.016	2.7	4.000	clayey silt to silty clay	0.13	15.14	531.58	6.82E-02
7.67	318.79	20.16	5.60	319.91	6.30	18.98	38.57	2.96	35.61	0.380	43.57	40.604	53.21	6.43	0.016	2.7	4.000	clayey silt to silty clay	0.14	14.69	523.21	7.70E-02
7.73	315.02	19.00	5.70	316.16	6.01	18.91	39.27	3.16	36.11	0.378	43.94	40.786	52.33	6.13	0.017	2.7	4.000	clayey silt to silty clay	0.14	14.16	511.43	9.00E-02
7.80	310.82	17.98	5.83	311.98	5.76	18.84	40.17	3.35	36.82	0.377	44.32	40.967	51.39	5.89	0.017	2.7	4.000	clayey silt to silty clay	0.15	13.65	502.75	1.00E-01
7.87	306.32	16.97	5.98	307.52	5.52	18.77	41.17	3.55	37.62	0.375	44.70	41.146	50.41	5.64	0.018	2.6	4.000	clayey silt to silty clay	0.16	13.13	493.93	1.11E-01
7.93	301.53	16.10	6.16	302.77	5.32	18.70	42.47	3.75	38.72	0.374	45.07	41.324	49.39	5.43	0.019	2.6	4.000	clayey silt to silty clay	0.17	12.62	488.61	1.17E-01
8.00	296.46	15.23	6.37	297.73	5.12	18.63	43.87	3.94	39.93	0.373	45.44	41.500	48.33	5.23	0.020	2.6	4.000	clayey silt to silty clay	0.18	12.10	483.08	1.24E-01

Project Name: -		2-6(119) RO-1			
GWT [ft]	6.66	M	1.2	κ	0.013

H [ft]	qc [psi]	fs [psi]	u [psi]	qt [psi]	R_f[%]	UW [kN/m3]	u2[kPa]	Uo [kpa]	Exc. Pore [kPa]	Δσv	σ_{vo} [kPa]	σ_{vo}' [kPa]	Qt []	Fr [%]	Bq []	Ic	Zone	Soil type	N	C	U_{adj}	k (ft/d)
8.07	291.24	14.50	6.60	292.56	4.96	18.57	45.47	4.14	41.33	0.371	45.81	41.676	47.27	5.07	0.021	2.6	4.000	clayey silt to silty clay	0.20	11.63	480.62	1.28E-01
8.13	286.45	13.78	6.82	287.81	4.79	18.51	46.97	4.34	42.63	0.370	46.18	41.850	46.28	4.90	0.022	2.6	4.000	clayey silt to silty clay	0.21	11.18	476.42	1.33E-01
8.20	282.24	13.05	7.03	283.65	4.60	18.44	48.47	4.53	43.94	0.369	46.55	42.022	45.40	4.71	0.023	2.6	4.000	clayey silt to silty clay	0.22	10.71	470.68	1.41E-01
8.27	278.91	12.47	7.22	280.35	4.45	18.38	49.77	4.73	45.04	0.368	46.92	42.194	44.67	4.56	0.024	2.6	4.000	clayey silt to silty clay	0.23	10.34	465.86	1.48E-01
8.33	276.73	11.89	7.38	278.21	4.27	18.32	50.86	4.92	45.94	0.366	47.29	42.364	44.13	4.38	0.025	2.6	4.000	clayey silt to silty clay	0.25	9.98	458.39	1.58E-01
8.40	275.72	11.46	7.51	277.22	4.13	18.28	51.76	5.12	46.64	0.366	47.65	42.533	43.79	4.24	0.025	2.6	5.000	silty sand to sandy silt	0.26	9.69	452.10	1.68E-01
8.47	276.01	10.88	7.61	277.53	3.92	18.22	52.46	5.32	47.15	0.364	48.02	42.702	43.66	4.02	0.025	2.6	5.000	silty sand to sandy silt	0.27	9.32	439.59	1.87E-01
8.53	277.46	10.44	7.72	279.00	3.74	18.18	53.16	5.51	47.65	0.364	48.38	42.869	43.71	3.84	0.025	2.6	5.000	silty sand to sandy silt	0.29	9.01	429.31	2.04E-01
8.60	279.92	10.15	7.80	281.48	3.61	18.15	53.76	5.71	48.05	0.363	48.74	43.036	43.93	3.70	0.025	2.6	5.000	silty sand to sandy silt	0.30	8.77	421.39	2.17E-01
8.67	283.26	9.86	7.89	284.84	3.46	18.12	54.36	5.90	48.46	0.362	49.11	43.202	44.29	3.55	0.025	2.5	5.000	silty sand to sandy silt	0.32	8.51	412.55	2.33E-01
8.73	287.18	9.72	7.99	288.77	3.37	18.11	55.06	6.10	48.96	0.362	49.47	43.368	44.74	3.45	0.025	2.5	5.000	silty sand to sandy silt	0.33	8.32	407.41	2.43E-01
8.80	291.67	9.57	8.09	293.29	3.26	18.09	55.76	6.30	49.46	0.362	49.83	43.534	45.27	3.35	0.025	2.5	5.000	silty sand to sandy silt	0.34	8.12	401.77	2.53E-01
8.87	296.31	9.57	8.21	297.95	3.21	18.10	56.56	6.49	50.07	0.362	50.19	43.700	45.83	3.29	0.025	2.5	5.000	silty sand to sandy silt	0.35	7.99	400.29	2.56E-01
8.93	301.53	9.72	8.33	303.20	3.21	18.12	57.36	6.69	50.67	0.362	50.55	43.866	46.47	3.28	0.025	2.5	5.000	silty sand to sandy silt	0.35	7.94	402.27	2.52E-01
9.00	307.19	9.86	8.46	308.88	3.19	18.15	58.26	6.89	51.37	0.363	50.92	44.033	47.18	3.27	0.025	2.5	5.000	silty sand to sandy silt	0.36	7.87	404.15	2.49E-01
9.07	313.43	10.01	8.59	315.14	3.18	18.17	59.16	7.08	52.08	0.363	51.28	44.200	47.97	3.25	0.025	2.5	5.000	silty sand to sandy silt	0.36	7.79	405.55	2.46E-01
9.13	320.10	10.30	8.72	321.84	3.20	18.21	60.06	7.28	52.78	0.364	51.65	44.368	48.82	3.28	0.024	2.5	5.000	silty sand to sandy silt	0.36	7.78	410.39	2.37E-01
9.20	327.21	10.59	8.83	328.97	3.22	18.25	60.86	7.47	53.38	0.365	52.01	44.537	49.73	3.29	0.024	2.5	5.000	silty sand to sandy silt	0.36	7.76	414.53	2.30E-01
9.27	334.46	10.88	8.96	336.25	3.24	18.29	61.76	7.67	54.09	0.366	52.38	44.707	50.65	3.31	0.024	2.5	5.000	silty sand to sandy silt	0.37	7.74	418.76	2.22E-01
9.33	341.42	11.17	9.08	343.24	3.25	18.33	62.56	7.87	54.69	0.367	52.74	44.877	51.52	3.33	0.024	2.5	5.000	silty sand to sandy silt	0.37	7.73	422.93	2.15E-01
9.40	347.80	11.60	9.18	349.64	3.32	18.38	63.26	8.06	55.19	0.368	53.11	45.049	52.30	3.39	0.023	2.5	5.000	silty sand to sandy silt	0.36	7.80	430.76	2.01E-01
9.47	352.88	12.04	9.28	354.73	3.39	18.43	63.96	8.26	55.70	0.369	53.48	45.221	52.87	3.47	0.023	2.5	5.000	silty sand to sandy silt	0.36	7.89	439.49	1.87E-01
9.53	356.07	12.47	9.38	357.95	3.48	18.47	64.66	8.45	56.20	0.369	53.85	45.394	53.14	3.56	0.023	2.5	5.000	silty sand to sandy silt	0.35	8.00	449.64	1.71E-01
9.60	356.79	13.05	9.47	358.69	3.64	18.53	65.26	8.65	56.60	0.371	54.22	45.569	53.04	3.72	0.023	2.5	5.000	silty sand to sandy silt	0.33	8.21	464.85	1.49E-01
9.67	354.91	13.63	9.56	356.82	3.82	18.58	65.85	8.85	57.01	0.372	54.59	45.744	52.55	3.91	0.024	2.5	5.000	silty sand to sandy silt	0.32	8.46	482.29	1.25E-01